AD NUMBER

AD836284

LIMITATION CHANGES

TO:

Approved for public release; distribution is unlimited.

FROM:

Distribution authorized to U.S. Gov't. agencies and their contractors; Critical Technology; JUN 1968. Other requests shall be referred to Air Force Technical Application Center, VELA Seismological Center, Washington, DC 20333. This document contains export-controlled technical data.

AUTHORITY

usaf ltr, 25 jan 1972

TR68-24

TECHNICAL REPORT NO. 68-24

FINAL REPORT, PROJECT VT/7703, DEEP WELL ARRAY OPERATIONS

GEOTECH
A TELEDYNE COMPANY

DISCLAIMER NOTICE

THIS DOCUMENT IS THE BEST QUALITY AVAILABLE.

COPY FURNISHED CONTAINED A SIGNIFICANT NUMBER OF PAGES WHICH DO NOT REPRODUCE LEGIBLY.

TECHNICAL REPORT NO. 68-24

FINAL REPORT, PROJECT VT/7703, DEEP WELL ARRAY OPERATIONS

by

Z. A. Der
E. J. Douze
A. W. Simmons

Sponsored by

Advanced Research Projects Agency
Nuclear Test Detection Office
ARPA Order No. 624

Availability

Qualified users may request copies of this document from:

Defense Documentation Center
Cameron Station
Alexandria, Virginia 22341

Acknowledgement

This research was supported by the Advanced Research Projects Agency, Nuclear Test Detection Office, and was monitored by the Air Force Technical Applications Center under Contract No. F33657-67-C-1224.

GEOTECH
A Teledyne Company
3401 Shiloh Road
Garland, Texas

25 June 1968

IDENTIFICATION

AFTAC Project No.:	VELA T/7703
Project Title:	Deep Well Array Operations
ARPA Order No.:	624
ARPA Program Code:No.:	7F10
Name of Contractor:	Geotech, A Teledyne Company 3401 Shiloh Road Garland, Texas 75040
Contract No.:	F33657-67-C-1224
Amount of Contract:	$278,800
Effective Date of Contract:	1 March 1967
Contract Expiration Date:	31 May 1968
Program Manager	David B. Andrew Garland, Texas 271-2561, A/C 214

TABLE OF CONTENTS

		Page
ABSTRACT		
1.	INTRODUCTION	1
2.	FIELD OPERATIONS PROGRAM	1
	2.1 Operation of triaxial array	1
	2.2 Computer operation and problems	5
	2.3 Film and digital tape recording	8
	2.4 Operate the online computer to test and compare real time vertical array signal enhancement data processing techniques	12
3.	ANALYSIS OF TRIAXIAL ARRAY DATA	12
	3.1 Determination of the ghosting filters for horizontal components	12
	3.2 Analysis of seismic noise	20
	3.3 Development of processors	30
4.	PROCESSING OF VERTICAL ARRAY DATA	38
	4.1 Inverse filters	42
	4.2 Optimum filtering	42
	4.2.1 Deghosting optimum filters	46
	4.2.2 Conventional optimum filters	48
	4.2.3 Prediction filters	53
	4.3 Non-optimum filters	55
	4.3.1 Multichannel deghosting filters	55
	4.3.2 Velocity filters	57
	4.3.3 Time-delay and sum	
5.	REFERENCES	60
6.	CONCLUSIONS AND RECOMMENDATIONS	61
	6.1 Conclusions	61
	6.2 Recommendations	61
APPENDIX -	Reproduction of Statement of Work to be Done, AFTAC Project Authorization No. VELA T/7703 and Amendments	

LIST OF ILLUSTRATIONS

Figure		Page
1	Facilities and equipment at GVTX	2
2	Triaxial seismometer module and switch	3
3	Triaxial seismometer outline drawing	4
4	Triaxial array system block diagram	6
5	Configuration of racks in recording van	9
6	Adage Ambilog 200 computer console	10
7	Adage Ambilog 200 equipment racks and tape deck	11
8	Teleseism recorded at GVTX, both analog and digital, MCD is a multichannel deghosted channel using DH1, DH2, and DH3 with a filter delay of 3.74 sec	13
9	Determination of Poisson ratio	15
10	Original and derived traces for the Greeley event, APOK	16
11	Original and derived traces (Haskell's method) Nicaragua event, GVTX	17
12	Deghosted deephole traces, Greeley event, APOK	19
13	Multichannel deghosted deephole traces	21
14	Triax array noise power spectra	22
15	Multiple coherences of computer transformed horizontal and vertical channels of the four short-period triax seismographs at GVTX	24
16	Observed and theoretical amplitude ratios for noise at GVTX, T = 6.0 sec	28
17	Observed and theoretical amplitude ratios for noise at GVTX, T = 4.0 sec	28
18	Observed and theoretical amplitude ratios for noise at GVTX, T = 3.0 sec	29
19	Observed and theoretical amplitude ratios for noise at GVTX, T = 2.0 sec	31

ILLUSTRATIONS (Continued)

Figure		Page
20	Observed and theoretical and amplitude ratios for noise at GVTX, T = 1.0 sec	31
21	Remode type processing	32
22	Multichannel deghosting filter amplitude response -- vertical components	35
23	Amplitude response of maximum likelihood filters on radial (angle of incidence = 34 deg)	36
24	Maximum likelihood - motion product processing Nicaragua event	37
25	Teleseismic signal operated on by techniques used to increase the signal-to-noise ratio a, surface; b, c, d, single-channel deghosting processes operating on DH3 (1060 m), DH2 (1980 m), and DH1 (2880 m); e, normalized sum of b, c, d; f, g, multichannel deghosting processes with one- and two-sided optimum filters; h, DH1 unfiltered; i, single-channel ghosting process	41
26	Deephole data processing techniques	43
27	Attenuation obtained from optimum techniques: a. single-channel deghosting (2880 m); b. single-channel deghosting (1980 m); c. single-channel deghosting (1060 m); d. sum of single-channels; e. one-sided multichannel deghosting; f. two-sided multichannel deghosting; g. sum of deghosted channels; h. single channels ghosting (2880 m); i. two-channel optimum filter; j. four-channel optimum	45
28	Teleseismic signal operated on by multichannel Wiener filters; a. surface signal; b. two-channel filter; c. four-channel filter	47
29	Noise spectrum of DH1 in solid line, noise spectrum after three-channel optimum filtering in dashed line, GVTX	49
30	Spectrum of the noise after three-channel prediction filter using DH4, DH3, and DH2 to predict DH1 (solid line), and spectrum of the noise at the surface (dashed line)	50
31	Multiple coherence of the four vertical seismographs at APOK, DH4, (surface) used as output	51
32	Multiple coherence of the four vertical seismographs at APOK, DH1 used as output	52

ILLUSTRATIONS (CONTINUED)

Figure		Page
33	Experimental results from prediction filtering (solid line) and theoretically predicted spectrum after prediction filtering (dashed line), APOK	54
34	Cosine inverse filter using (a) all four deephole channels, (b) bottom channels, GVTX	56
35	Noise (from spectra) and signal attenuation resulting from fan-filtered deephole array, APOK	58
36	Attenuations obtained at GVTX in time delay and sum processing	59

TABLES

Table		Page
1	Signal-to-noise ratios for deephole triax array operating at GVTX	8
2	Velocity model for Grapevine, Texas, with surface taken as zero reference and the first layer 137 m thick, etc	26

ABSTRACT

A deephole array consisting of 12 short-period triaxial seismometers was operated at a test site near Grapevine, Texas (GVTX), until 23 February 1968. The system was then put in a standby status until additional software could be developed to provide additional filtering capabilities. The complete system was shut down and all of the instrumentation and equipment was moved into storage areas at the Geotech plant in Garland, Texas, during the last week of May.

The information gathered from the short-period triaxial array at the GVTX site was used to study short-period noise and signals, to develop signal enhancement, and filtering techniques. Most of the time was used in trying techniques based on least-mean-square filtering. In general, it can be concluded that because the noise is not stationary, these filters degrade too rapidly to be of practical interest for online processing. Several non-optimum filtering techniques were also tried and were found to be as effective as the optimum filters.

FINAL REPORT, PROJECT VT/7703
DEEP WELL ARRAY OPERATIONS

1. INTRODUCTION

This report discusses the work accomplished and the problems encountered during the field operations program conducted under Project VT/7703. The work reported herein covers field operation of a 12-component short-period triaxial array system (4 vertical components), modifications, improvements, programming, signal and noise analysis, and processing from 1 March 1967 through 31 May 1968. It is submitted in compliance with paragraph 5, Reports of the Statement of Work to be Done, Project VT/7703. This project was under the technical direction of the Air Force Technical Applications Center (AFTAC) and under the overall direction of the Advanced Research Projects Agency (ARPA).

This report is generally presented in the same sequence as the tasks in the Statement of Work. A copy of the Statement of Work is included as Appendix 1.

2. FIELD OPERATIONS PROGRAM

2.1 OPERATION OF TRIAXIAL ARRAY

The short-period triaxial deephole array and the associated equipment that was assembled for Project VT/5051, was moved from the site near Apache, Oklahoma (APOK), to the site near Grapevine, Texas (GVTX), see figure 1, during the first two weeks of March, 1967. All of the downhole instruments were disassembled, thoroughly checked, and marginal components replaced where necessary before installation. The downhole instrumentation consists of four short-period triax seismometers that have three sensitive modules directionally orientated 120 degrees to each other. Figure 2 is a photograph of one of these modules and figure 3 shows an outline drawing of one seismometer assembly. The instruments were operated in the GVTX deephole at the following depths:

DH4	Surface
DH3	1067 m
DH2	1982 m
DH1	2915 m

With the exception of moisture getting into a downhole connector, all of the instruments were checked out and calibrated without incident. Satisfactory operation of all downhole instruments continued until the middle of July when the bottom seismometer in the deephole started to leak. This required pulling all of the deephole instruments. The leak was found in the switching module. While it was being repaired, a routine inspection revealed a heat distorted calibration coil in module No. 1 of the bottom seismometer. After repair and replacement, the array was lowered to the desired depths and put

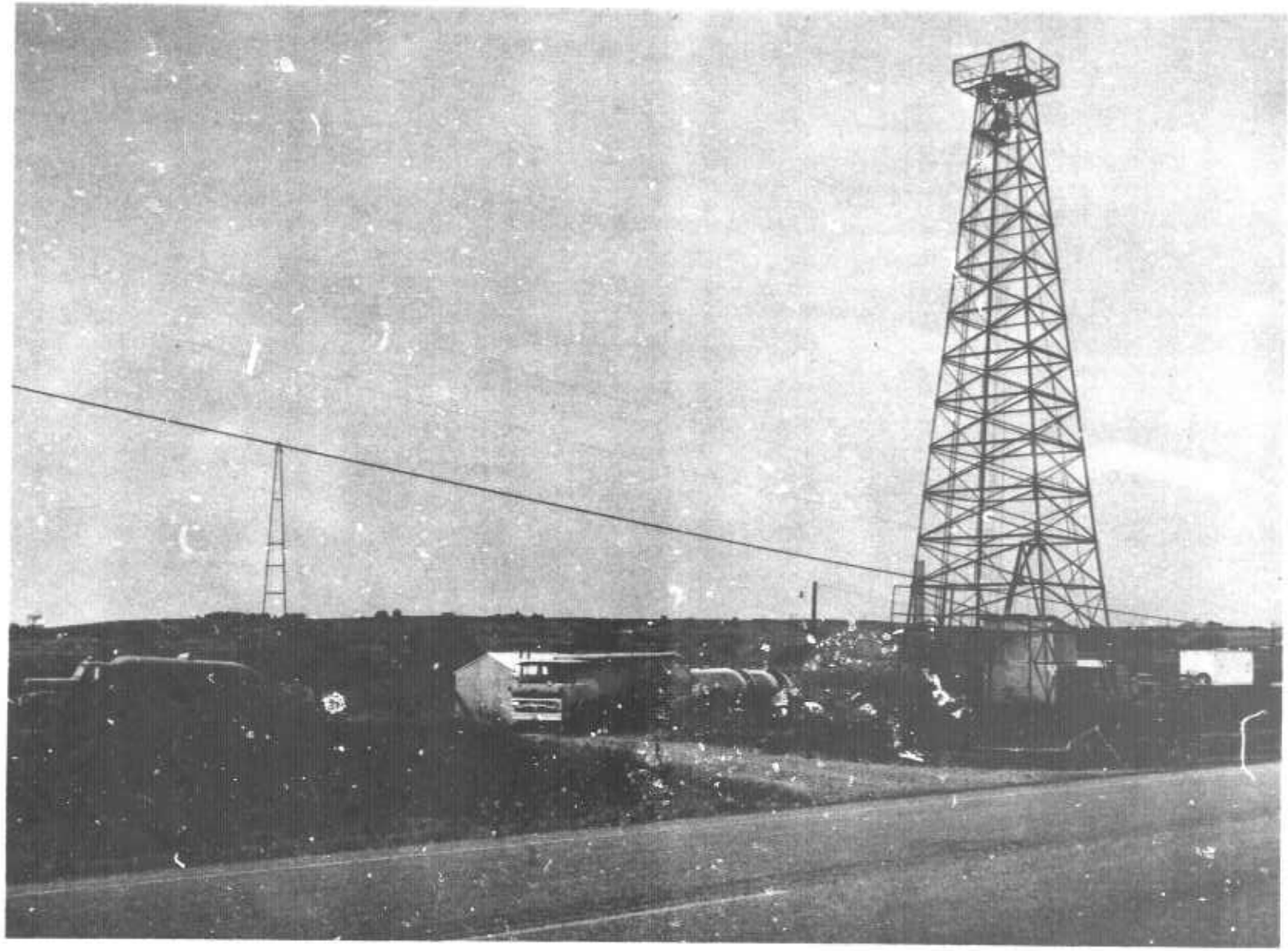

Figure 1. Facilities and equipment at GVTX

G 4171

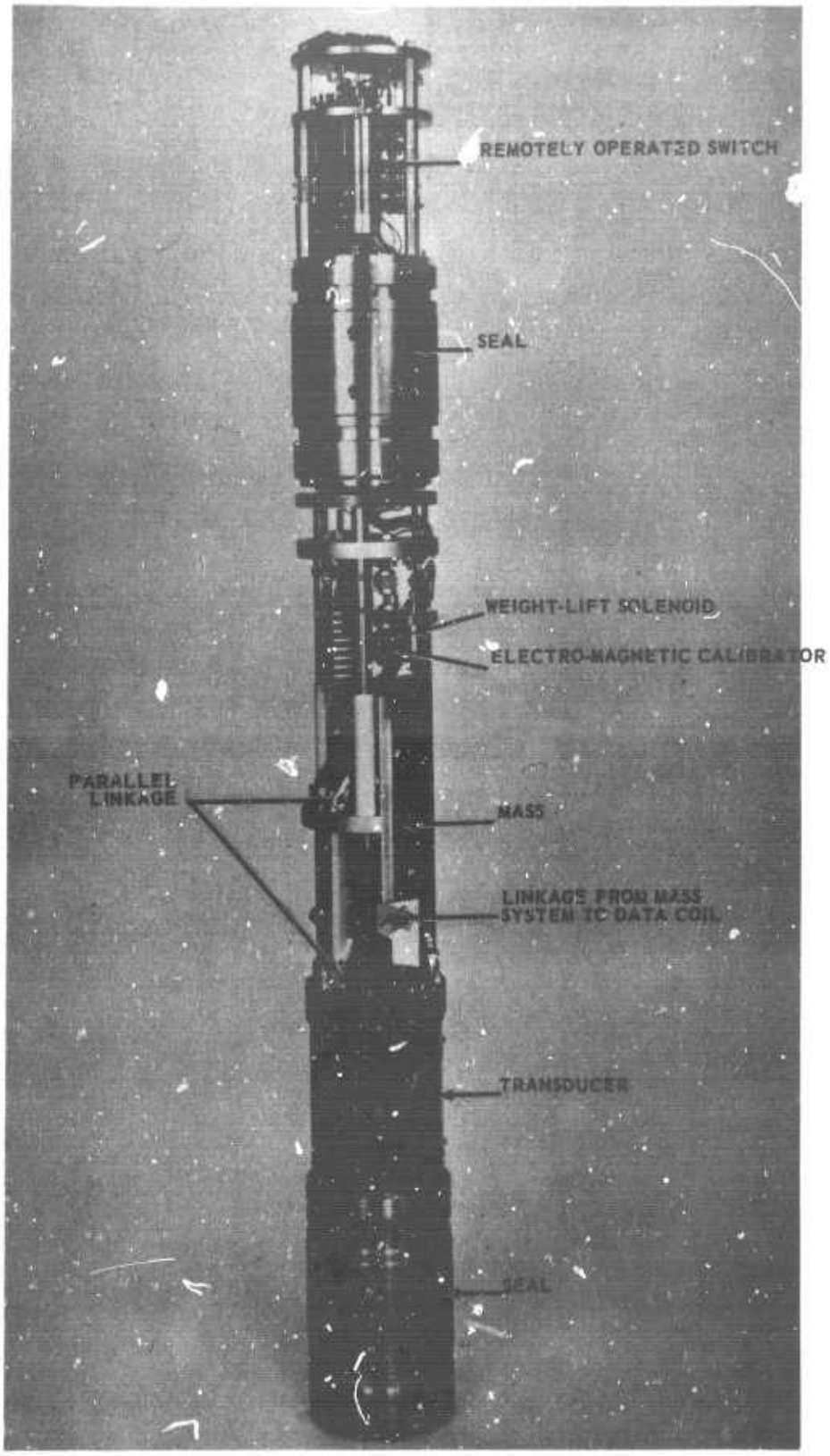

Figure 2. Triaxial seismometer module and switch

G 1348

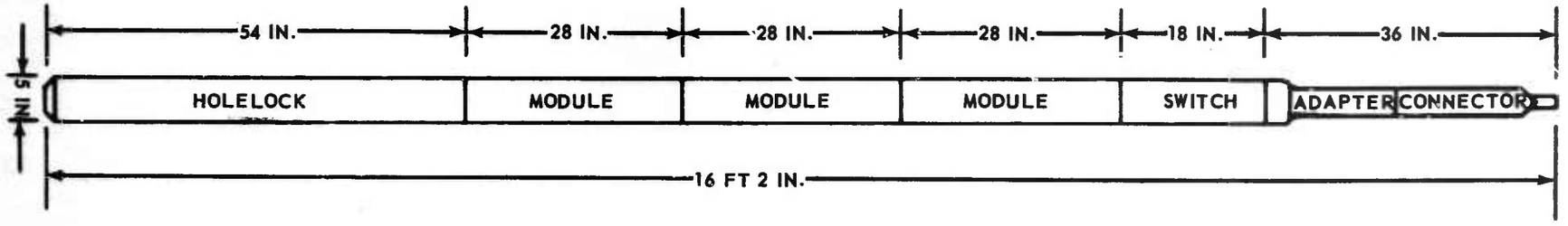

WEIGHT OF ASSEMBLY 520 LB

Figure 3. Triaxial seismometer outline drawing

G 1347

into operation. During calibration, the mass position motor in No. 1 module of seismometer No. 2 failed. This required removing seismometer No. 3 and seismometer No. 2 from the deephole. The motor, and Bendix flexures damaged when removing seismometer No. 2 from the well, were replaced. Check out after installation revealed that the cable attached to No. 3 seismometer showed low insulation resistance from the electrical conductors to ground. This required No. 3 seismometer to be removed from the well for cable repair. A cable serviceman was called in to repair this cable and another known short in a spare cable on a winch truck not being used at that time. Number 3 seismometer was then attached to the repaired cable on the winch truck, previously not in use, and lowered to desired depth. All instruments were operational the last week of August, 1967, and have continued to operate satisfactorily until 23 February 1968 when the entire system was put in a standby status.

All of the peripheral analog equipment, including the film recording equipment operated satisfactorily. The failures that did occur were caused mainly by wear from normal operation. These failures were anticipated and spare parts were available, thereby keeping downtime on these pieces of equipment to an absolute minimum.

After digitizing several magnetic tapes of data for noise studies, a decision was made to increase the gain of the system. This was accomplished by decreasing the input impedance of the multiplexer in the computer. After digitizing the required amount of data, the gain was raised again. This time, operational amplitifers (op-amps) were added to the system between the phototube amplifiers and the data control modules as shown in figure 4. The multiplexer inputs were then restored to their original configuration with the system gain increased about 35 dB. The first week of October, the initial op-amps were removed from the system and were replaced by two op-amps in series in each data channel. The total additional gain was now 60 dB. Signal-to-noise ratios for the system with the op-amps in operation are listed in table 1.

2.2 COMPUTER OPERATION AND PROBLEMS

The majority of the system downtime can be attributed to the problems that have existed in the Ambilog 200 computer. During the 4-month period from the third week of March 1967, to 1 August 1967, the computer was considered operational 337 hours as far as listing and editing programs was concerned. The computer was capable of digitizing raw triaxial data and performing system response calibrations for approximately 116 hours of the 337 operational hours mentioned. It was not possible to digitize data for the full 116 hours as software programs had to be checked and debugged, and system calibrations had to be made before data could be digitized.

The major problems resulting in computer downtime follows.

1. 21 March 1967 — Analog to digitial converter (ADC) failed, oscillations on some channels, others putting out random spikes. The ADC section was sent to the manufacturer in Fullerton, California, for repair and calibration. The Fullerton, California, division was unable to

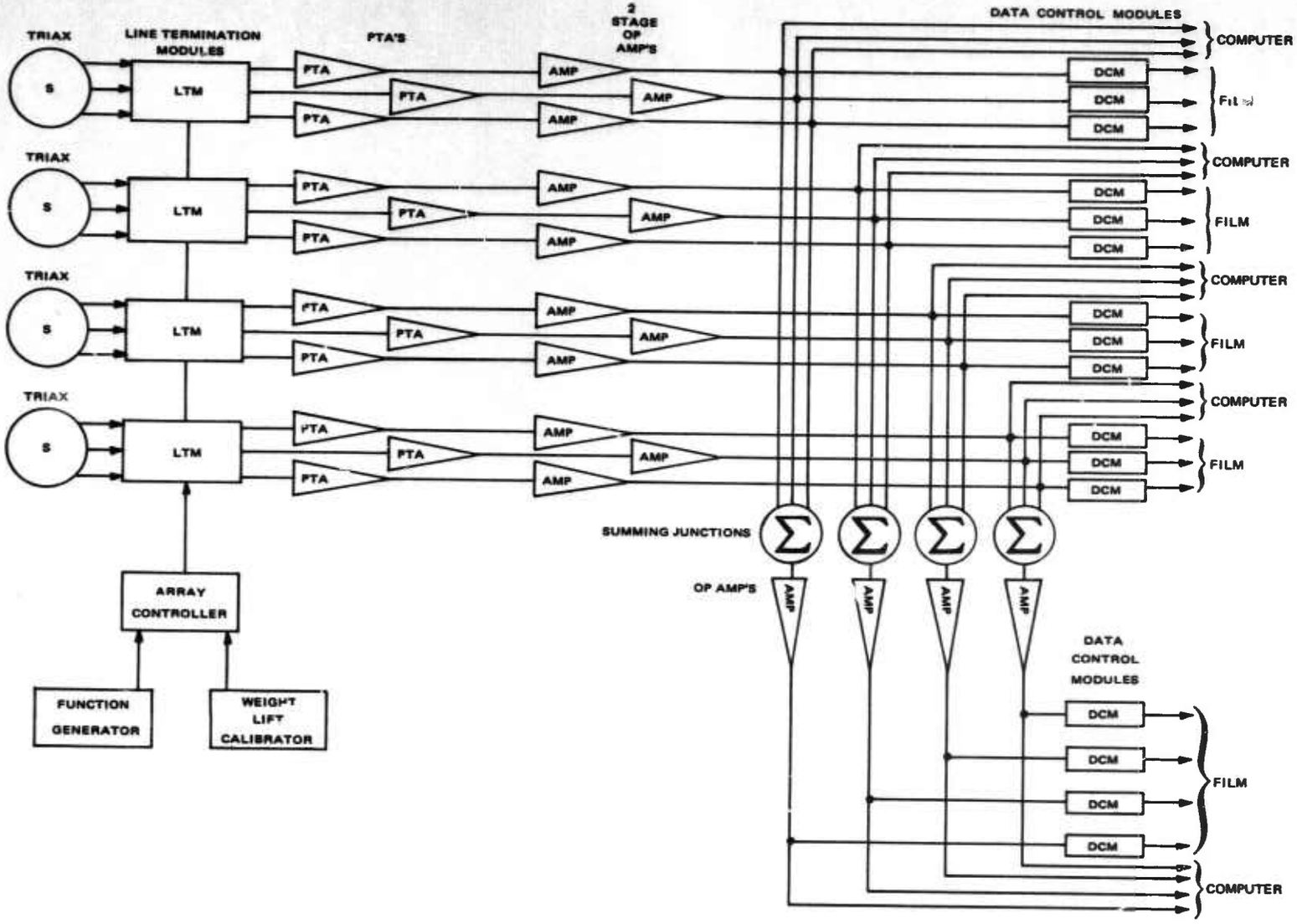

Figure 4. Triaxial array system, block diagram

G 4172

repair the unit. They sent the complete section to the factory in Boston, Massachusetts, where it remained for approximately 6 weeks before repairs were completed. The unit was received 11 May 1967; after two days of testing, problems still existed in the ADC unit and it was sent back to the manufacturer again for repair. It was received from the factory on 12 June, checked out, and this time performed satisfactorily.

2. 14 June 1967 — Relay failure in the Dura typewriter caused semiconductor failures in the OPI section of the computer. The replacement components were received and installed and the computer was operational again on 20 June.

3. 21 June 1967 — A microswitch in the Dura typewriter failed and again caused semiconductor failure in the OPI section of the computer. Repairs were made and the OPI section readjusted. The computer was operational again on 23 June.

4. 3 July 1967 — Another microswitch failure caused the computer to stick in the "type-out" stage. A new microswitch was installed and the computer was again operational on the afternoon of 3 July.

5. 7 July 1967 — Another Dura typewriter failure occured and this time the Dura serviceman removed the old typewriter and installed a rebuilt typewriter. After the typewriter exchange was made and checked out, it became obvious that another problem existed. This problem was found in the voltage reference section. Two shorted transistors were found on the Ref 8 card. After repair and adjustments were complete, the computer was operational on 17 July.

6. 26 July 1967 — This failure was in the SCU section. The serviceman was called and arrived on site on 28 July and replaced a shorted transistor. The computer was operational on 29 July.

7. 15-23 August 1967 — The Adage serviceman performed complete ambilogical calibrations. Several marginal components were discovered and replaced while performing the calibration. Calibration was delayed for 2 days because an OP4 printed circuit board had to be shipped from the factory in Boston, Massachusetts, to replace one that would not meet specifications.

8. 20 February 1968 — Intermittant operation was detected in the accumulator section. The trouble was found to be a cold solder joint on a printed circuit board. The computer was operational the afternoon of 20 February after 4 hours of downtime.

Table 1. Signal-to-noise ratios for deephole triax array operating at GVTX

Seismometer	Module	Seismic background (counts)	Dummy PTA (counts)	S/N, background dummy PTA
1	1	3950	560	7.1:1
	2	5500	570	9.6:1
	3	3800	500	7.6:1
2	4	6300	590	11.1:1
	5	4250	300	14.1:1
	6	4200	550	7.6:1
3	7	6100	500	12.0:1
	8	8000	450	17.5:1
	9	8750	600	14.5:1
4	10	10100	650	15.5:1
	11	7750	350	22.0:1
	12	9450	250	38.0:1

These tests were made at operational magnifications which recorded a normal seismic background level for each triax seismograph, in counts (plus to minus) for a 15-bit binary digital form.

Computer downtime had become such a serious problem by the middle of June that it became necessary to initiate a 3-month maintenance contract with the computer manufacturer. This arrangement worked so well that the contract was kept in effect for a total of nine (9) months. Reliable and routine operation of the computer was possible after 23 August when the ambilogical sections were calibrated.

Several engineering changes have been made to the computer during this contract period. Seven (7) engineering changes have been made by Adage, the computer manufacturer. One (1) engineering change was made by Fabritek, the manufacturer of the computer memory. Two (2) corrections were made to the Potter tape deck by the Adage serviceman. Twelve (12) other corrections of problems were made by the Adage serviceman and Geotech personnel during normal computer downtime. These corrections and adjustments did not result in any computer downtime during normal working hours. Figures 5, 6, and 7 show the rack configuration, the computer console, and the tape deck as installed in the instrumentation van.

2.3 FILM AND DIGITAL TAPE RECORDING

Considerable signal and noise data have been digitized and recorded on film and tape during the operational period of this project. Some of the first digitized data recorded on tape was of low amplitude and had low level spikes in it caused by the tape advance mechanism in the tape deck. This particular problem, and a similar problem of intermittant spikes, were corrected and all of the data since the last of August, 1967, is free from detrimental responses.

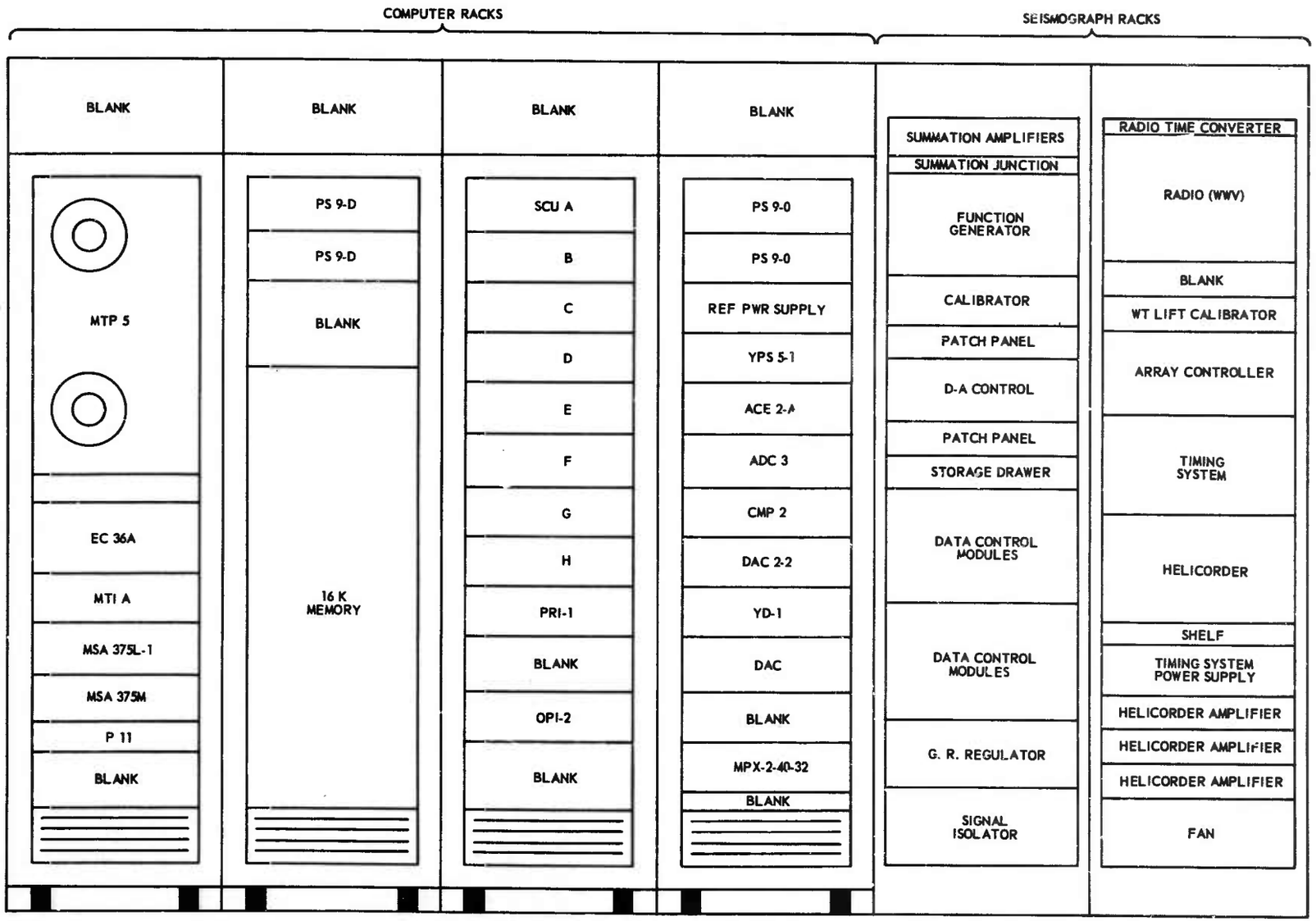

Figure 5. Configuration of racks in recording van

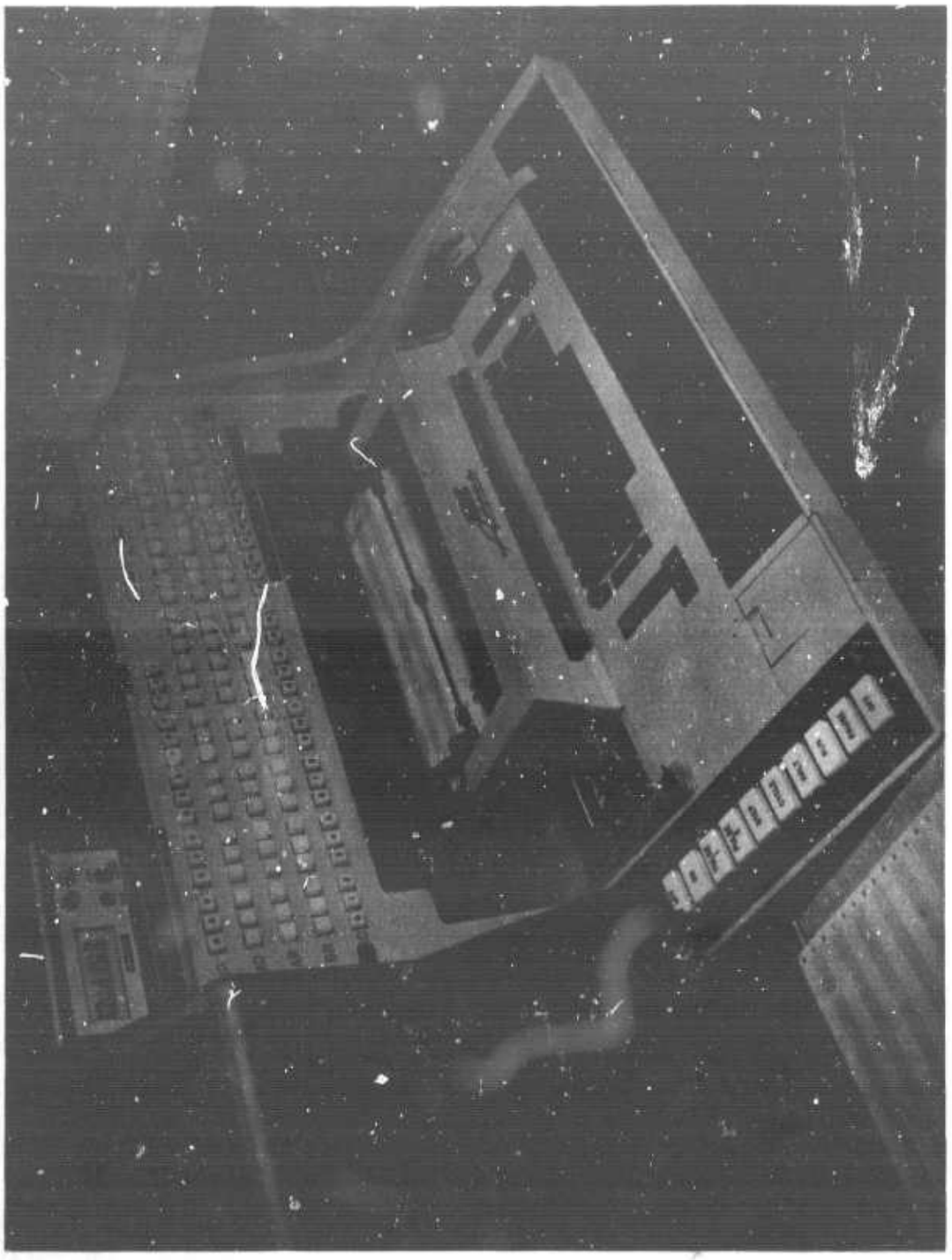

G 4173

Figure 6. Adage Ambilog 200 computer console

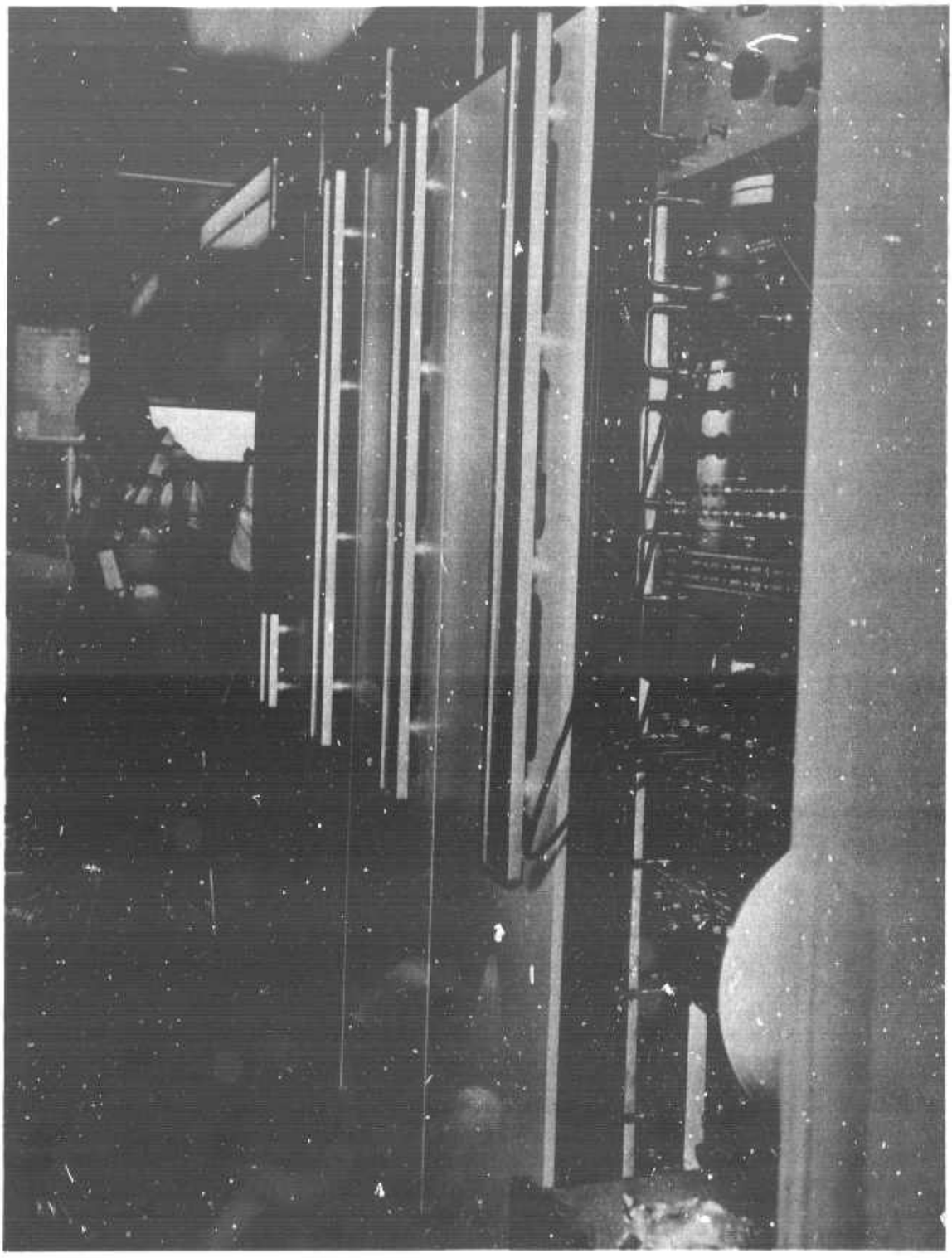

Figure 7. Adage Ambilog 200 equipment racks and tape deck

G 4174

2.4 OPERATE THE ONLINE COMPUTER TO TEST AND COMPARE REAL TIME VERTICAL ARRAY SIGNAL ENHANCEMENT DATA PROCESSING TECHNIQUES

The hardware problems encountered during the early part of the project delayed the processing of data with existing programs; however, a general filter program was written and ehecked out. This program will add any set of filter weights to 10 channels of seismic data and output the summation of the filtered data and the raw data on the film. The type of filtering performed depends on the method by which the filter weights are computed. Initial tests were run using Weiner optimum filter weights.

The online filter program was checked out and several days of data were recorded on film. Figure 8 shows the operational results of this program. Traces 5, 6, and 7, counting from the top, are identical traces to 1, 2, and 3, respectively, except that they have been digitized prior to online processing. They are then discriminated and recorded for comparison with the raw analog data. These are the results of processing three channels of data using 149 weights per channel. Only the three deepest seismometer outputs were used because the high noise levels close to the surface degraded the output when included.

In order to permit simultaneous recording of data on film and magnetic tape, and to incorporate the additional filter routine requested by the Project Officer, the above filter program was rewritten. The program had not been completely checked out at the contract termination date. Data was not being properly recorded on magnetic tape even though the magnetic tape read-write routines were operating properly.

3. ANALYSIS OF TRIAXIAL ARRAY DATA

Analysis of triaxial data does not involve any new principles compared to the vertical component deephole arrays. The signal waveforms change with depth on the horizontals as well as on the verticals. The change of signal waveforms from level to level and component to component can again be described in terms of relative simple filters.

The noise on the horizontals is different from the noise on the verticals; and contributions from both Rayleigh and Love modes can be expected on the horizontals. As a result of angular spread in the directions of approach of surface waves, the coherence between the vertical and horizontal components and the two perpendicular horizontals is expected to be very low.

The directional orientation of the triaxial seismometers was determined using several large teleseisms. This determination seems to be fairly accurate, the deviations of direction is less than 10 degrees.

3.1 DETERMINATION OF THE GHOSTING FILTERS FOR HORIZONTAL COMPONENTS

Determination of the effect of ghosting on the signal (P wave) waveforms at depth can be done similarly to the methods used for vertical component arrays. There are, however, some complicating factors. While the waveforms on the

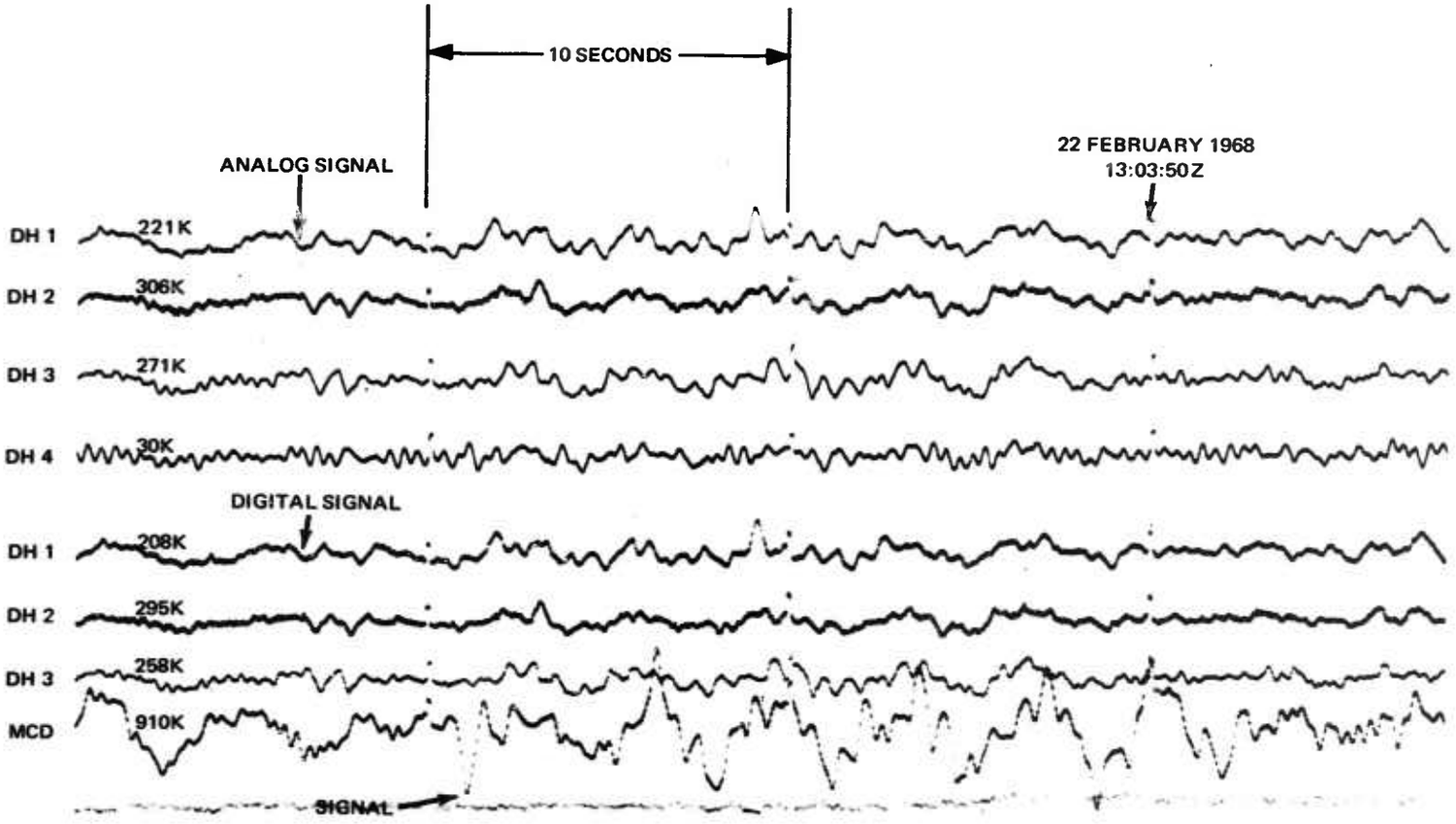

Figure 8. Teleseism recorded at GVTX, both analog and digital MCD is a multichannel deghosted channel using DH1, DH2, and DH3 with a filter delay of 3.74 seconds

G 4175

verticals can be approximated well by considering only incident and surface reflected P waves, for the horizontals, the surface reflected SV wave contributes significantly to the shape of waveforms. The arrival time of the SV wave and its amplitude depends critically on the Poisson ratio (or S wave velocity) of the medium and the angle of incidence of the wave. No direct measurement of S velocity is available at the present deephole sites. In order to determine the average Poisson ratio for a site, the following procedure was used:

A set of filters was derived to simulate the effect of ghosting at the deepest radial component by filtering the near surface vertical component recording of a seismic event. Various values of Poisson ratios, σ, were used to derive the individual filters in the set. The resulting set of simulated deephole radial components was compared to the actual deephole radial. The filter designed with the "best" average Poisson ratio gives the waveform which agrees most favorably with the actual deephole radial components. Such an analysis was performed for both the Grapevine and Apache sites. Figure 9 shows the output of several filters with varying Poisson ratios obtained for the Greeley nuclear explosion as recorded at Apache, Oklahoma. It shows that the best agreement found is $\sigma = 0.3$. Fairly good agreement is found also for $\sigma = 0.35$. Vertical waveforms (not shown) found for this Poisson ratio, however, do not agree with the observed waveforms. For Grapevine, the procedure yielded the same value $\sigma = 0.3$.

To test the adequacy of filters to simulate ghosting, a set of deephole traces were derived from the near surface vertical using the Poisson ratio $\sigma = 0.3$. Figure 10 shows the results for the Greeley explosion recorded at Apache, Oklahoma. The figure shows that the waveforms agree very well. For this case, an elastic halfspace model was used with only incident P, reflected P, and SV considered.

Figure 11 shows the results of a similar test for the Grapevine, Texas, site for a Nicaragua earthquake. Again, good agreement in the waveforms is found. The filters used for this test were cauculated by computing the response of a layered elastic medium by Haskell's method. A computer program written by Hannon was modified to yield the response as a function of depth (Hannon, 1967). The frequency response functions were inverse Fourier transformed and convolved with the surface vertical trace.

In several previous processing schemes, deghosting was applied to deephole traces (see final Report, Project VT/5051, TR67-3, 1967). Deghosting filters for vertical components turned out to be especially simple two-point recursive filters. This is not true for the radial components. The ghosting filters for radial components (filters which derive the ghosted radial trace from the incident P waveform) are not minimum phase and inverse filtering must be implemented by forward and reverse recursion.

Although all waveforms can be reduced to an impulse through filtering recursively by the waveform itself, in general, recursive filtering leads to instability. This means that the impulse response of the recursive filter increases without bounds. Any small deviation from the exact waveform can initiate this unstable condition. Recursive filters are stable only if the filter used is minimum phase or minimum delay, and are unstable if they are maximum or mixed delay.

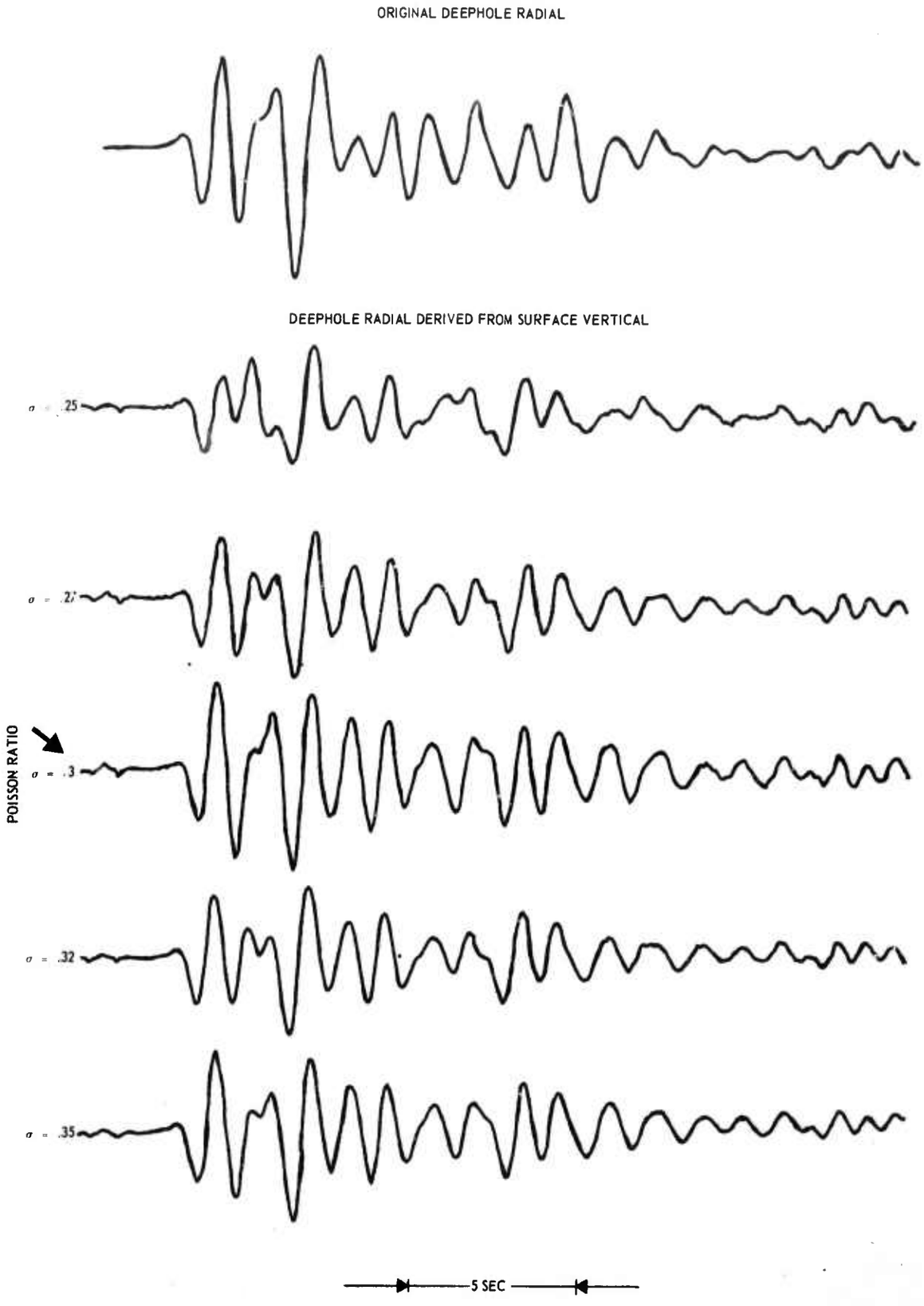

Figure 9. Determination of Poisson ratio

G 3253

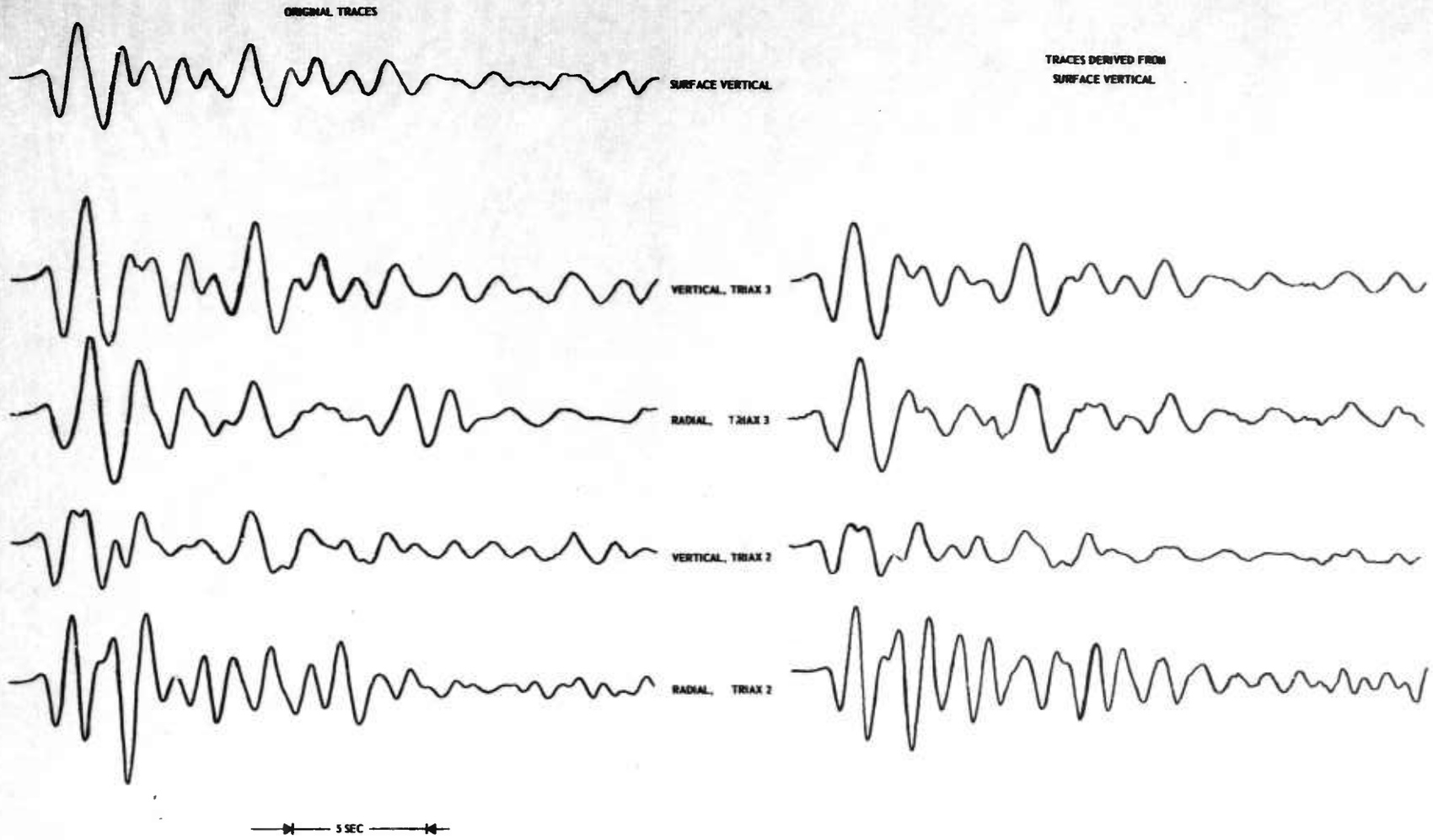

Figure 10. Original and derived traces for the Greeley event, APOK

G 3254

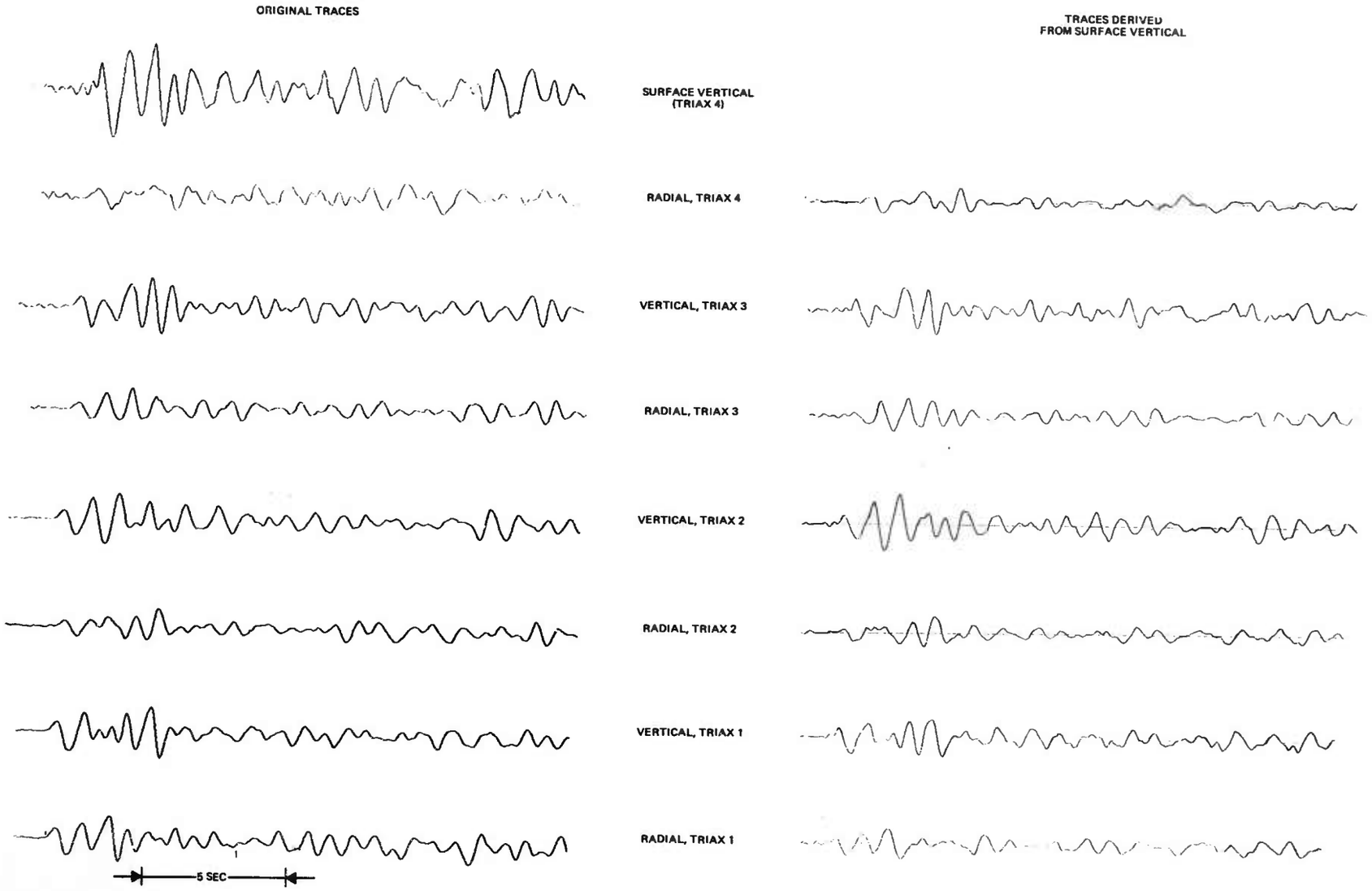

Figure 11. Original and derived traces (Haskell's method) Nicaragua event, GVTX

G 4176

It is easy to determine to which group a particular filter belongs. If the filter weights are a_0, a_1, a_2 . . . a_n, and the polynomial (Z transform) is

$$P(Z) = a_0 + a_1 Z + a_2 Z^2 + \ldots + a_n Z^n$$

and the roots of this polynomial are r_1 . . . r_n (real or complex conjugate pair). The filter is minimum delay if $[r_i] > 1$ for all roots. The filter is maximum delay if $[r_i] < 1$ for all roots.

Mixed delay has roots both larger and smaller than zero in absolute value. Our filters are mixed delay, therefore, if applied recursively, they are unstable and the filter polynomial can be factored into two polynomials,

$$P(Z) = P_1(Z)\ P_2(Z)$$

where $P_1(Z)$ is minimum delay and $P_2(Z)$ is maximum delay.

$P_1(Z)$ can be applied recursively without any difficulty; $P_2(Z)$ cannot; but it can be used in reverse recursion if we replace Z by $1/Z$ which is equivalent to reversing the time scale and thus $P_2(1/Z)$ becomes minimum phase.

A detailed discussion of these concepts may be found in the references. For our case, the forward and reverse recursive filters are derived by taking the root of the Z transform polynomial where a_0, a_1, . . . a_n are the filter weights for the filter which derives the particular deephole trace from the surface vertical. The roots are separated into two groups, one with absolute values smaller than unity, $|r_1| < 1$, and the other with absolute values larger than unity $|r_i'| > 1$, forming two (Z) polynomials;

$$P_1(Z) = (Z - r_1)\ (Z - r_2) \ldots (Z - r_k)$$

and,

$$P_2(Z) = (Z - r_1')\ (Z - r_2') \ldots (Z - r_m'),\ m + k = n.$$

The coefficients of these polynomials are the desired filter weights. After normalization, the coefficients of the first polynomial are used as inverse recursive filters taken in inverse order and those of the second polynomial are used as forward recursive filters. A computer program for factoring Z transforms in this manner has been written. It was found that many roots of the Z polynomials for horizontal ghosting filters are extremely close to the unit circle in the complex plane. This indicates that the inverse recursive filters would be very close to instability.

Figure 12 shows some deghosted traces using the Greeley recordings at APOK. No difficulty was encountered in deghosting the deephole vertical traces. This is not the case for the horizontals. For the deepest radial component, the forward and reverse recursion filters were found to ring severely, as indicated by the location of roots, and the best results were obtained by using a 150 point Wiener filter. The waveforms obtained from the horizontals are poor.

It is desirable to deghost the deephole traces at some point during the processing sequence. The ghosted deephole traces are not easy to interpret. Since deghosting the traces involves amplification at frequencies where the signal has been attenuated by interference of incident and surface reflected

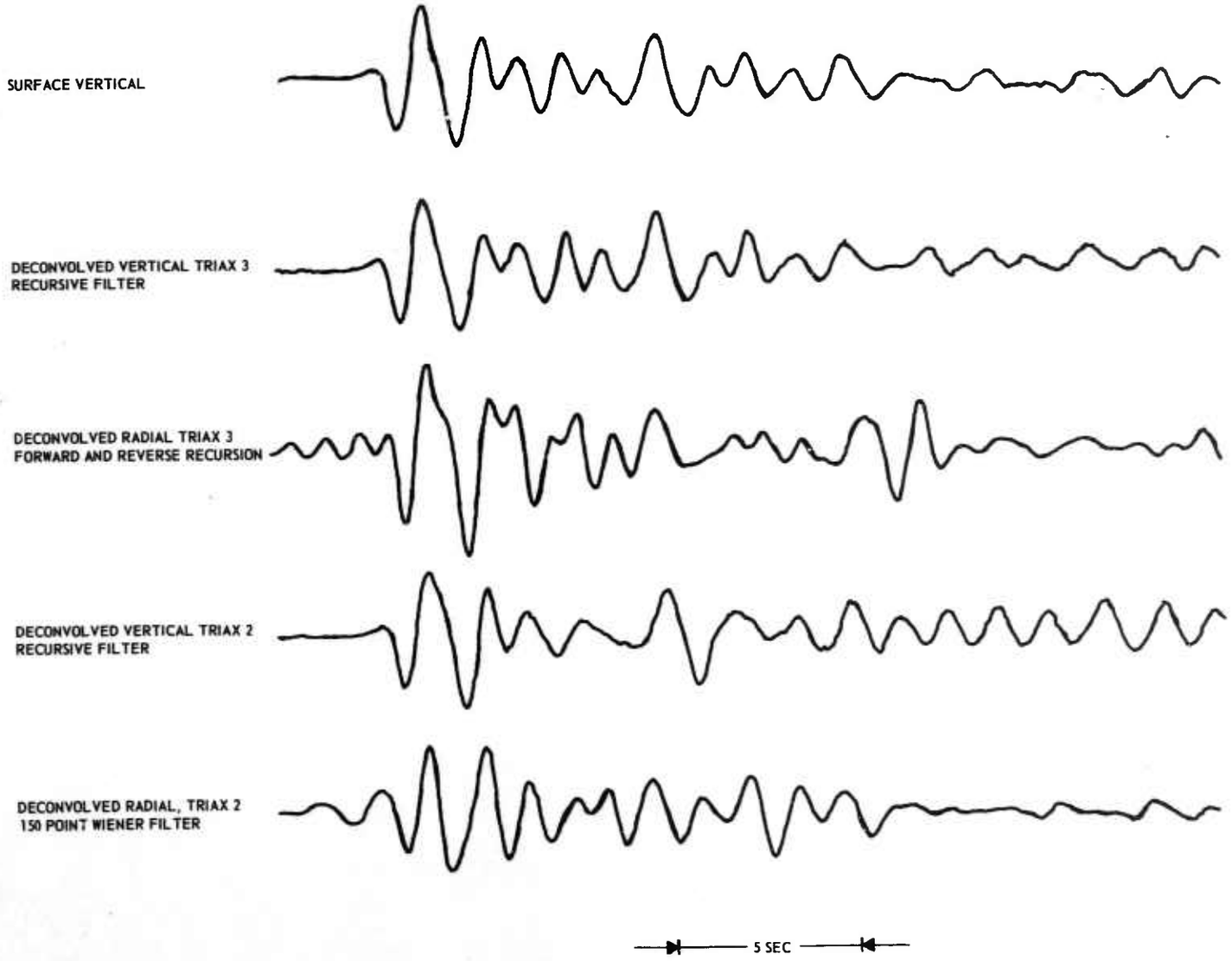

Figure 12. Deghosted deephole traces, Greeley event, APOK

G 3255

waves, single channel deghosting will amplify a considerable amount of noise. This is especially evident for horizontals where excessive ringing is the result of small deviations of waveforms from the theoretically assumed one (which can also be considered noise).

If, as in our case, several traces are available, multichannel deghosting seems to be a more attractive approach. It can avoid increasing the noise at certain frequencies by taking the contribution at that frequency from traces where the signal-to-noise (S/N) ratio is higher.

Figure 13 shows several multichannel deghosted traces for a Nicaragua event.[1] Multichannel deghosting filters proposed by the Project Officer also satisfy the above requirements.

The top trace shows the desired output which is the actual near surface vertical component. The next two traces are obtained by multichannel maximum likelihood filters. The bottom trace was obtained by Wiener filtering of the two deepest radial components. For the design of this filter, the incident P wave was considered signal and the reflected SV and P as noise. The filter was designed to reject SV and reflected P. The two noise components were assumed to be independent.

For maximum likelihood filters, there still seems to be some difficulty with the inverse filters on radials, although the filter no longer rings. The Wiener filters are not optimized with respect to deephole noise, while the maximum likelihood filters are.

3.2 ANALYSIS OF SEISMIC NOISE

In order to study the general character of noise at Grapevine, several noise samples have been analyzed. Power spectra and cross spectra were computed for various combinations of traces. For analysis of noise between 10 and 0.5 second periods, 3000 point samples were used; 128 lags were considered for the correlation functions. The length of these samples is 2.5 minutes. The horizontal components for these analyses were not oriented to the customary north and east directions, the component H1 is oriented south-southeast, H2 west-southwest, but this does not affect the analysis.

Figure 14 shows the noise power spectra computed for all of the triaxial components. Inspection of these plots shows that the horizontal noise spectra are quite different from the vertical spectra, which is to be expected. The spectra on the two perpendicular horizontals are very similar. The surface is very noisy on verticals and horizontals as compared to instruments located at deeper levels. Surface noise power around 0.5 sec is as much as 40 dB above the noise power level at the maximum depth of the array. The high surface noise level is partially due to local geology, near surface low velocity layer which

---

[1]Recorded on 2 October 1967 (location 11.7 N latitude, 86.8 W longitude, origin time 15 h 59 m 43.4 s, h = 39 km USGS)

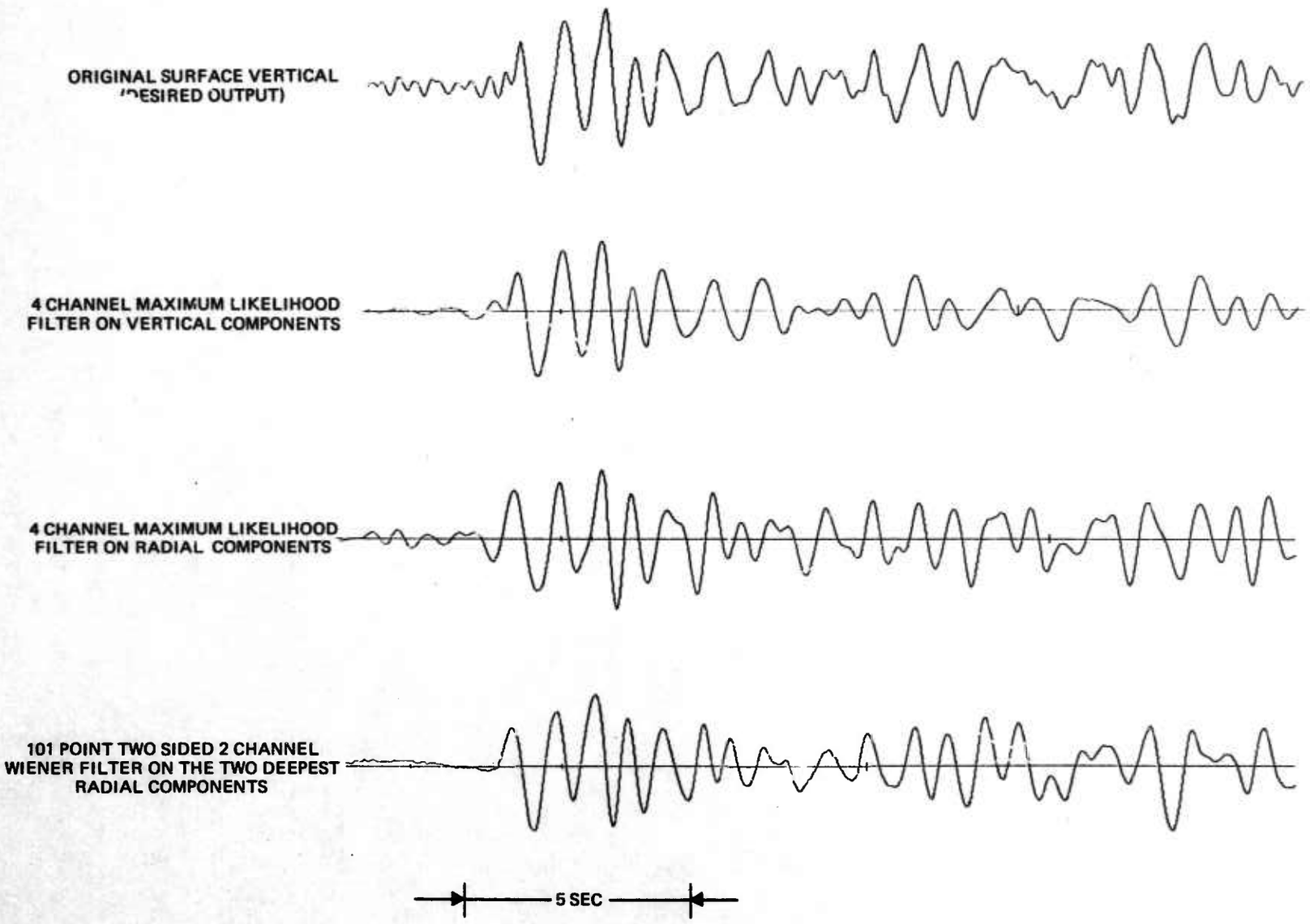

Figure 13. Multichannel deghosted deephole traces

G 3761

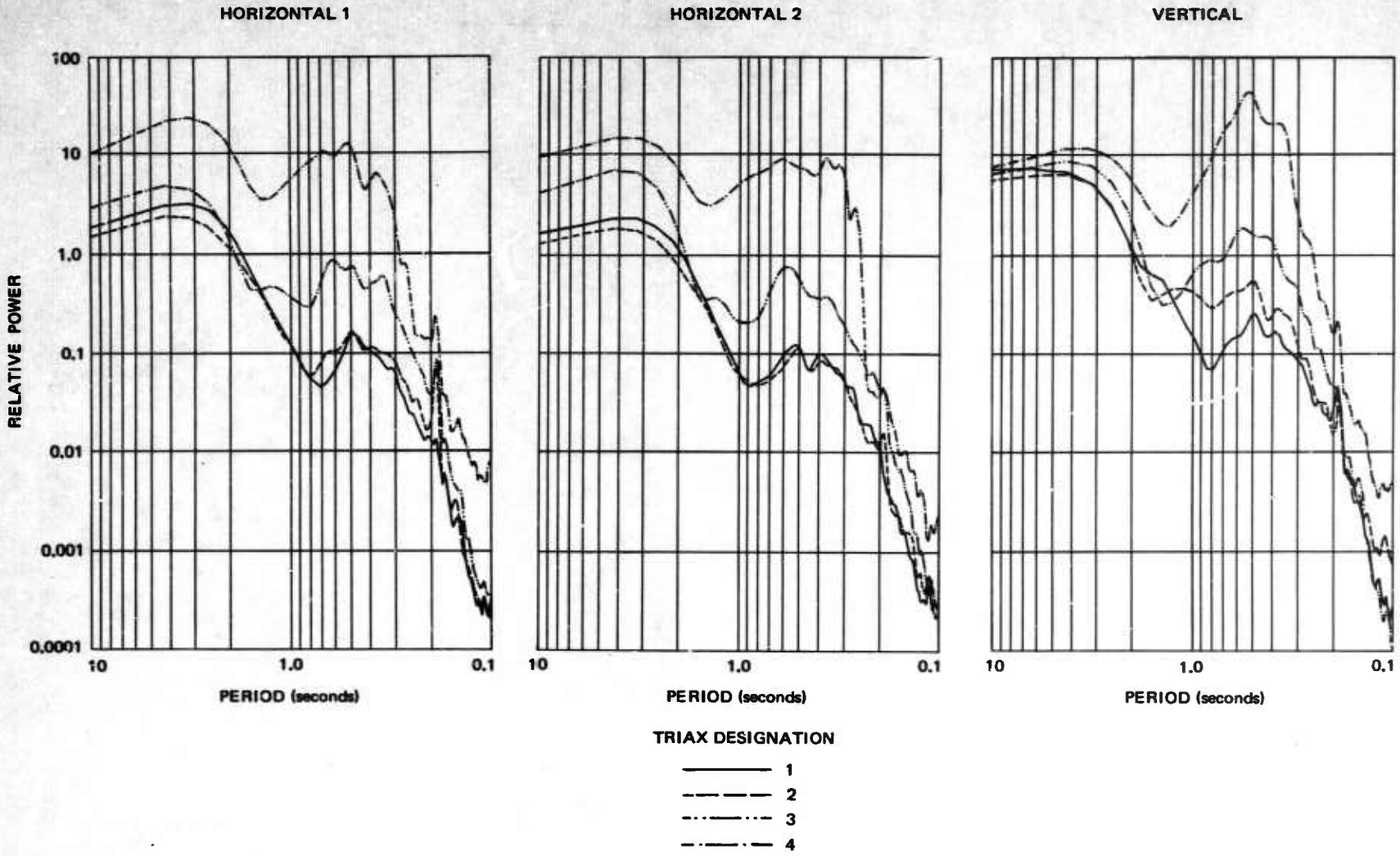

Figure 14. Triax array noise power spectra

facilitates the channeling of seismic energy close to the surface, and partially to the proximity of Dallas which is a source of cultural noise.

This noise sample showed very little directionality; the coherence between perpendicular components of motion was found to be very low.

The coherences between parallel components of motion at various depths were very low below 1 second period while between 1 and 10 second period higher coherence values were found.

A set of multiple coherences were computed for three sets of outputs; all of the H1, H2, and vertical components. Multiple coherence is defined by Bendat and Piersol, 1966, as

$$C_i^2(f) = 1 - [G_i(f)G^i(f)]$$

where $G_i(f)$ is the i-th diagonal element of the spectral matrix G of inputs to be analyzed and $G^i(f)$ is the corresponding element of the matrix G^{-1}.

If n inputs are being analyzed, n multiple coherences are obtained. C_i denotes the relative amount of power in the i-th input trace which can be obtained from the rest of the inputs by linear multichannel filtering. Its value is unity if the i-th input can be predicted entirely at the frequency specified for the rest of the inputs, and is zero if it cannot be obtained at all.

Multiple coherences are indicative of the number of independent noise processes present if all the inputs contain these processes, as in the case of a vertical array where the motion at each level can be considered a superposition of independent surface wave modes. Theoretically, if the number of processes is less than the number of inputs, the multiple coherence should be unity.

"Independent process" in the context of a vertical array may mean a mode with amplitude depth relationship which is significantly different from the rest of the components and is not correlated with them. Several modes with roughly the same depth behavior may behave as one single process. The values of multiple coherence depend also on the relative amplitudes of independent components. Multiple coherences, therefore, should be used with some caution in interpreting vertical array noise data. Low multiple coherences indicate that an excessive number of independent components (modes) contribute significantly to the observed inputs.

The squared multiple coherences computed are shown in figure 15. For the vertical components, the multiple coherences are high between periods of 1 to 10 seconds. Below the 1 second period, all of the curves decline steeply and remain at very low coherence values. The horizontal curves behave similarly, but they decrease fast at a longer period (1.5 second). The higher multiple coherences for verticals can be explained by the fact that only Rayleigh modes contribute to the vertical motion (a small number of independent components is present). Low values (below 1 second period) mean that linear filtering schemes are not very effective at these periods and the best array processing possible is some kind of weighted sum. These low values indicate that decomposition of noise into different modes is not possible at these periods. The only mode which can positively be identified below 1 second is the

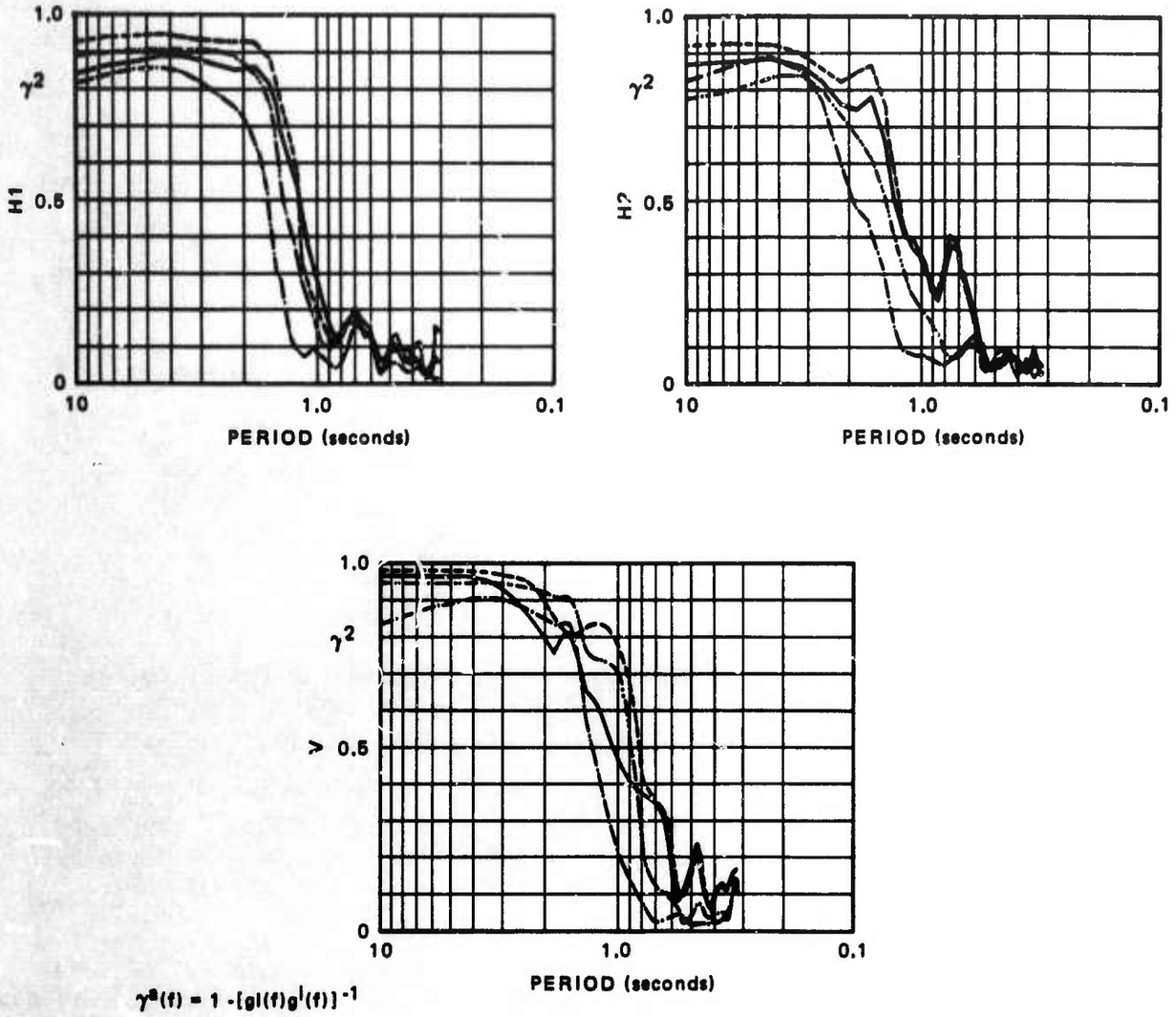

Figure 15. Multiple coherences of computer transformed horizontal and vertical channels of the four short-period triax seismographs at GVTX

G 3705

fundamental, causing high amplitudes on the near surface instruments.

In general, the lowest multiple coherences are obtained if the surface instruments are assumed as output. This is caused by the fundamental mode surface waves which decrease fast with depth and do not correlate with noise at the deepest levels.

Comparing the coherences below 1 second prior to theoretical coherences for P and S waves incident uniformly within a cone of 45 degrees aperture at the bottom of the array did not reveal any similarity. A previous study revealed such a similarity at Apache, Oklahoma, indicating the presence of mantle P waves in the noise (Douze, 1967). At Grapevine, this part of the short-period noise seems to be more complicated.

To obtain better estimates of noise spectra at periods higher than 1 second, the noise has been bandpass filtered and decimated by a factor of five. A 3600 point sample with time length of about 15 minutes was taken and a set of spectra was computed.

These spectra have a much higher resolution and they show the similarity between the two horizontal spectra and differences from the vertical. There is some directionality in the noise around the 6 second period showing that Rayleigh waves arrive predominantly from the northeasterly direction, presumably generated by storms located in the Newfoundland area.

To obtain some picture about the composition of the noise, the amplitude behavior of noise on the horizontal and vertical components has been compared to theoretical Rayleigh and Love wave amplitude-depth curves.

The velocity model used to compute the amplitude-depth curves for Grapevine, Texas, is given in table 2. For the long-period (2-10 sec) part of the computation, a rough crustal model was used which is a scaled down version of the model of Tryggvason and Qualls (1966). For computing the shorter period curves, the layered model is terminated by a halfspace. The added crustal section is not expected to influence the results decidedly.

There is some uncertainty in the amplitude depth curves since the geology below the array is not well known. The igneous basement rock is estimated to be about 1 km below the deepest seismometer. If no drastic changes occur in velocity, a few kilometers below the array, the curves are a reasonable approximation. The densities were assumed appropriate, considering the lithology. The S velocities are computed from the P velocities by assuming an average Poisson ratio $\sigma = 0.3$ and multiplying the P velocities by the appropriate constant factor

$$\sqrt{\frac{1 - 2\sigma}{2(1 - \sigma)}} \quad .$$

The P velocities were obtained from a velocity log.

In an attempt to interpret the noise data in terms of the first few Rayleigh and Love modes, several deephole to surface amplitude ratios have been plotted

Table 2. Velocity model for Grapevine, Texas, with surface taken as zero reference and the first layer 137 m thick, etc

Layer	Thickness (km)	P velocity km/sec	Density
1	0.137	2.43	2.0
2	0.061	2.75	2.0
3	0.081	3.50	2.3
4	0.053	2.88	2.0
5	0.137	3.50	2.3
6	0.173	3.04	2.0
7	0.091	3.35	2.0
8	0.137	3.50	2.3
9	0.259	3.65	2.3
10	0.563	3.97	2.3
11	0.122	4.27	2.6
12	0.365	4.60	2.6
13	0.107	4.74	2.6
14	0.076	4.27	2.6
15	0.061	3.82	2.6
16	0.122	4.60	2.6
17	0.045	5.50	2.8
18	0.015	4.27	2.6
19	0.030	5.80	2.8
20	0.152	4.12	2.6
21	0.076	6.10	2.8
22	0.137	5.50	2.8
23	0.030	5.80	2.8
24	0.106	6.40	2.8
Added crustal layers			
25	9.3	6.40	2.8
26	14.2	6.66	2.8
27	18.4	7.20	2.8
28	∞	8.30	3.3

Poisson ratio $\sigma = 0.3$

and compared to the corresponding theoretical amplitude depth curves. No attempt was made to indicate heavy modes or body waves in the interpretation, although they may be present.

The observed ratios of the deephole vertical to surface vertical and the average deephole vertical to surface vertical were superimposed on the plots of Rayleigh amplitude depth curves. The ratios of the averaged deephole horizontals to the averaged surface horizontals were superimposed on the Love wave amplitude-depth curves.

The averaged amplitude ratios for horizontals were obtained by averaging the horizontal power spectra, taking the appropriate ratio, and finally, taking the square root of the result. This method approximates the effect of complete isotropy in the noise. In plotting the ratios, the relative phase angles (0 degrees or 180 degrees) were also considered. Phase angles were only considered if the coherences between the respective components were relatively high (0.3 and up).

The theoretical horizontal amplitudes on the plot were reduced by a factor $1/\sqrt{2}$ relative to the ratios obtained from the Rayleigh wave program to simulate the effect of isotropy of noise.

Plotting the amplitudes with positive or negative signs is not entirely correct since both in phase and 180 degrees out of phase components may be present. The plots are, however, suitable for preliminary analysis. Figure 16 shows the plot obtained for the 6 second period. For this period, there is relatively little difference in the Rayleigh amplitude depth relationship on the vertical components; the horizontal ratios, however, differ considerably. The amplitude depth behavior of the first three Love modes is practically identical.

The observed vertical ratios are the closest to the curve for fundamental Rayleigh modes. The horizontal to surface vertical ratios are however, too high for isotropic Rayleigh waves only. The observations can be explained by the presence of fundamental Rayleigh waves mixed with indifferentiated Love modes. Accuracy of the data does not permit us to say whether any higher mode Rayleigh waves are present in the noise.

Figure 17 depicts a similar plot for the noise at the 4 second period. The picture resembles the previous illustration, but the vertical ratios are closer to the first higher mode curve. The fundamental Love mode curve begins to separate from the next three higher modes. The observations can be explained here by the presence of first higher mode Rayleigh waves mixed with (preferably higher) Love modes.

Figure 18 shows the amplitude ratio plot for noise at the period of 3 seconds. The vertical ratios on this figure follow the first higher Rayleigh mode fairly closely. The horizontal ratios behave quite differently; the average phase between the deepest and the rest of the seismometers is approximately 180 degrees and the horizontal amplitudes are again too large. The curve for the horizontal ratios is not smooth, an error resulting probably from the fact that both in phase and 180 degrees out of phase components are present between the bottom of the hole and the near surface seismometer.

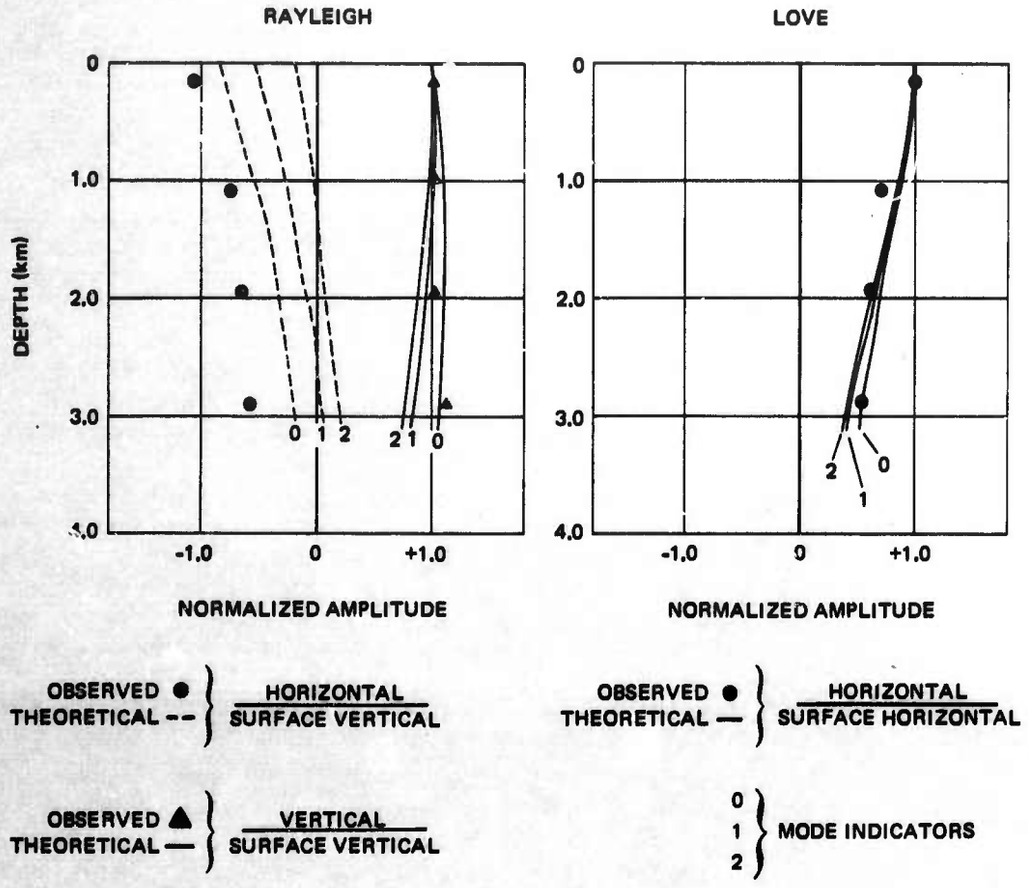

Figure 16. Observed and theoretical amplitude ratios for noise at GVTX, T = 6.0 sec

G 3706

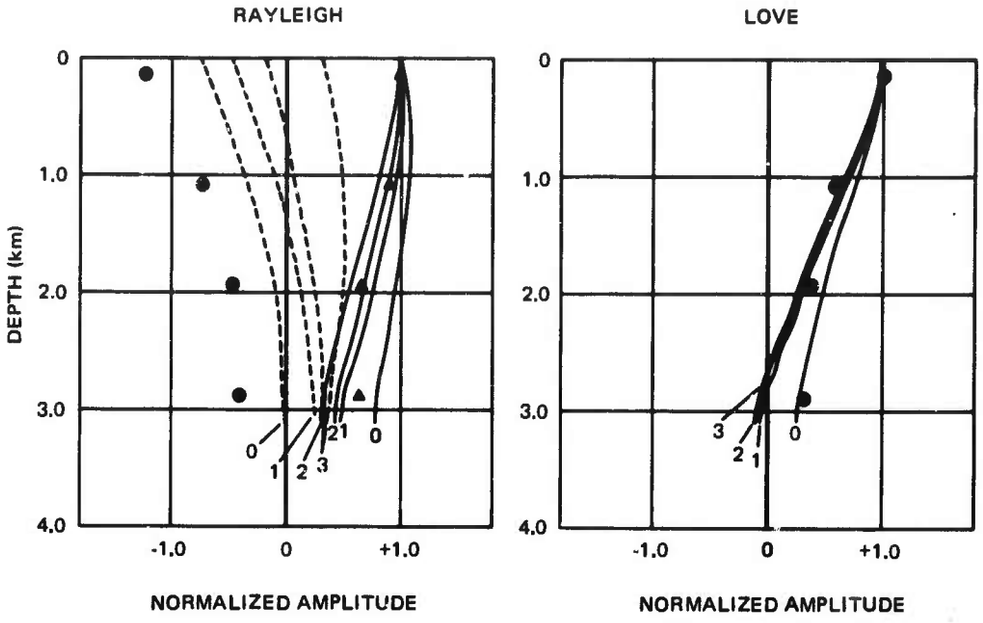

Figure 17. Observed and theoretical amplitude ratios for noise at GVTX, T = 4.0 sec

G 3707

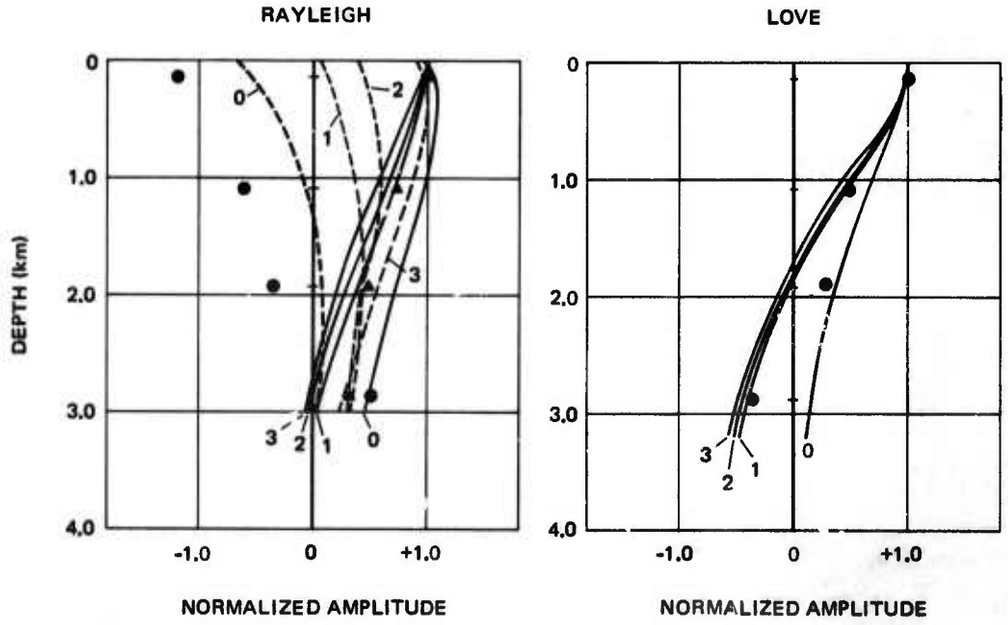

Figure 18. Observed and theoretical amplitude ratios for noise at GVTX, T = 3.0 sec

G 4179

The dominant modes on horizontals are probably the higher Love modes with a smooth amplitude depth curve which can be obtained by shifting the points slightly as indicated on the figure.

Figure 19 shows a similar situation for a 2 second period. Some Rayleigh modes at this period have a large horizontal amplitude and may be contributing to the noise.

For the noise at 1 second periods, the only modes which can be identified with some confidence are the fundamental Love and Rayleigh and this is illustrated in figure 20. Coherences between levels are low and the phase angle is uncertain.

3.3 DEVELOPMENT OF PROCESSORS

Work has been done on two types of processors for the short-period triaxial array. Each is explained in some detail below.

a. A REMODE type processor was developed that tests the character of spectral ratios inside a time window on all deephole traces. This processor chooses one trace as a reference and spectral ratios are computed between the references and each of the other deephole traces. The number obtained constitutes a complex vector $\vec{A}$. The normalized complex "dot" product of vector $\vec{A}$ and the theoretical amplitude ratio for incident waves, vector $\vec{B}$ results in factors:

$$\alpha(f) = \sqrt{\frac{|\vec{A} \cdot \vec{B}|}{|\vec{A}| \cdot |\vec{B}|}}$$

These factors can be used as a measure of the similarity of the motion to P motion at each frequency. The factors are used to weight the Fourier components of the reference trace. The weighted spectra are transformed point by point back to the time domain and added together continuously as the window moves along the traces.

The method was applied to the verticals 1, 2, and 3 with radial 1 as reference; however, other combinations of vertical and horizontal traces can also be used. The output traces show some signal-to-noise improvement, especially at the shorter periods (figure 21) but it is minor. It seems that at the longer periods, the signal and noise is very similar (the deephole array moves as a single unit) and the parameters are not sensitive enough for improving the signal-to-noise ratio. Redefinition of the parameter α can probably improve the method.

Due to the contract schedule and the slowness of this processing scheme, the work on processors based on similar principles was not investigated further.

b. A maximum likelihood-REMODE processor is the second data processor developed. Since similarly oriented components show fairly high coherency between various levels, it is conceivable that linear processors will offer some improvement over straight summing. Even if the coherence is low, linear processors can give an optimum way of summing (optimum weighting) and

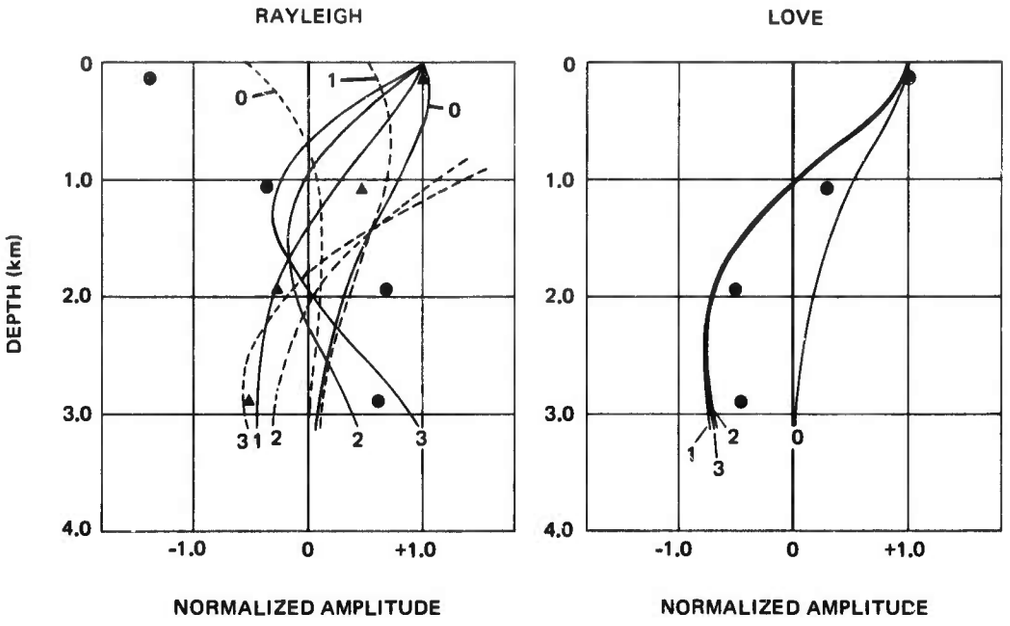

Figure 19. Observed and theoretical amplitude ratios for noise at GVTX, T = 2.0 sec

G 3708

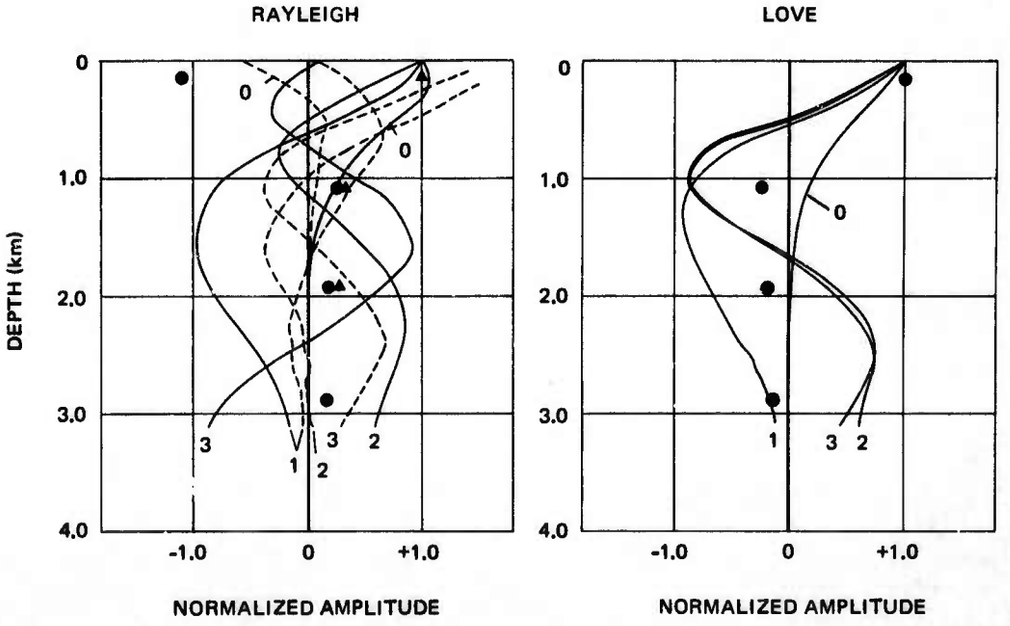

Figure 20. Observed and theoretical amplitude ratios for noise at GVTX, T = 1.0 sec

G 3709

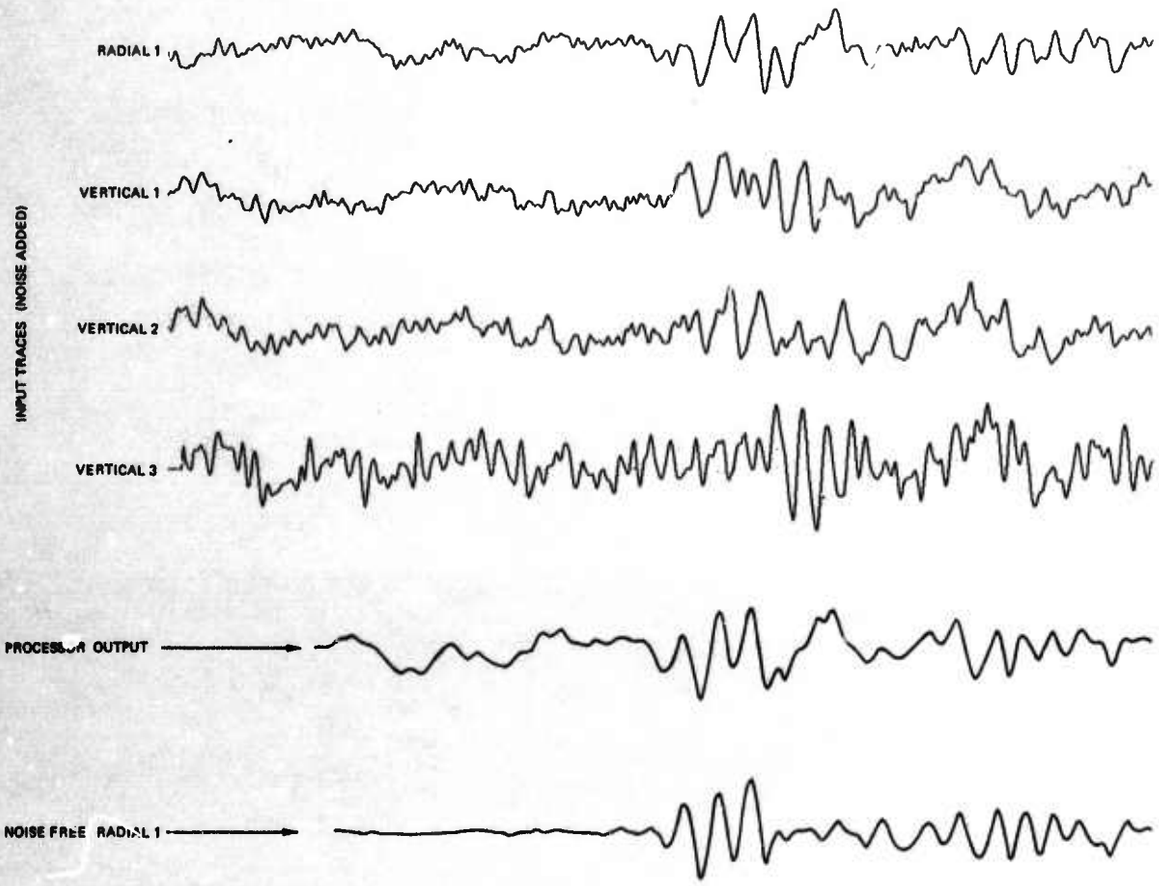

Figure 21. Remode type processing

G 3699

deghosting the traces. A REMODE type processor can then be used to accentuate linear motion on the deghosted, optimum summed traces that were derived from the group of radials and the group of verticals. Deghosting is necessary to make the motion linear and the REMODE process is expected to enhance rectilinear motion since the noise between the horizontal and vertical traces was found to be incoherent. The maximum likelihood filters applied here are influenced by the fact that the signal shape is not identical on all traces.

The problem can be formulated in the frequency domain as follows: It is desired to minimize the noise output power P of the filters F,

where F is a multichannel filter (complex row vector),

$$P = FP_N F^{*\prime} \tag{1}$$

and P_N is the noise power spectral matrix. The asterisk denotes complex conjugates and the prime denotes transpose.

The filters are subject to the condition,

$$FG' = 1 \tag{2}$$

where G is a complex vector denoting the response of "ghosting" filters. The condition is equivalent to stating that we want to have a deghosted waveform passed by the filters.

Transposing condition (2) and taking the complex conjugate, one obtains

$$G^*F^{*\prime} = 1$$

We want to minimize the quantity

$$FP_N F^{*\prime} + \Lambda G^* F^{*\prime} \text{ where } \Lambda \text{ is a Lagrange multiplier.}$$

Differentiating with respect to $F^{*\prime}$ leads to the equation

$$FP_N + \bar{\Lambda}\, G^* = 0 \quad \bar{\Lambda} = \Lambda/2$$

multiplying this on the right with P_N^{-1} and rearranging one obtains

$$F = -\bar{\Lambda} G^* P_N^{-1}$$

substituting into condition (2)

$$FG' = -\bar{\Lambda} G^* P_N^{-1} G' = 1$$

rearranging, one obtains

$$\bar{\Lambda} = \frac{-1}{G^* P_N^{-1} G'}$$

substituting, one arrives at the final result

$$F = \frac{G^* P_N^{-1}}{G^* P_N^{-1} G'} \qquad (3)$$

Equation (3) reduces to the form given by Capon and Greenfield (1965) if the components of G are unity (signal waveform is identical on all traces). This formula was used to determine the spectral response of the maximum likelihood filters.

The multichannel filters were applied to two groups of traces, one consisting of all radial, the other of all vertical components. For the verticals, the ghosting filters were assumed here to be the simple (no phase shift) amplitude response of form $F(\omega) = 0.5 \cos \omega t$ where t is the uphole time delay. For designing the filters, the quad spectra were neglected in the noise spectra matrix. This is justified in general since these elements were found to be small compared to the elements in the real part of the spectral matrix.

These assumptions led to simple, no phase shift digital filters which perform well for a fairly wide range of the angle of incidence. The filtering has been performed in the time domain.

The precursors resulting from the use of two sided filters are found to be small. As an experiment, all cospectra were neglected for the design of some filters. This did not result in an appreciable deterioration of the performance of the filters indicating that the noise is essentially uncorrelated between the traces which are the most heavily weighted by the process in the frequency range of interest. The amplitude responses of the filters for vertical components are shown on figure 22. The figure shows that for long periods, all traces contribute to the output; at short periods, the contributions from the near surface traces are negligible due to the relatively high near surface noise. The surface vertical could be easily eliminated from the processing scheme.

The ghosting filter responses for horizontal components were found by the use of Haskell's method. The upward curvature of the raypath at Grapevine is due to the near surface velocity decrease. The horizontal signal-to-noise ratio is considerably lower on the two instruments nearest to the surface.

The filters resulting from the computation have a phase shift and the time domain representatives are no longer symmetric. The amplitude responses of the filters for horizontals are shown on figure 23.

Figure 24 shows the result of the application of these filters to an event in Nicaragua. The noise sample used in the design of filters was amplified and added to the event to create a synthetic noisy record. The groups of vertical and radial components have been processed using the maximum likelihood filters. The resulting two traces are shown in figure 24. Also shown in this figure are the results of processing the Nicaragua event with noise added to the input artificially and the final step is a simple motion product processor of the Shimshoni-Smith type.

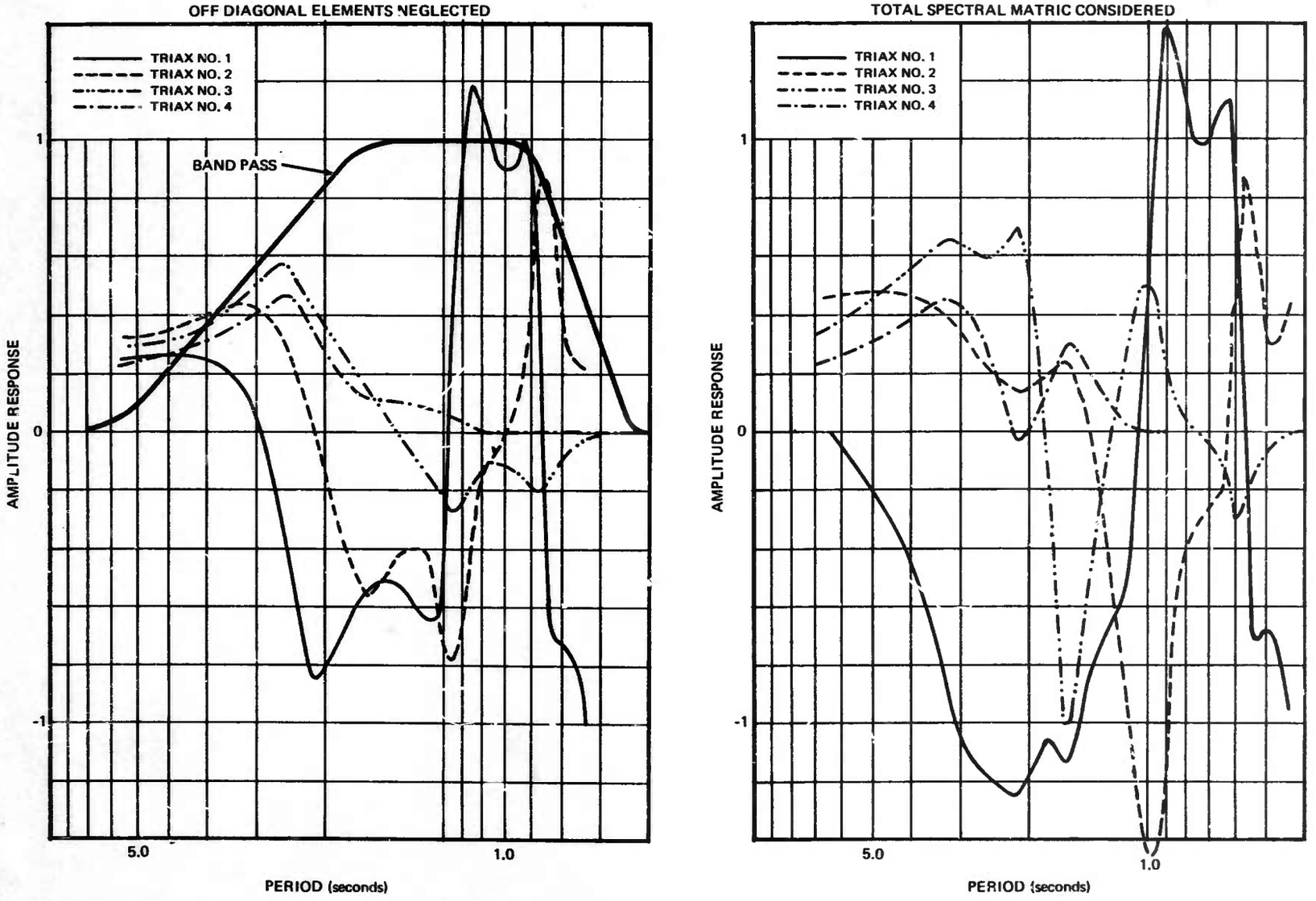

Figure 22. Multichannel deghosting filter amplitude response -- vertical components

G 3700

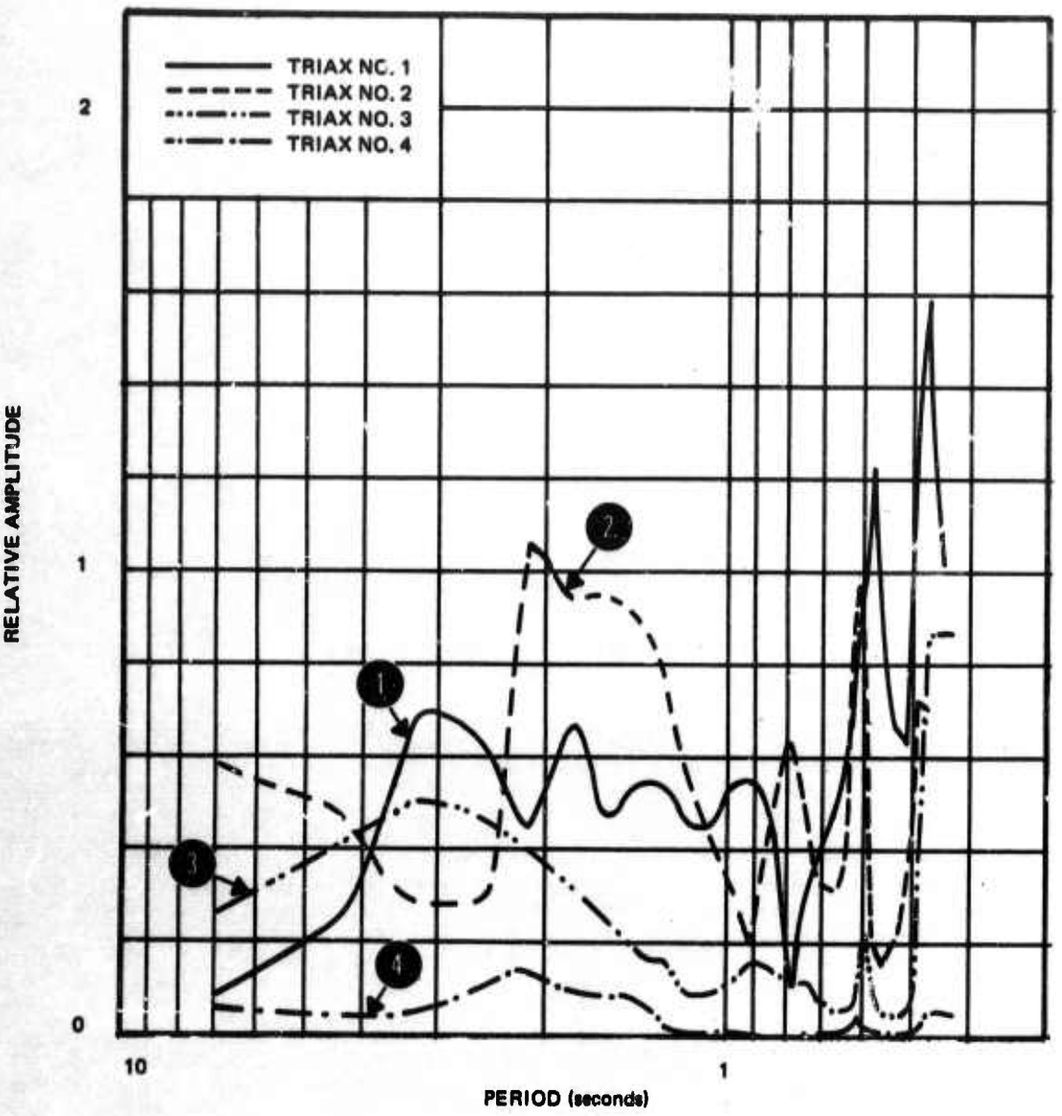

Figure 23. Amplitude response of maximum likelihood filters on radial (angle of incidence = 34 degrees)

G 4185

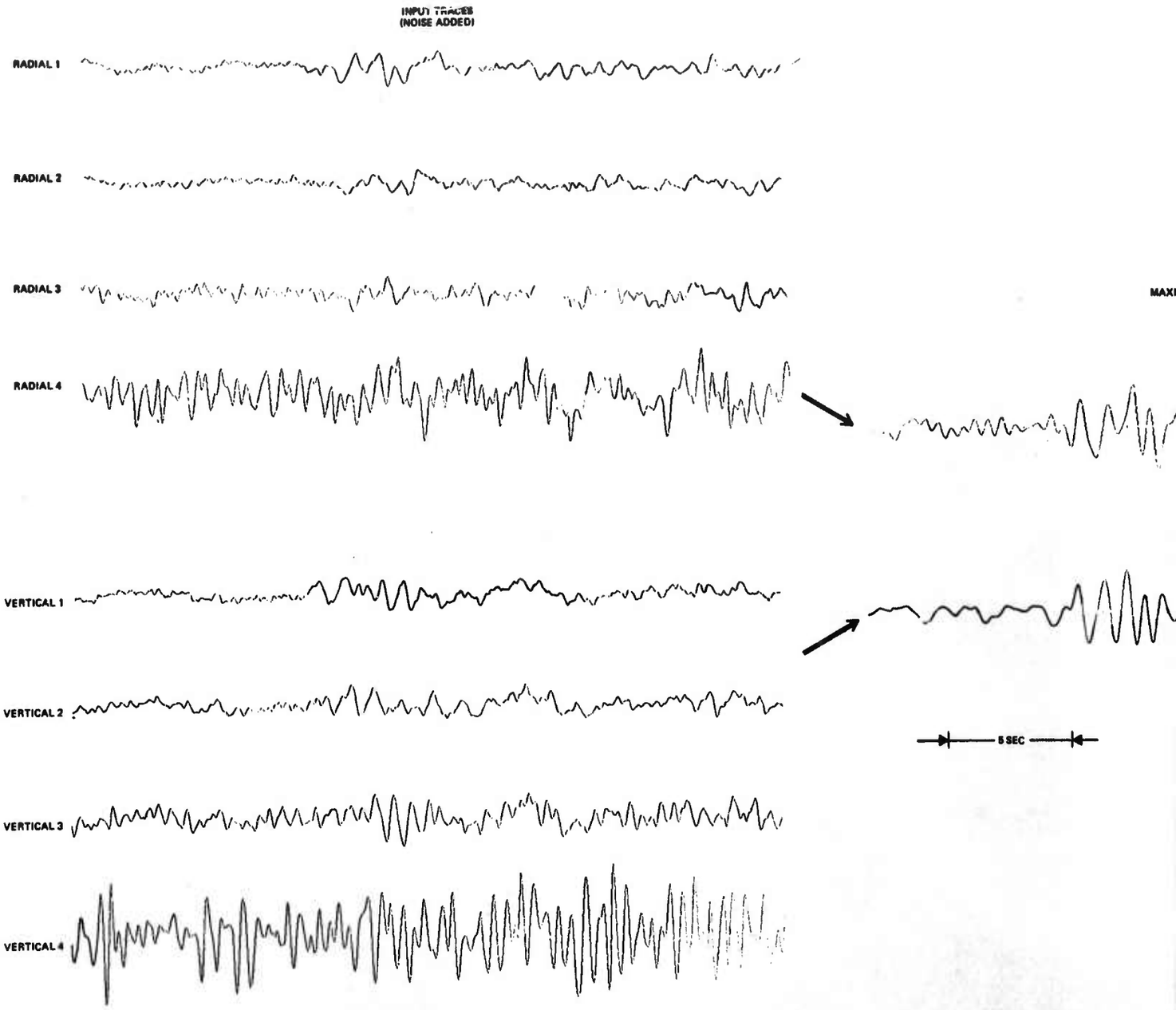
INPUT TRACES
(NOISE ADDED)
RADIAL 1
RADIAL 2
RADIAL 3
RADIAL 4
VERTICAL 1
VERTICAL 2
VERTICAL 3
VERTICAL 4
MAXI
5 SEC

A

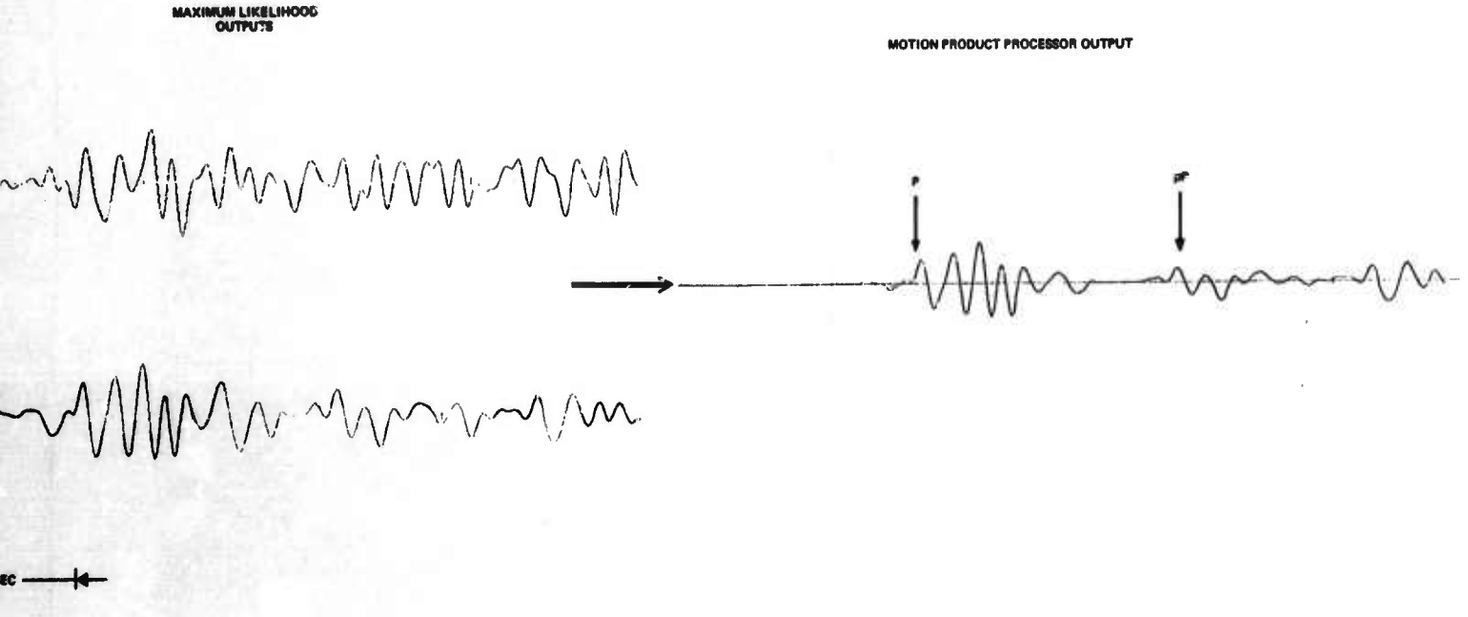

Figure 24. Maximum likelihood - motion product processing Nicaragua event

G 3762

The gain factor, (essentially a correlation coefficient)

$$f\left(\frac{t_1 + t_2}{2}\right) = \frac{\int_{t_1}^{t_2} v(t) \cdot r(t) \cdot dt}{\sqrt{\left(\int_{t_1}^{t_2} v^2(t)\, dt\right)\left(\int_{t_1}^{t_2} r^2(t)\, dt\right)}} \text{ (positive only),}$$

operates on the maximum-likelihood filtered vertical output v(t) where, r(t) is the maximum likelihood radial output, and $t_2 - t_1$ is 2 seconds (length of the moving window). Negative values of f(t') are put equal to zero.

The output shows that the noise is essentially uncorrelated between the vertical and radial outputs (as was expected) and is eliminated quite well. A second arrival (likely pP) is considerably enhanced. These results look very promising, but because of the poor deghosting achieved on the horizontals, it will be desirable to process more events to better evaluate the method. The process is quite fast and is probably suitable for online processing.

4. PROCESSING OF VERTICAL ARRAY DATA

In this section of the report, a brief discussion is presented of all the filtering techniques that have been used with the vertical arrays of vertical seismographs. The triax seismograph discussed throughout this report may be treated as a vertical seismograph after summation of the three module outputs of a particular instrument. Therefore, the 12-element triax array may be summed to provide 4 vertical seismographs operating at four depths in the deephole. In order to obtain a coherent presentation, some portions include work done under previous contracts, e.g., the section on inverse filters.

Most of the time was employed in trying techniques based on least-mean-square filtering. In general, it can be concluded that because of the lack of stationarity of the noise, these filters degrade too rapidly to be of practical interest for online processing.

When the inadequacy of optimum filtering became apparent, several non-optimum filtering techniques such as velocity filtering were tried. In general, these non-optimum techniques were as effective as the optimum filters.

4.1 INVERSE FILTERS

One of the main differences between array processing of deephole and surface arrays is that in surface arrays, the signal recorded by each seismometer is usually assumed to be identical with only a time delay introduced by the apparent surface velocity. The signal recorded at different depth changes from that recorded at the surface because of the interfering reflections from the free surface and velocity interfaces. Two general approaches can be employed: (a) the use of processes such as optimum Wiener filtering with assumptions about the spectrum of signals, in which case the signals do not need to be changed, (Burg, 1964) or (b) processes such as maximum likelihood filters or the techniques discussed later in this report in which case the signals must be inverse filtered. We shall call the filters that change a signal recorded at one depth to the signal at some other depth inverse filters. The simplest approach to inverse filtering is to filter the deephole signals in such a way as to make them look like the surface (deghosting filters); however, it is also possible to change the signal from any depth into the signal that would be recorded at another depth (ghosting filters). Throughout the present work, the filters are designed so that all signals are normalized to the surface amplitude. The filters are designed to operate on signals from teleseismic distances between 60 and 90 deg.

The filters can be expressed as rational functions of z, where the z transform (Jury, 1964) method is employed.

$$F(z) = \frac{A(z)}{B(z)} = \frac{a_0 + a_1 z^{-1} + a_2 z^{-2} + \ldots + a_n z^{-n}}{b_0 + b_1 z^{-1} + b_2 z^{-2} + \ldots + b_m z^{-m}}$$

By rewriting the formula as $B(z) \cdot F(z) = A(z)$, it is apparent that F(z) is the filter that changes the time series B(z) into the time series A(z). In terms of inverse filtering as applied to deephole signals, the filter should change the signal recorded at one depth to that recorded at another depth. The time series A(z) and B(z) are the response that would be recorded at the different depths if the incoming signal were a unit impulse; that is, the impulse response of the layered half space taken as a model of the section penetrated by the hole.

F(z) can be expanded by long division into a simple polynomial:

$$\frac{A(z)}{B(z)} = f_0 + f_1 z^{-1} + f_2 z^{-2} + \ldots + f_k z^{-k} + \ldots .$$

In general, the expansion of F(z) will result in an infinite series. In the filters used in this work, the deephole inverse filters are stable and the coefficients converge to zero. They converge slowly because of the large reflection coefficient at the free surface. The series actually used was truncated to a length of 125 points and a cosine taper was applied to smooth the results. Instead of obtaining an inverse filter by long division and truncation, we also designed a one-channel optimum Wiener filter on the same length. The difference in the results was negligible; therefore, the long division process was employed.

In order to obtain shorter filters that would function more effectively in online processing, it was decided to use recursive filters (Shanks, 1967). Consider the following filter, where X(z) is the input and Y(z) is the output:

$$Y(z) = \frac{a_0 + a_1 z^{-1} + a_2 z^{-2} + \ldots + a_n z^{-n}}{1 + b_1 z^{-1} + b_2 z^{-2} + \ldots + b_m z^{-m}}$$

where b_0 can always be made equal to 1 (unless it is zero) by dividing numerator and denominator by b_0. By rearranging the formula can be changed into:

$$Y(z) = (a_0 + a_1 z^{-1} + \ldots a_n z^{-n}) X(z)$$
$$-z^{-1} Y(z)(b_1 + b_2 z^{-1} + \ldots b_m z^{-m+1})$$

The output Y(z) is thus equal to the input multiplied by A(z) minus the output delayed one sample interval and multiplied by B(z). In processing where the deephole signals are usually filtered to approximate the surface signals, it is possible to go one step further and design a filter that uses only the present input and past outputs. This approach is possible in the present case because A(z), the impulse response of the medium at the surface, consists of one large impulse and some very minor reverberations. The incoming pulse as recorded by the deepest seismometer is taken as the reference in this example. The desired filter is:

$$F(z) = \frac{A(z)}{B(z)} \approx \frac{1}{C(z)}$$

C(z) can be obtained by synthetic division of B(z) by A(z). Because of the nature of A(z), the result is very nearly B(z) and the length of the filter has not increased because the values at lags greater than m [the length of B(z)] are extremely small and can be neglected. Thus, the feedback filter presently being used is:

$$Y(z) = X(z) - z^{-1}Y(z)\ (b_1 + b_2 z^{-1} + \ldots + b_m z^{-m+1}).$$

It must be noted that the recursive filter is an exact inverse filter and not an approximation like the tapered inverse filter discussed previously. Figure 25 b, c, and d shows the same signal inverse filtered by the ghosting and deghosting techniques with the long inverse filters discussed first.

Because of recent innovations in the methods of the Fourier transform, it is also feasible to do the inverse filtering in the frequency domain. Cooley and Tukey (1965) have published an algorithm which allows very fast computation of the Fourier transform.

The Fourier transform of the desired inverse filter is calculated by transforming the untapered inverse filter using a large number of values obtained by synthetic division. This approach gives a third method of inverse filtering online; but, it is not expected to be more efficient for online processing than the recursive filter. However, if more than one filtering operation has to be done, such as bandpass and inverse filtering or optimum and inverse filtering, they can generally be done faster by operating in the frequency domain. The

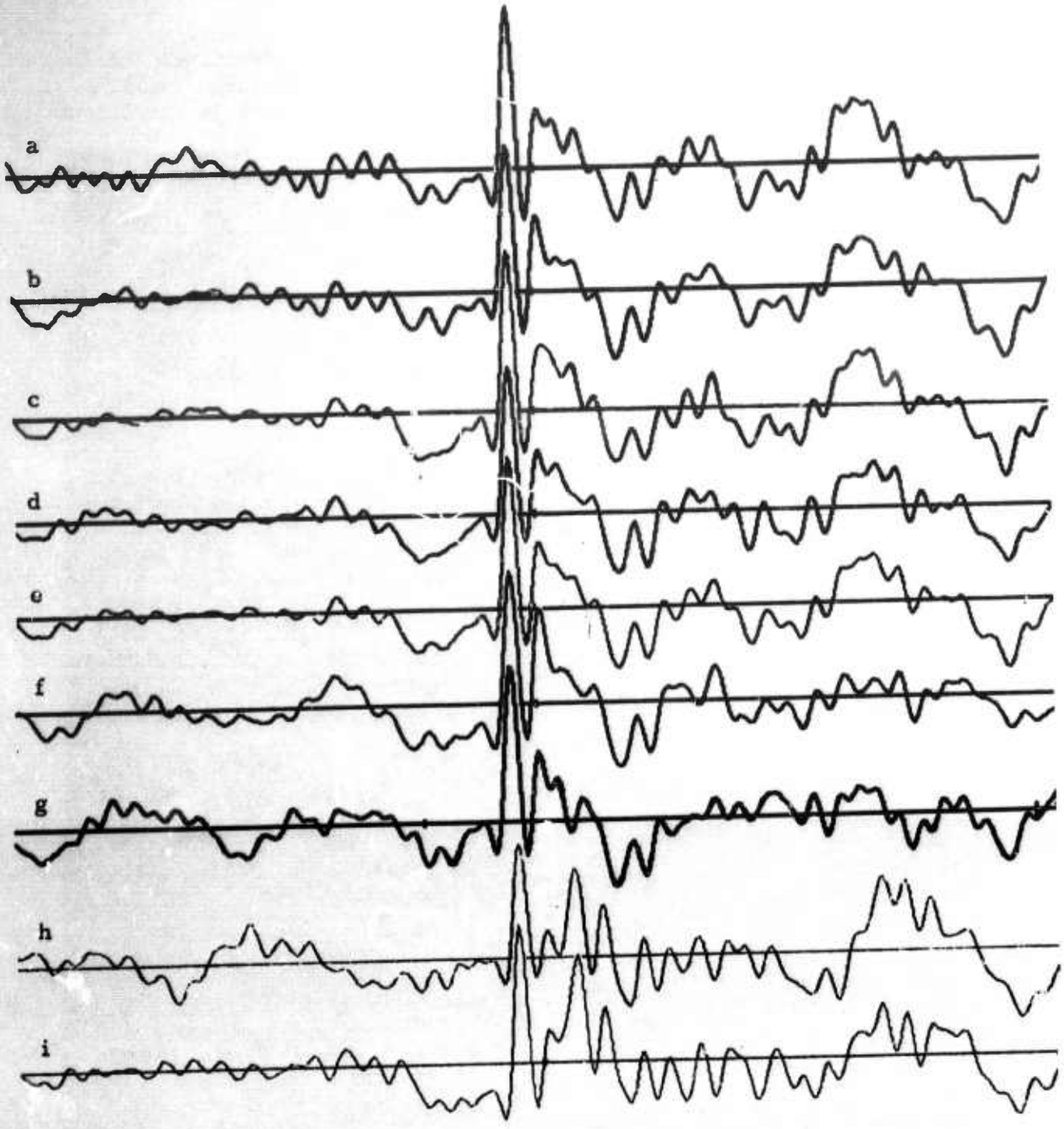

Figure 25. Teleseismic signal operated on by techniques used to increase the signal-to-noise ratio a, surface; b, c, d, single-channel deghosting processes operating on DH3 (1060 m), DH2 (1980 m), and DH1 (2880 m); e, normalized sum of b, c, d; f, g, multi-channel deghosting processes with one- and two-sided optimum filters; h, DH1 unfiltered, i/ single-channel ghosting process

G 2241

transform method essentially computes a Fourier series; therefore, some care must be employed in using the method for filtering. Convolutions as usually computed, assume the time series to be zero outside the region of interest. The new method assumes the input to be periodic with a period equal to the length of the record. When multiplying in the frequency domain, the periodicity implies that elements shifted past the end of the time series appear again at the beginning (personal communication, McCowan). This problem can be avoided by adding a number of zeros to the end, equal to the number of filter points in the time domain. When this is done, no end effects are present and frequency domain filtering will result in a smooth time series with no discontinuities at the points where the time series divided and transformed into the frequency domain and back. It is, of course, possible to compute the inverse filters in the frequency domain. However, the computer program used allows specifications of the filter in either the time domain or frequency domain and adds the correct number of zeros or the number of zeros needed if the filter is defined in the frequency domain. In the frequency domain, the number of frequency points must be equal for filter and data; thus, a large number of zeros are usually added to the time domain filter to make the length of filter and data equal. Inverse filtering in the frequency domain resulted in a deghosted signal identical to that shown in figure 25 b, c, and d.

4.2 OPTIMUM FILTERING

Two methods of optimum filtering have been tried. In the first, the signals are equalized at all depths by the use of inverse filters and the signals were eliminated by subtraction; optimum filters operating only on the noise were then computed. The second approach used consists of standard optimum least-mean-square filters in which assumptions about the signal must be made. Discussion of optimum filtering in this report will be confined to Wiener least-mean-square technique discussed by Burg (1964).

4.2.1 Deghosting Optimum Filters

The processes used are shown in figure 26. These processes are logical extensions of a technique discussed briefly by Bendat (1958). It must be noted that the inverse filters must be quite exact for the process to operate correctly. It was expected that for large signals, small errors in the inverse filters would result in the subtraction shown in figure 26 not being exact and errors would be introduced. This phenomenon is unavoidable when a range of distances and angles of incidence are covered by a single set of inverse filters. However, large signals with a good signal-to-noise ratio are of little interest in array processing because all the necessary parameters can be measured from a single seismograph. As will be shown later in the discussion, the inverse filters are sufficiently exact to allow the process to operate correctly.

These processing schemes are based on the concept that elimination of the assumptions made about the signal in conventional optimum filtering would result in a more effective processor. Figure 26 shows the filtering technique used in the first attempts to improve the detection capability of the site. As shown by the schematic, the signals are first equalized by the inverse filters discussed in the previous section. After inverse filtering, each

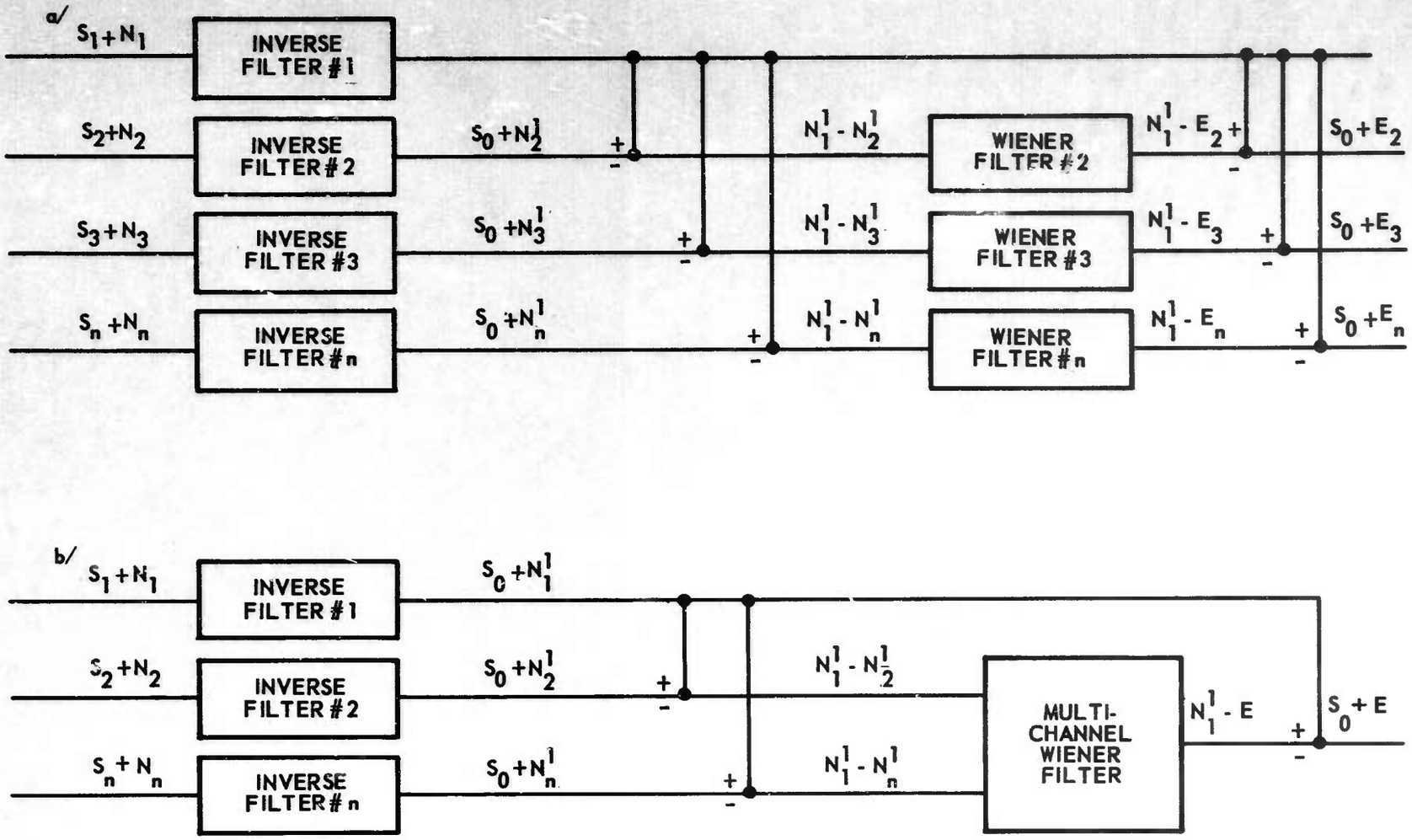

Figure 26. Deephole data processing techniques

G 543A

deephole channel is subtracted from the reference channel to produce a trace that consists of noise only. Although the surface channel has been used as a reference channel throughout the present analysis, any channel can be used as a reference. In fact, at sites where there is an appreciable increase of signal-to-noise ratio with depth (which is not the case at APOK), the surface must not be used as a reference because it would introduce excessive noise into the process.

An optimum filter was then constructed where the desired signal is the noise at the surface and the actual noise recorded in the deephole is to be suppressed. It must be noted the usual assumption that desired signal (surface noise) and noise are uncorrelated is not correct; the optimum filters are designed from actual data (including correlation of signal and noise) and no assumptions about the signal are made. The optimum filter output is then subtracted from the surface to obtain the desired signal (surface noise). The process can use either multi- or single-channel optimum filters. Both the inverse filters and optimum filters are operating correctly as shown in figure 25. The shape of the signals (for 25b through 25g) is identical to that recorded by the surface seismograph. It must be noted that this sharp signal constitutes a severe test for the inverse filters (recursive).

Figure 27 shows the decrease of the noise level obtained by some of these processes. The single-channel filters are all one-sided filters using only past data because experimental comparisons indicated that no further improvement is obtained by two-sided filters in this situation.

The filter length employed was 71 points, corresponding to 3.5 sec of real time. In comparing the three single-channel outputs, it is apparent that the noise level was only reduced by a small amount except at 0.5 sec. The reason for this behavior is probably that the amplitude-depth relationships of signal and noise are almost identical. The peak at 3.0 sec period was not reduced appreciably by any of the filters mainly because the filter length was not sufficient; however, as these waves are not at the periods where teleseisms are usually detected, no attempt was made to improve the performance.

The 2 Hz peak shown on all spectra is one main obstacle to visual detection at the APOK site. Comparison of the results of the single-channel cases indicate that deephole 1 (2880 m) was the most effective and reduced the power in the 2 Hz peak by 12 dB. The single channel process operating on deephole 3 (1060 m) did not reduce the power while deephole 2 (1980 m) achieved a reduction of 5 dB. Therefore, a single-channel optimum filter operating on the bottom seismograph is the best processor for this technique.

Figure 27 also shows the results of using a single-channel ghosting technique, in which case, all the recordings were filtered to simulate deephole 1 before subtraction. For reasons that are not understood at present, the results are inferior to the single-channel deghosting filter technique if the attenuation of the spectral peak at 2 Hz is used as the criteria. At 0.5 Hz, the ghosting technique resulted in a greater attenuation of the noise. The process is working correctly as indicated in figure 25 in which deephole 1 (unfiltered) and the final output of the process are shown.

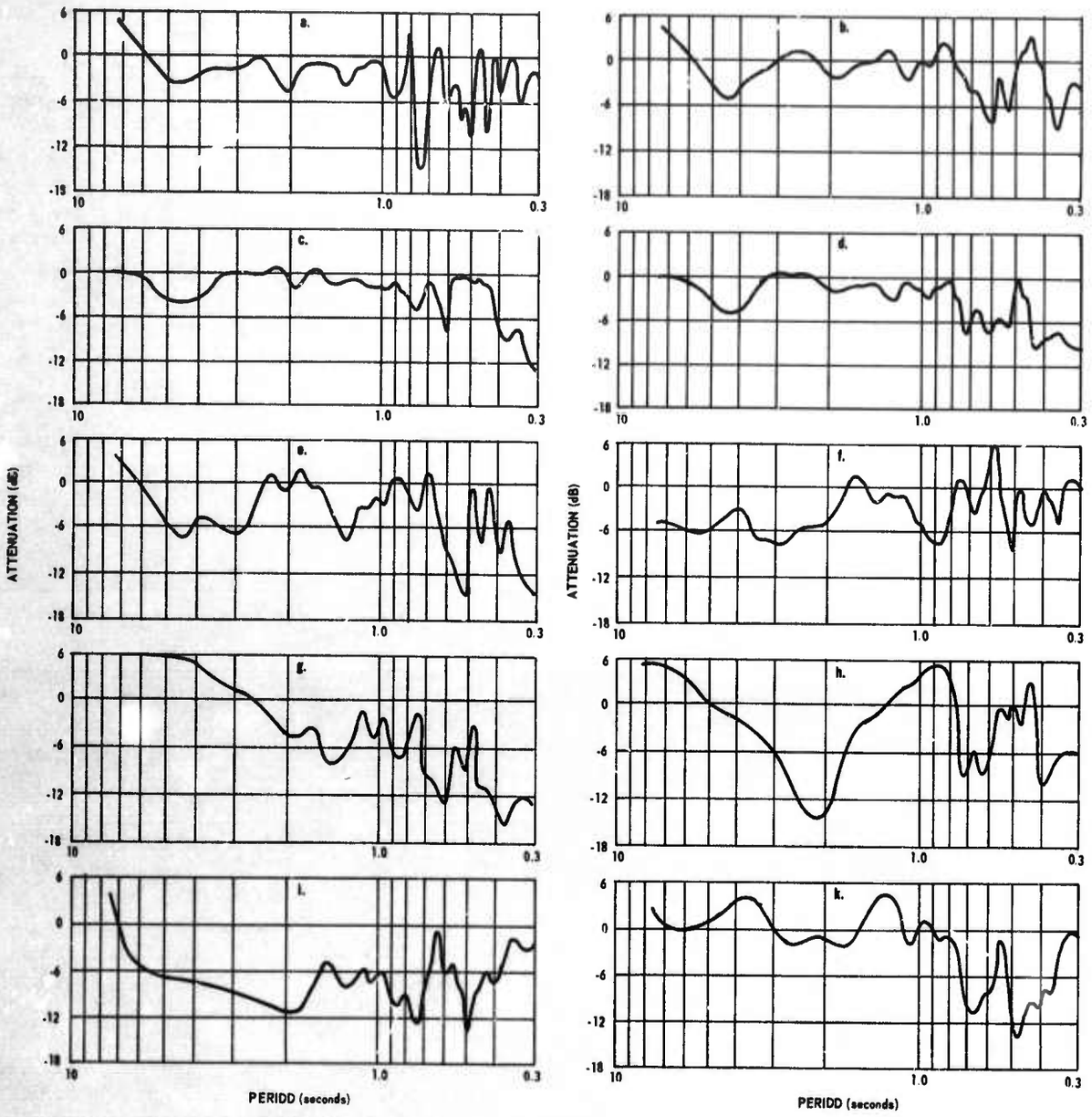

Figure 27. Attenuation obtained from optimum techniques: a/ single-channel deghosting (2880 m) b/ single-channel deghosting (1980 m) c/ single-channel deghosting (1060 m) d/ sum of single-channels e/ one-sided multi-channel deghosting f/ two-sided multi-channel deghosting g/ sum of deghosted channels h/ single-channels ghosting (2880 m) i/ 2-channel optimum filter, k/ 4-channel optimum filter

G 4186

A two-channel Wiener optimum filter set for GVTX was computed using the technique in which the signals are eliminated by subtracting the inverse filtered traces. DH1 was used as a reference and the surface seismograph was not used. Only slight attenuation in the noise was obtained when the filters were applied to the noise from which they were calculated. When operating on noise samples several days later, no attenuation of the noise was obtained. It is of interest to note that the signal shape remained undistorted for several cycles. This phenomenon may indicate that signal generated noise is not as much of a problem at GVTX as it is at APOK.

4.2.2 Conventional Optimum Filters

For comparison with the results discussed above, optimum filters of a more conventional type were also calculated. The technique consists of assuming a model of the signal. In the case discussed here, the signal is assumed to be white between 2.0 and 0.3 sec period and a cosine taper starting at the cutoff is zero at 4.0 and 0.4 sec period. The impulse response of the velocity section in the hole is convolved with the theoretical signal to obtain the model of the signal at any depth. Signal and noise are taken to be uncorrelated. The correlation matrix then consists of the measured noise added to the theoretical signal for the various depths. The desired signal is the signal as recorded by the surface seismograph. It should be noted that an assumption must be made as to the signal-to-noise ratio. A signal-to-noise of 2 was assumed in these calculations.

Using the deghosting techniques discussed previously, it was found that a single-channel filter at APOK was as effective as a multichannel filter. Therefore, it was decided to try both 2-channel and 4-channel optimum filters. Figure 27 shows the noise reduction that was obtained; if the 2 Hz peak is again used as a criteria, these optimum filters are as effective as the single-channel filter using deghosting technique in reducing the noise. Examination of figure 27 indicates that the 2-channel filter is more effective than the 4-channel filter. Examination of figure 28 illustrates that the filter also reduces the signal amplitudes approximately 3 dB. It is of course possible to use a number of different signal models and signal-to-noise ratios to try to improve on the results obtained here. However, it would appear likely that an improvement in noise reduction would result in a further reduction of signal amplitude.

The results obtained to date indicate that the one-sided single-channel optimum filter using the deephole 1 and the surface (as reference) is as effective a technique as any multichannel set of filters at APOK. However, because of the complexity of programming the first technique online, it is probably preferable to use conventional multichannel filters.

A three-channel optimum Wiener filter was computed using the three deepest seismometers at GVTX. The surface seismograph was not included. In theory, inclusion of the high noise level at the surface would result in a set of filters which would heavily attenuate the signal contribution from the surface seismograph. In practice, the filter could not hope to respond to the large burst of noise from nearby traffic without degrading the performance from the array. The signal model used consists of a white signal between 0.25 and 2.0 second period, with a cosine taper at each end. This model appears

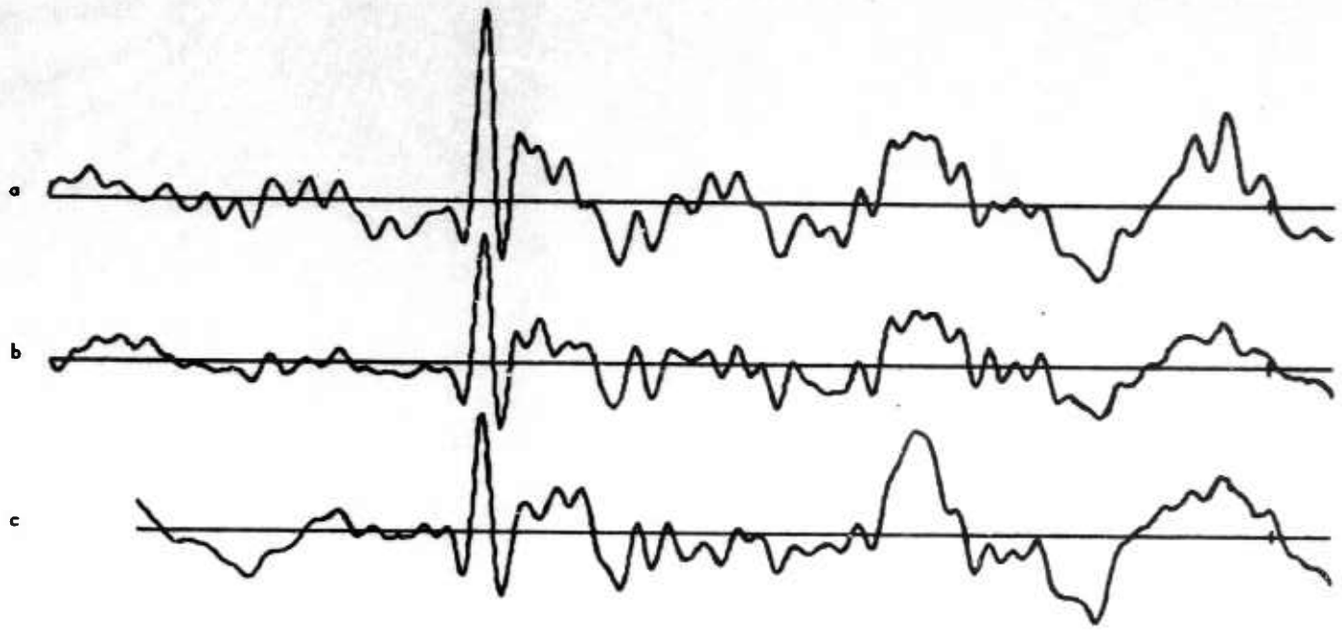

Figure 28. Teleseismic signal operated on by multichannel Wiener filters; a. surface signal; b. two-channel filter; c. four-channel filter

to cause less trouble in computation of filters than the model without the tapers. The results are shown in figure 29, together with the noise level of DH1, which has the best signal-to-noise ratio of the individual seismographs. Only a small amount of noise reduction was obtained.

4.2.3 Prediction Filters

A set of optimum prediction filters were computed for the APOK vertical seismographs. These filters do not predict noise in the future, but take advantage of the fact that the signal has already been received by the bottom seismograph while the other seismographs are still recording noise. Thus, a set of filters operating on the noise from the top seismographs can be used to predict the noise from the bottom seismograph; subtracting the two time series should eliminate some of the noise and improve the signal-to-noise ratio of the first break. Of course, it must be noted that when the signal arrives at the other seismographs, the signal will be distorted. Because of the similarity between noise and signal at the site, the signal is severely attenuated after the first break. Figure 30 shows the noise after 3-channel prediction filtering and the unfiltered noise at the surface. In this case, the noise reduction is greater with increasing numbers of seismographs. As noted previously, optimum filtering using other techniques does not always result in further improvements when more seismographs are added.

It was decided to try long prediction filters (>200 points, 20 samples/sec) to determine if further improvements are possible. The total amount of data used was 3276 sec of noise with a spectral lag of 12.8 sec. The results are high confidence, high resolution, spectral and cross spectral estimates. The multiple coherences were calculated to determine the improvement that can theoretically be obtained. The multiple coherence is defined by Bendat (1966):

$$\gamma^2_{ij}\ (f) = 1 - \left[G_i(f)\ G^i(f)\right]^{-1}$$

where, $G^i(f)$ is the ith diagonal element of the inverse of the spectral matrix.

The noise reduction that can theoretically be obtained is:

$$G_p(f) = \left(1 - \gamma^2_{ix}\right) G_i(f)$$

where $G_p(f)$ is the theoretically predicted spectrum.

Figures 31 and 32 show the multiple coherences at APOK when the surface and DH1 (2880 m) are the outputs. The multiple coherences are high for periods greater than 1.0 sec and decrease rapidly towards the shorter periods. When the surface is taken as the output, the 2 Hz peak shows a coherence somewhat higher than the adjacent frequencies. With DH1 as the output, the coherence at the 2 Hz peak is no more than adjacent frequencies. In general, the plot shows the higher frequency noise is not very predictable when averaged over long samples.

A 210 point set of 3-channel prediction filters were computed in the time domain from the correlation matrix obtained from the long sample discussed

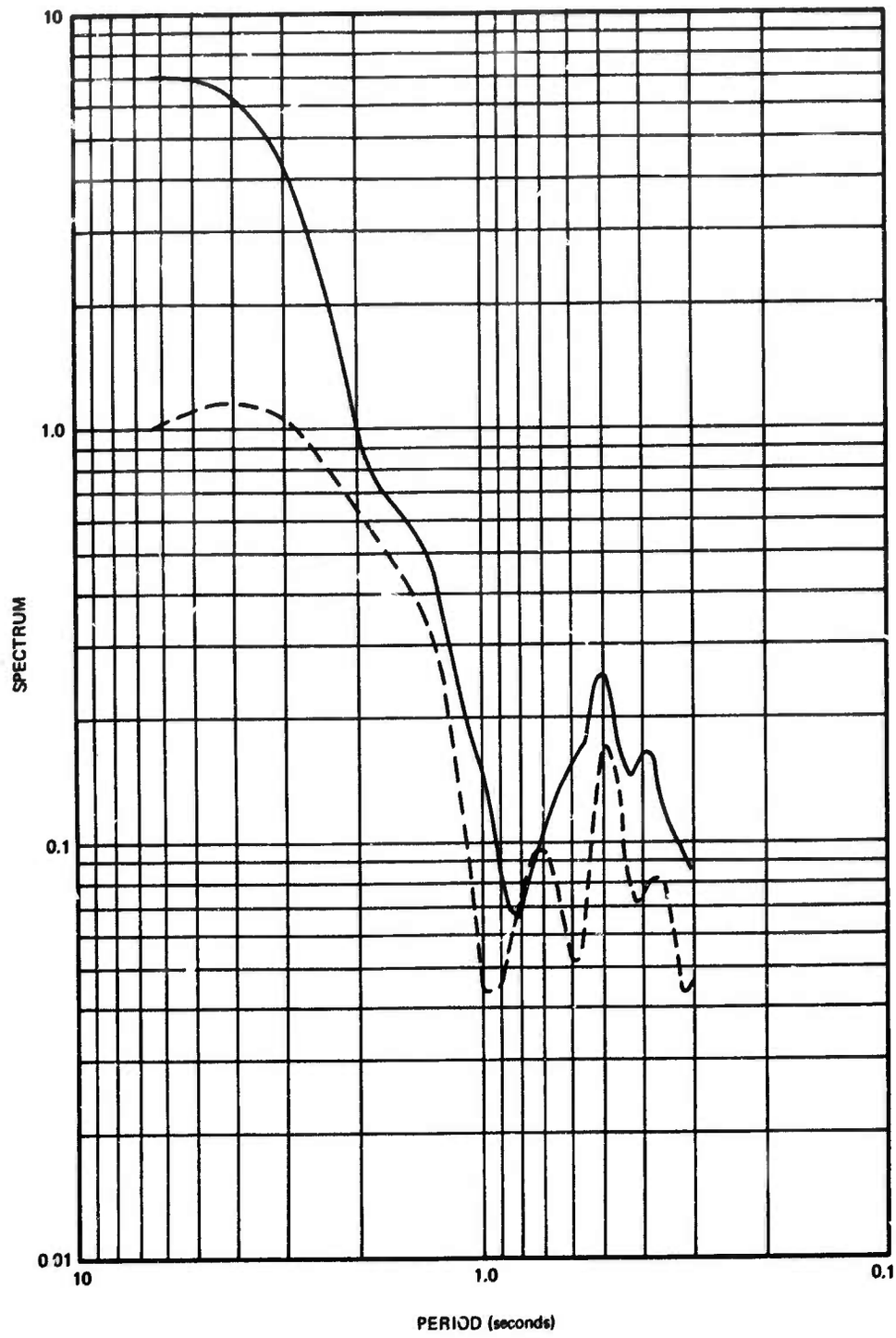

G 3383

Figure 29. Noise spectrum of DH1 in solid line, noise spectrum after 3-channel optimum filtering in dashed line, GVTX

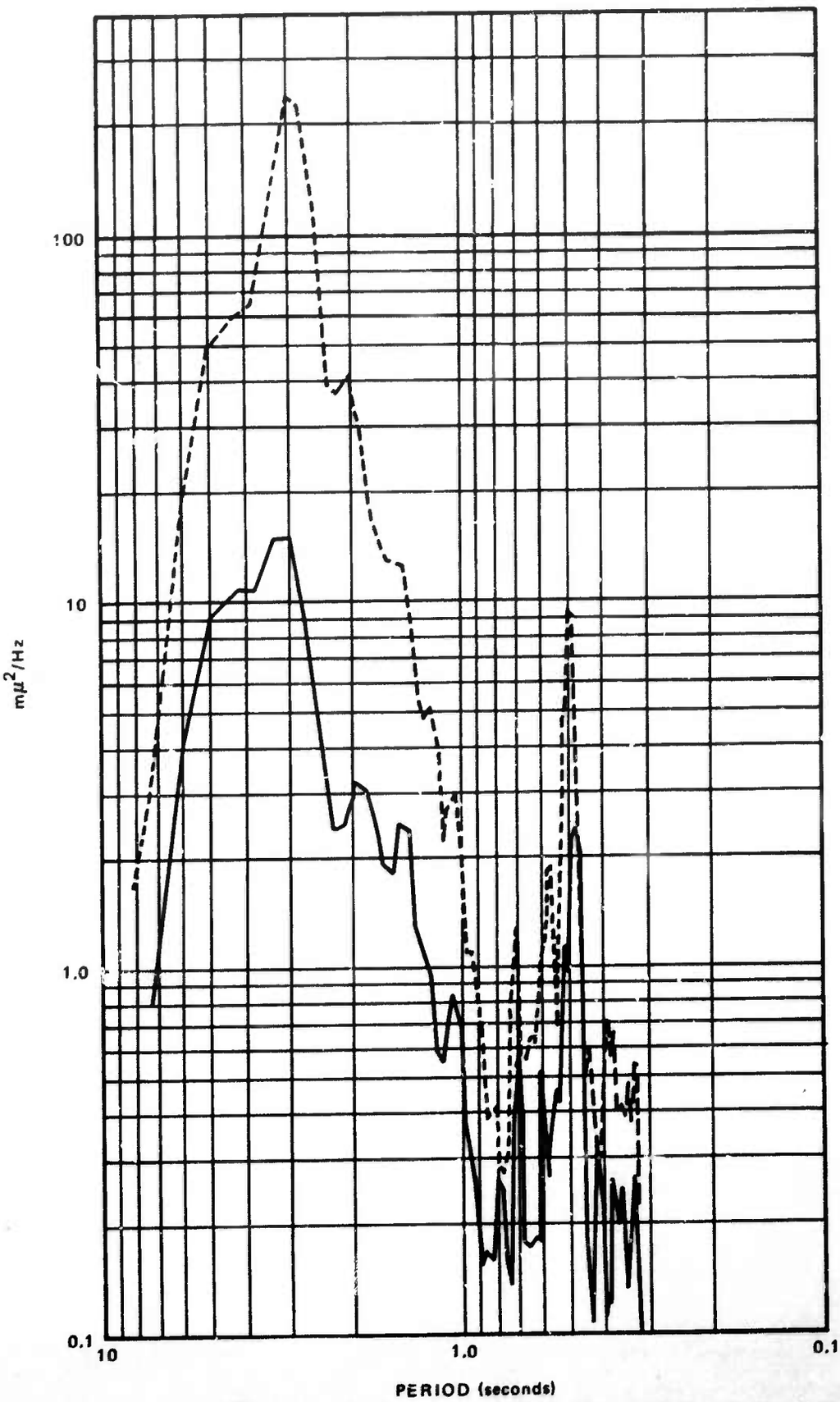

Figure 30. Spectrum of the noise after three-channel prediction filter using DH4, DH3, and DH2 to predict DH1 (solid line), and spectrum of the noise at the surface (dashed line)

G 4187

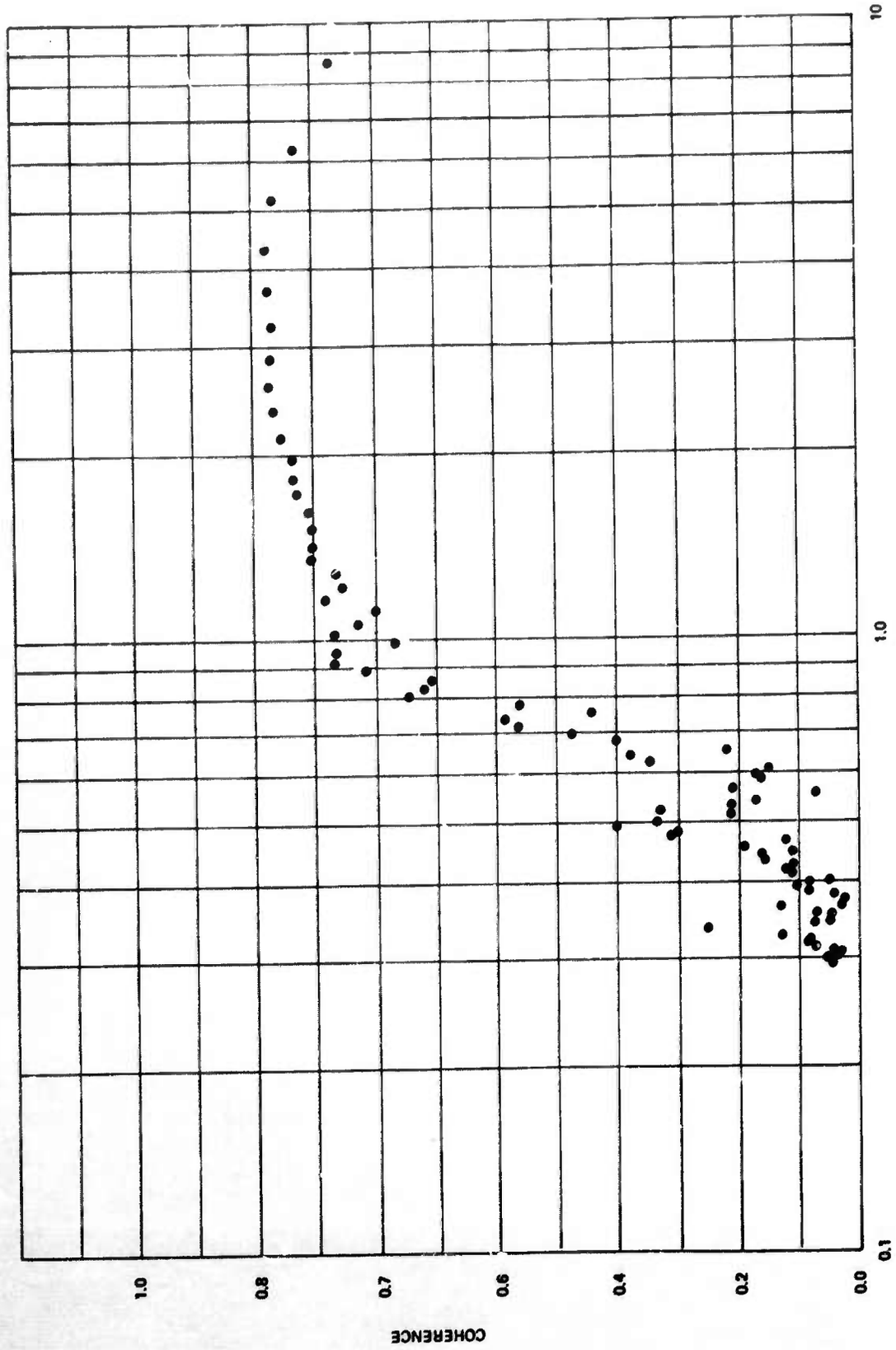

Figure 31. Multiple coherence of the four vertical seismographs at APOK, DH4 (surface) used as output

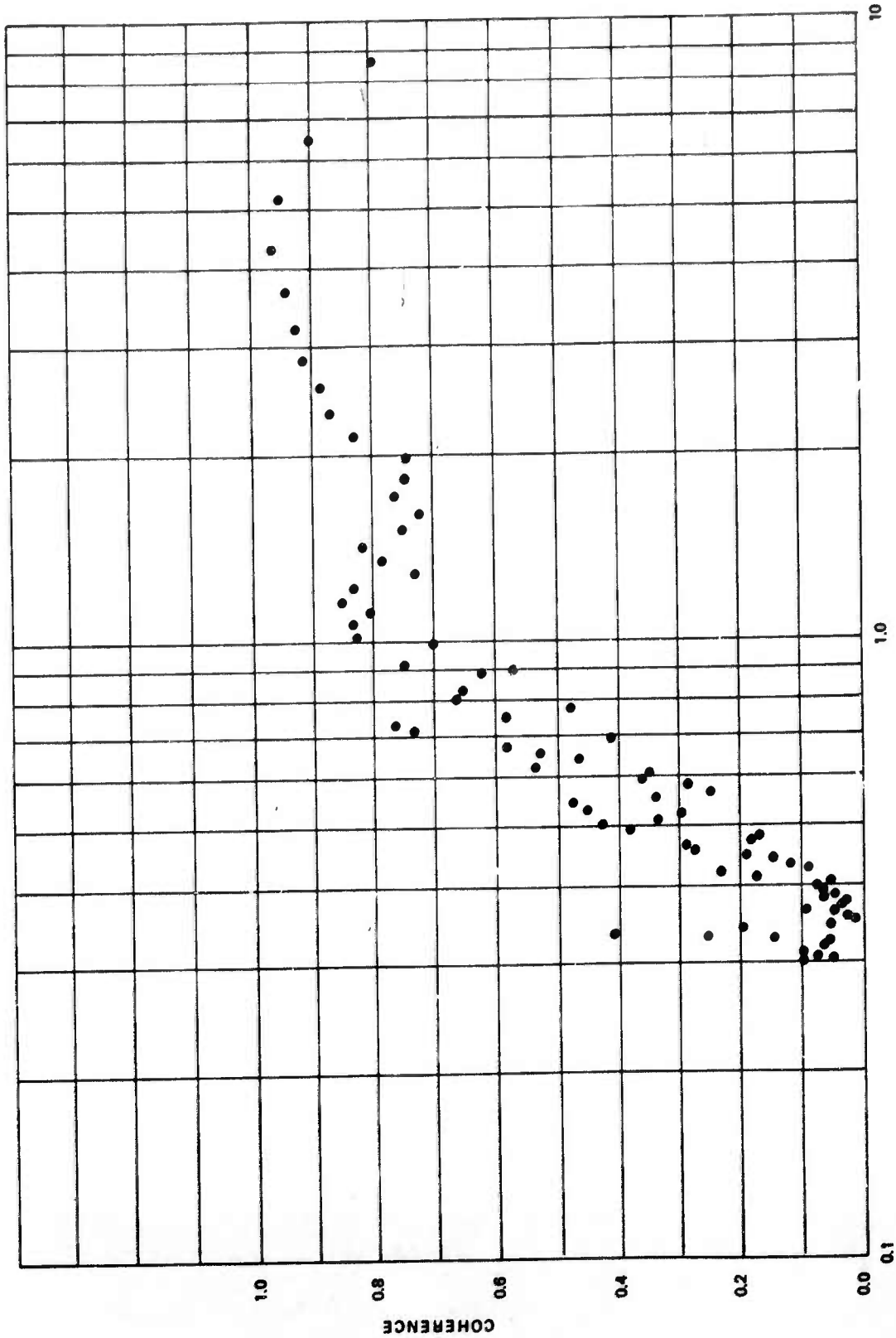

Figure 32. Multiple coherence of the four vertical seismographs at APOK, DH1 used as output

before. Figure 33 shows the theoretically predicted noise spectra after prediction filtering and the actual spectra obtained experimentally by applying the set of filters to the first 240 sec of the data from which the filters were computed. At no frequency are the experimental results as good as the multiple coherence indicates they should be. At 2 Hz, no improvement was obtained. It is concluded from these experiments that the noise is not stationary at 2 Hz over periods on the order of an hour. At 1 Hz, the noise is not completely stationary, but some improvements can be obtained by optimum filtering.

In order to compute long prediction filters, a program has been written to obtain spectral and cross spectral estimates from large noise samples. The program uses the Fast Fourier Transform and operates by sectioning the record, taking the spectra and averaging these spectra.

Let $X(t)$, $t = 0, \ldots N-1$ be a sample from a seismic time series. We take non-overlapping segment $X_n(t)$, $t = 0, 1, \ldots L-1$, where $n(L-1) = N-1$.

The Fourier transform of each segment is computed

$$F_n(k) = \frac{1}{L} \sum_{t=0}^{L-1} X_n(t)\, W(t) e^{-2\pi i k n/L}$$

where $W(t)$ is the smoothing window; to date a Hanning window has been used.

$$F_n(k) = 1/4F_{n-1} + 1/2F_n + 1/4F_{n+1}$$

The spectral and cross spectral of each segment are:

$$S_n(k) = F_i(k)\, F_j^*(k)$$

where $i=j$ gives the spectra and $i \neq j$ gives the cross spectra.

The final step consists of averaging over all the spectra to obtain the final spectral estimate of $X(t)$,

$$S(k) = \frac{1}{N} \sum_{n=0}^{N} S_n(k)$$

The average of this method consists of not being limited, in the length of sample that can be analyzed, by the core of a small computer. For example, we have calculated the spectral matrix from 1 hour of short-period data with 256 lags in only 25 minutes of CDC 3200 computer time. The program is specially useful in obtaining high resolution and high confidence multiple coherences.

4.3 NON-OPTIMUM FILTERS

As an alternative to the use of optimum filters, which deteriorate rapidly with time because of the non-stationary noise, a number of non-optimum filtering techniques (in the least-mean-square sense) were tried. The methods tried during the present contract were multichannel deghosting filters, velocity filters, and time delay and sum.

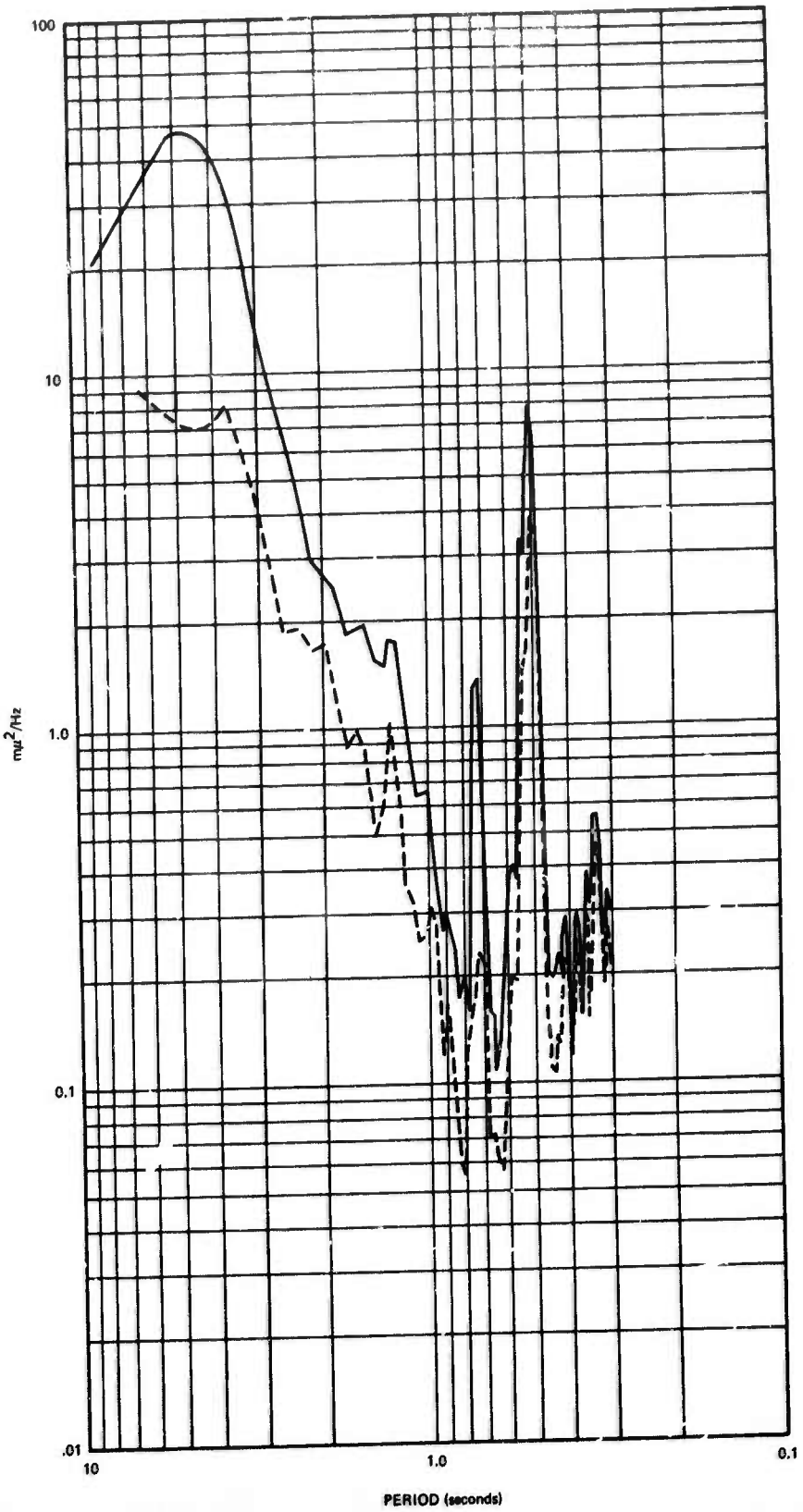

Figure 33. Experimental results from prediction filtering (solid line) and theoretically predicted spectrum after prediction filtering, (dashed line) APOK

G 4188

4.3.1 Multichannel Deghosting Filters

A set of multichannel filters were computed from a formula suggested by the Project Officer.

$$\begin{bmatrix} Z_o(f) \\ Z_1(f) \\ Z_n(f) \end{bmatrix} = \begin{bmatrix} \alpha_o \cos 2\pi f t_o \\ \alpha_1 \cos 2\pi f t_1 \\ \alpha_n \cos 2\pi f t_n \end{bmatrix} \cdot S(f)$$

where n is the number of seismographs, t_n is the uphole time, S(f) is the surface signal and α_n a weighting factor obtained from the noise level of the nth seismometer. The filter applied to each channel is,

$$F(\omega) = \frac{\alpha_n \cos 2\pi f t_n}{\sum_{m=0}^{N} \alpha_n^2 \cos^2 2\pi f t_n}$$

The advantage of this filter is that the noise level cannot increase above the level of an individual seismograph. The filters were computed in the frequency domain and transformed into the time domain. Filters obtained in this fashion are two sided and small precursors appear on the filtered seismograms in front of the signal. Figure 34 shows the filter result obtained using all four seismographs at GVTX and the three bottom seismographs. The slight difference in amplitudes is caused by the presence or absence of the surface trace with the associated weighting factor. A small precursor is visible on both examples, but is more noticeable on the lower trace. A comparison with the surface trace indicates that the filters are operating correctly. The main advantages of this method are the simplicity of computation and the fact that it does not allow for an increase in the noise levels. The main disadvantages are that long filters (150 points were used) are necessary and that precursors appear in front of the signals.

4.3.2 Velocity Filters

While body-wave signals travel uphole with known velocity, that part of the noise which consists of Rayleigh waves is either in phase or 180 deg out of phase with the surface. Under these conditions, it appeared that velocity (fan) filters might be effective in reducing the noise level.

This approach was used only with data from APOK, where the signal-to-noise ratios are close to constant with depth. The technique is not applicable to GVTX where the surface seismograph should not be used and therefore only a small linear array is available.

A simple set of velocity (fan) filters were calculated for the APOK deephole site. The data were single-channel inverse filtered and then fan filtered to pass only waves traveling at the uphole velocity of P waves. The filters used were calculated from the following formula (Embree, et al, 1963):

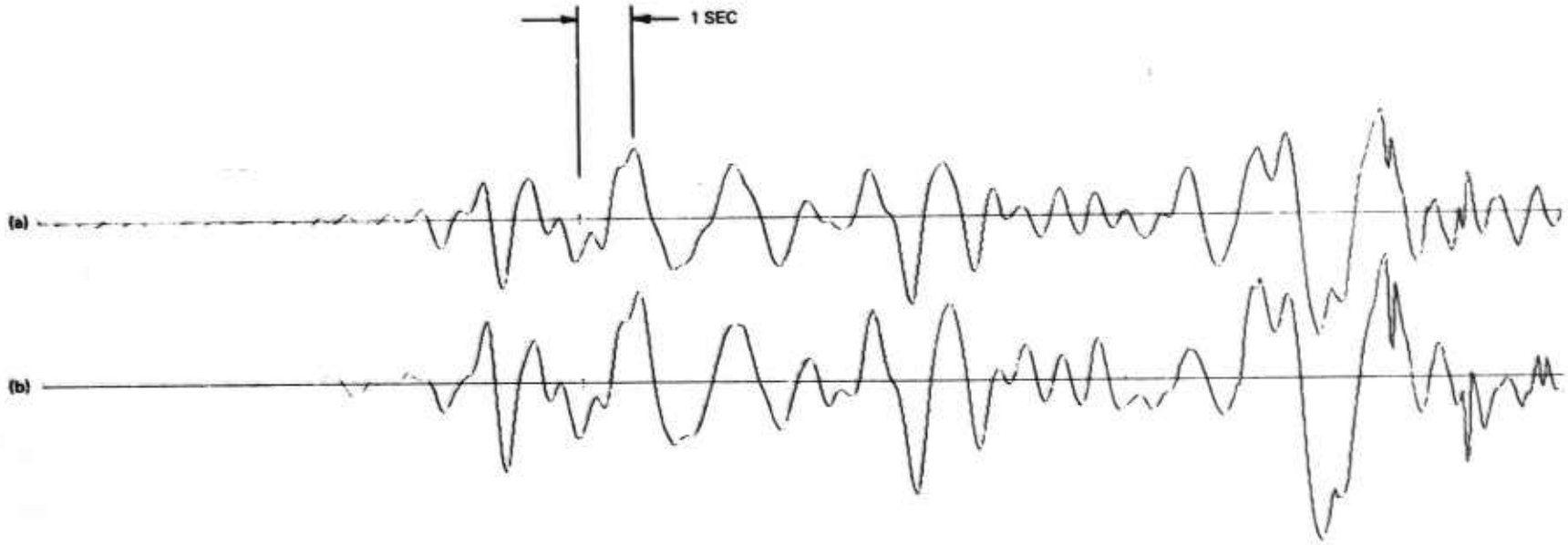

Figure 34. Cosine inverse filter using (a) all 4 deephole channels, (b) bottom channels, GVTX

G 3691

$$y(T_n, X_m) = \frac{1}{\pi^2 \left[\left(\frac{X_m}{\Delta_x} \right)^2 - n^2 \right]}$$

where: T_n =$n\Delta t$ a given sampled value of time t

Δ_x =seismograph separation

x_m =distance from array center of m^{th} seismograph.

Because of the small array available, the filters attenuated both the signal and the noise. Figure 35 shows the noise attenuation obtained together with a signal before and after filtering. Comparison of signal and noise attenuations shows that for periods less than 1.0 sec, a small improvement was obtained. Improved fan filters can be calculated and should be tried. Finally, it must be noted that with this very small array, only a limited improvement on the signal-to-noise can be expected.

4.3.3 Time-Delay and Sum

In order to compare with the results of filtering techniques described in the previous sections, it was decided to include simple time delay-and-sum filtering. The major disadvantage of the method is that for vertical arrays, the resulting signal shape is not the one that is recorded at the surface. The major advantage is the simplicity of the operation.

Several different weighting functions were used in various time-delay and sum operations at GVTX and are listed below:

	No. 1	No. 2	No. 3
DH4	0.149	0.227	0.000
DH3	0.373	0.555	0.373
DH2	0.612	0.833	0.612
DH1	1.000	1.000	1.000

The weighting factors for example No. 1 were provided by the Project Officer. Weighting factors for example No. 2 were calculated from the mean square noise level of the spectra. The spectra are corrected to equal signal level. Figure 36 shows the results obtained and neither resulted in an improvement over the noise level at the bottom of the hole. Figure 36 also shows the results from the weighting factors of example No. 3 where the noise surface seismograph was not included. The results show a modest improvement over the noise level at the bottom of the deephole. From these experiments, it appears that it is better not to include the surface seismographs at sites with high level surface noise.

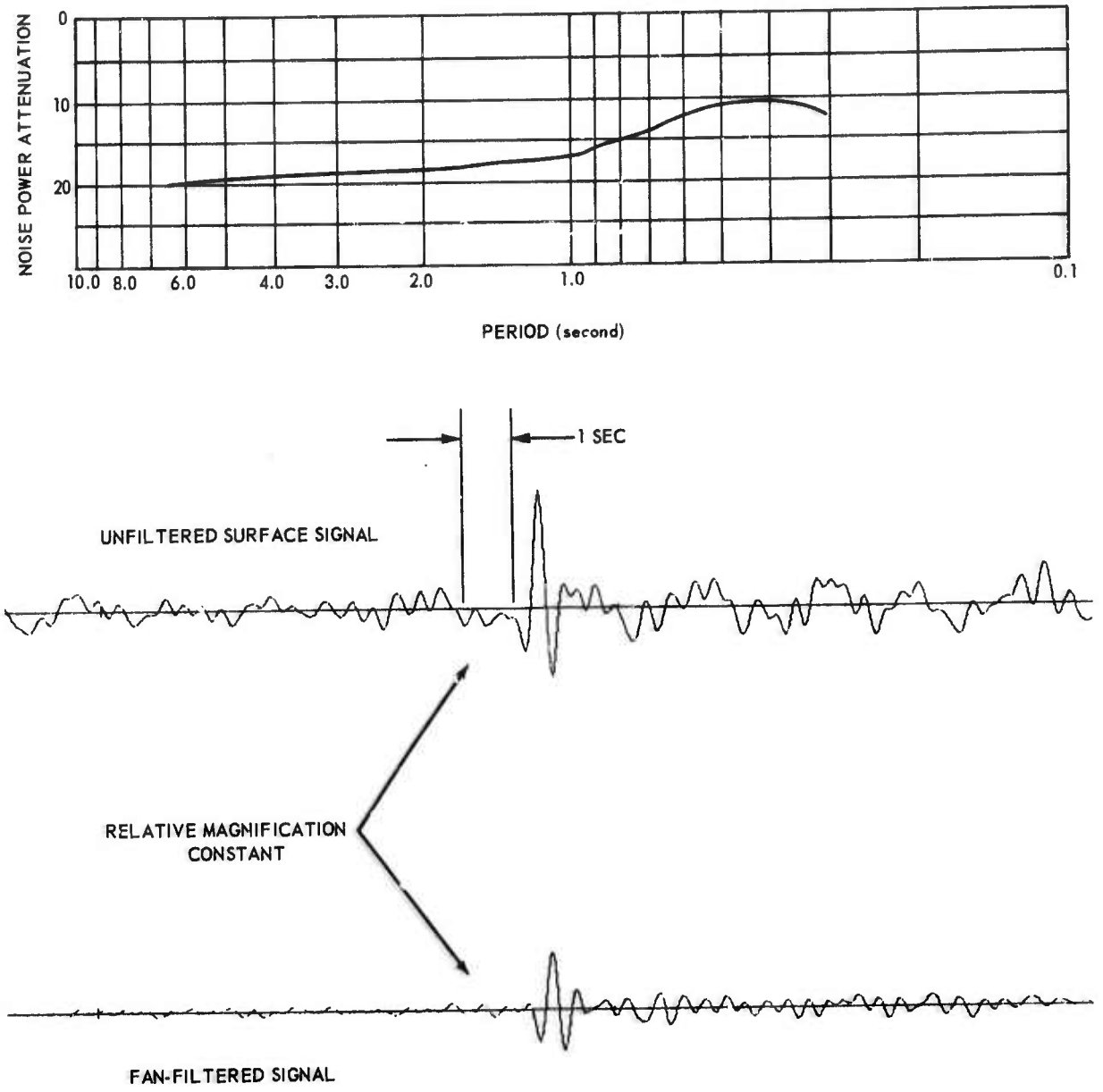

Figure 35. Noise (from spectra) and signal attenuation resulting from fan-filtered deephole array, APOK

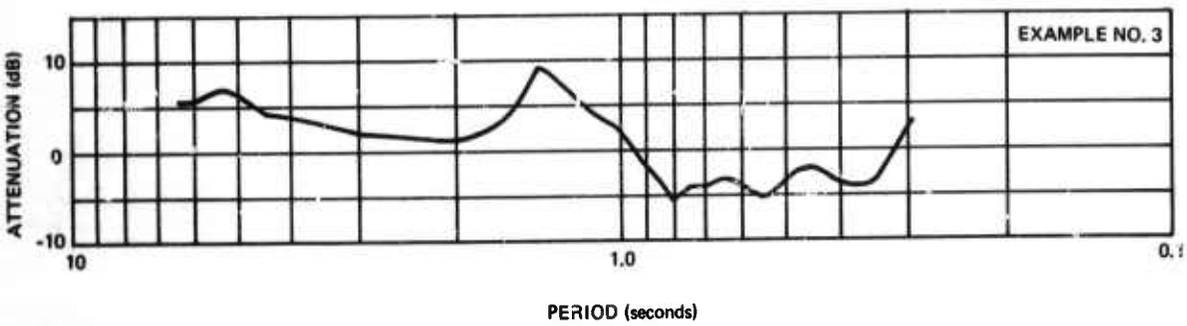

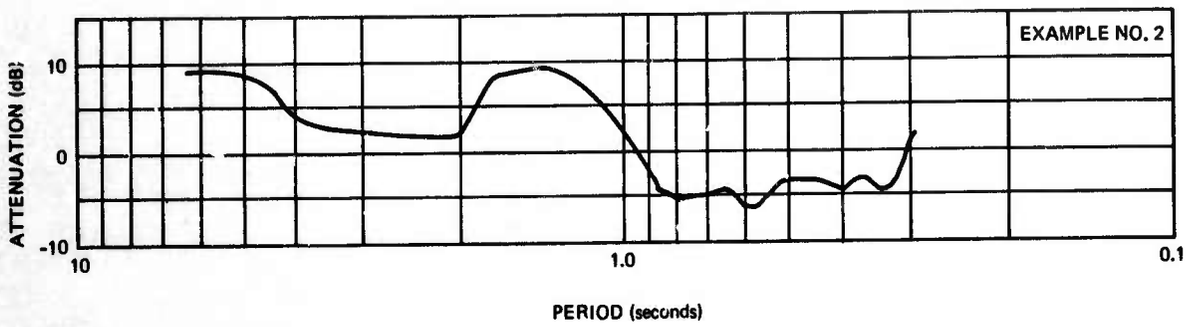

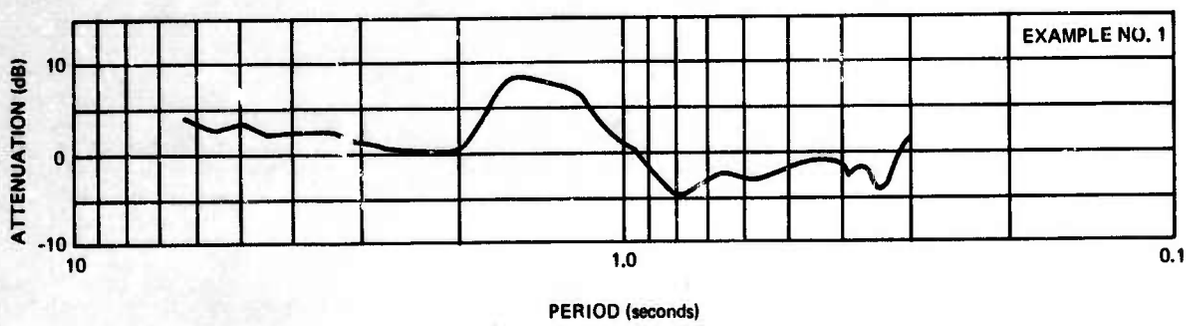

G 3704

Figure 36. Attenuations obtained at GVTX in time-delay and sum processing

It is, of course, always possible to include the surface by assigning it a weighting factor consistent with the noise level when large bursts of noise are present. However, in this case, the weighting factor for the surface at Grapevine would be about 0.05 and is therefore essentially negligible.

At APOK, the time delay and sum operations were done without weighting factors because the signal-to-noise ratio is almost identical for all depths. Only a small increase in the signal-to-noise ratio (3 dB) was obtained in this fashion.

5. REFERENCES

Capon, J., and Greenfield, R.J., 1965, Asymptotically optimum multichannel filtering for sampled data processing of seismic arrays: MIT, Lincoln Laboratory, Technical Note 1965-1967.

Douze, E.J., 1967, Short period seismic noise: Bull. Seis. Soc. Am., v. 57, p. 55-81.

Hannon, W.T., 1964, An application of the Haskell-Thompson matrix method to the synthesis of the surface motion due to dilatational waves: Bull. Seis. Soc. Am., v. 54, p. 2067-2079.

Potter, T.F., and Roden, R.B., 1965, Theoretical capability of systems of horizontal seismometers for predicting a vertical component in ambient trapped-mode noise: Special Report No. 7, Texas Instruments, Inc.

Sax, R.L., 1966, Feasibility of linear polarization measurements for detecting and measuring seismic body waves: SDL Report No. 163, Earth Sciences Division, Teledyne Industries, Inc.

Shanks, J.L., 1967, Recursion filters for digitizing processing: Geophysics, v. 32, p. 33-52.

Shappee, R.M., and Douze, E.J., 1967, Deepwell research, Final Report, Project VT/5051, Technical Report No. 67-3: Geotechnical Corporation.

Shimshoni, M., and Smith, S., 1964, Seismic signal enhancement with three component detectors: Geophysics, v. 29, p. 664-671.

Simons, R.S., 1967, A surface wave particle motion discrimination process: Geotechnical Corporation, Manuscript.

Treitel, S., and Robinson, E.A., 1967, The stability of digital filters: IEEE Transactions or Geoscience Electronics, November, 1967, p. 6-18.

Tryggvasson, E., and Qualls, B.R., 1966, Seismic refraction measurements of crustal structure of Oklahoma: J. Geophysical Research, v. 72, p. 3738-3740.

6. CONCLUSIONS AND RECOMMENDATIONS

6.1 CONCLUSIONS

The short-period triaxial seismometer has proven to be a very stable and reliable instrument, requiring a minimum of attention and adjustments. It is also much easier to work with and transport than earlier deephole instruments. Nearly all of the malfunctions encountered in the downhole instrumentation can be attributed to dc motor failure or to insulation breakdown in the 7H4 cable. The insulation in the 7H4 cable used on this contract has broken down on several occasions due to age and long periods of use in high temperature deepholes. Cable insulation problems were the cause of most of the seismometer downtime.

Considerable time was lost due to the computer hardware problems. As a result, online program development was delayed during the beginning of the contract year. After an on-call service contract was made with Adage, Inc., the computer manufacturer, satisfactory operation was maintained. Normal operation of the computer was possible from the last week of August, 1967, until the Grapevine, Texas site was shut down the last week of May, 1968.

None of the filtering techniques employed in the recordings of the vertical array have resulted in improved detection capability of the magnitude originally expected. Least-mean-square processing methods are not acceptable because the filters computed from a given noise sample degrade rapidly (< 1 hour) with time. Therefore, these techniques are not usable for online processing.

It must be noted that adaptive optimum filtering could invalidate this conclusion. However, it appears unlikely that adaptive filtering will be any better than Wiener optimum filters used on the sample from which they are computed. Therefore, even with adaptive filtering improvements in signal-to-noise of 3-4 dB over the period range of interest appears to be the best that can be expected. The non-optimum techniques of multichannel deghosting and velocity filtering are almost as effective as optimum filtering and need only be computed once for each site. These techniques are therefore to be preferred for online processing.

6.2 RECOMMENDATIONS

Dc motors were the only components within the seismometer that failed and caused damage to the instrument itself. Oxidation and corrosion of the armature and brushes appear the major cause of motor failure. These failures prevent the seismometer masses from being caged and consequently the suspensions are very often damaged while removing the seismometers from the deephole. In order to correct this motor problem, it is recommended that brushless stepping motors be tested and used to replace the existing motors.

Armored electrical cable (7H4) used on this program is becoming quite unreliable because of normal usage over several years. It is recommended that new cable be supplied if the system is transported to another location for data acquisition.

A large amount of valuable equipment is now in storage as a result of the termination of this contract. This equipment will, in all likelihood, be scattered within other programs if it is not put back in operation in a reasonable length of time. It is recommended that this short-period triaxial system be used to replace older equipment at some location where high quality deephole data may be recorded for further research work.

The maximum likelihood REMODE nonlinear processor discussed in section 3.3 appears quite promising. Because of the shortage of time and funds, this technique has not been fully evaluated. It is recommended that additional analysis of three-component deephole data be included in future work.

APPENDIX

REPRODUCTION OF STATEMENT OF WORK TO BE DONE AFTAC PROJECT AUTHORIZATION NO. VELA T/7703 AND AMENDMENTS

APPENDIX 1

F33657-67-C-1224
16 DEC 1966

STATEMENT OF WORK TO BE DONE
(AFTAC Project Authorization No. VT/7703/S/ASD)

1. Using the deep-well-array field system assembled for Project VT/5051, conduct a field-operations program at two or more available VELA-UNIFORM deep-well sites to be designated by the AFTAC project officer. The sites near Pinedale, Wyoming (PIWY), Grapevine, Texas (GV-TX), and Franklin, West Virginia (FNWV), may be considered for planning purposes. In the course of this work, accomplish the following subtasks at each site visited:

a. Routinely operate and maintain an easily-transportable deep-well vertical-array system employing 4 to 6 triaxiam and vertical component short-period borehole seismometers, appropriate surface instrumentation, and an on-line digitizing/recording/computing device.

b. Record on film and digital-tape vertical and three-component data from the deep-well array. Establish an interim library of digitized raw seismic data from the array, including records of background noise and signals and appropriate identifying logs, suitable for use in this and other projects.

c. Operate the on-line computing device to test in real-time different vertical-array signal-enhancement data-processing techniques. Record the results on film and tape. Operate at each site long enough to compare the different techniques and determine the better signal-enhancement processing methods for each site. Relate the results of each technique to site conditions, such as seismic noise field, geological structure, and geographic location. This work is to be accomplished in close coordination with the AFTAC project officer, who will assist in selecting the techniques to be tested.

2. Process the raw seismic data obtained from field operations and perform detailed analysis and evaluation of the horizontal components of surface and subsurface noise at the designated sites, making comparisons between observations and theoretical studies, to improve our understanding of noise composition. Particular emphasis is to be placed on using horizontal data to ascertain the true form of noise constituents which appear from their vertical components to be compressional body-waves. Computer programming and computational services will be accomplished by the contractor; commercial high-speed-computer services will not be arranged for under this project without prior AFTAC concurrence.

3. Tailor various borehole-array data-processing techniques, for improving signal-to-noise ratios and detecting low-level signals, for implementation at the designated deep-well sites and demonstrate them in off-line tests. The processes should be ultimately suitable for real-time use and shall include, but not necessarily be limited to: optimum filtering, both with and without ghosting and deghosting pre-filters; prediction filtering, using vertical data exclusively and three-component data; correlation processing and other non-linear techniques; and possibly, other processes suggested by the AFTAC project officer. Adapt selected signal-enhancement techniques to on-line real-time operation.

Attachment 1 F33657-67-C-1224

REPORTS

(AFTAC Project Authorization No. VT/7703)

1. Monthly Management Report: A monthly letter-type management report, summarizing work for the calendar month and generally not exceeding 3 pages of text, will be submitted to AFTAC in 15 copies by the 20th day of the following month. The heading of each report will contain the identification data listed in paragraph 7. These reports should not contain detailed technical descriptions, formulae, equations, graphs, or other technical documentation. Instead, they will present a narrative summary of work performed during the report period, including reference to the following topics:

a. Research Program and Plan - a brief statement of objectives and plan of research.

b. Major Accomplishments - a brief description, written in lay terms, of any finding or accomplishment considered worthy of being brought to the attention of management.

c. Problems Encountered - make reference to difficulties associated with personnel, facilities, contracts, availability of literature, funds, strikes, disasters, etc., which significantly affect the progress of the work involved. Problems of a technical nature should also be included, but in brief, nontechnical terms.

d. Fiscal Status - include an estimate of contractor funds required to complete the work if an overrun is anticipated.

e. Government Actions Required - specify any AFTAC assistance required in resolving "Problems Encountered."

f. Future Plans - a brief statement of any significant change which is planned in the course of work under way or on any new item which is considered to be of interest to management. In addition, the initial monthly report should include an introduction outlining the background, objectives, and assignment of responsibility for the project.

2. Monthly Financial Statement: The contractor will submit 5 copies of financial data in an Alternate Management Summary Report.

3. Quarterly Technical Reports: Quarterly letter-type technical reports, summarizing work for calendar quarters, will be submitted to the AFTAC project officer in 2 copies within 15 days after the close of each such period. Each report will present a factual discussion of technical findings and accomplishments for the quarter, supported by technical descriptions, mathematical developments, graphs, and illustrations as necessary.

4. Site Reports: A Site Report will be submitted to AFTAC in 50 copies within 60 days after the completion of operations at each site visited. Each report will be identified by the data listed in paragraph 7 and will include the notices specified in paragraph 8. Each site report should be comprehensive, presenting a complete and factual discussion of technical methods and findings of all aspects of project work connected with the particular site, using a format similar to that of the site and analysis reports published under Projects VT/1139 and VT/5051. DD Form 1473, Document Control Data - R&D (reference AFR 80-29) will be included in each report. The appropriate availability/limitation notice for use on the Form 1473 will be designated by AFTAC/TD-7.

5. Final Report: A final report, identified by the data listed in paragraph 7 and including the notices specified in paragraph 8, will be submitted to AFTAC/TD-7 in 50 copies within 60days after the completion of all work. The report will present a concise and factual discussion of technical findings and accomplishments of the entire project, using the site-report format. DD Form 1473, Document Control Data - R&D (reference AFR 80-29) will be included in each report. The appropriate availability/ limitation notice for use on the Form 1473 will be designated by AFTAC/TD-7.

6. Special Reports:

a. Special reports of major events will be forwarded by telephone, telegraph, or separate letter as they occur and should be included in the following monthly report. Specific items are to include, but are not restricted to, strikes and disasters, program delays, technical breakthroughs, major decisions, and requirements for increase in funds.

b. Special technical reports may be required for instrument evaluations, project recommendations, and special studies when it is more desirable to have these items reported separately from the periodic and site reports. Specific format, content, number of copies, and due dates will be furnished by AFTAC as required.

c. All seismograms and operating logs, including pertinent information concerning time, date, type of instruments, magnification, etc., will be provided when requested by the AFTAC project officer.

7. Identification Data: All monthly, site, and final reports will be identified by the following data:

AFTAC Project No. VELA T/7703

Project Title: Deep-Well Array Operations

ARPA Order No. 624

ARPA Program Code No. 7F10

Name of Contractor:

Contract Number:

Amount of Contract:

Effective Date of Contract:

Contract Expiration Date:

Name and phone number of Project Officer, Scientist, or Engineer:

8. Notices:

a.. All site and final reports will include the following notice on the cover:

Sponsored by
Advanced Research Projects Agency
ARPA Order No. 624

b. All site and final reports will include the following notices on the first or title page:

This research was supported by the Advanced Research Projects Agency, Nuclear Test Detection Office, under Project VELA-UNIFORM, and accomplished under the technical direction of the Air Force Technical Applications Center under Contract No. F33657-67-C-1224.

Qualified users may request copies of this document from:

Defense Documentation Center
Cameron Station
Alexandria, Virginia 22314

CONTRACTOR'S COPY

STANDARD FORM 30, JULY 1965
GENERAL SERVICES ADMINISTRATION
FED PROC REG (41 CFR) 1-16.01

AMENDMENT OF SOLICITATION/MODIFICATION OF CONTRACT

PAGE 1 OF

1. AMENDMENT/MODIFICATION NO.	2. EFFECTIVE DATE	3. REQUISITION/PURCHASE REQUEST NO.	4. PROJECT NO. (If applicable)
P001	4 Aug 1967	Not Applicable	

5. ISSUED BY — CODE
UNITED STATES AIR FORCE
AFSC AERONAUTICAL SYSTEMS DIVISION
WRIGHT-PATTERSON AIR FORCE BASE, OHIO
Buyer: J. A. McKinley/ASNKS 45433

6. ADMINISTERED BY (If other than block 5) — CODE
DCASR, Dallas
500 South Ervay Street
Dallas, Texas 75201

SEP 5 1967
52412

7. CONTRACTOR — CODE — FACILITY CODE
NAME AND ADDRESS (Street, city, county, state, and ZIP Code)
TELEDYNE INDUSTRIES, INC.
(Geotech Division)
3401 Shiloh Road
Garland, Texas 75401

8.
☐ AMENDMENT OF SOLICITATION NO. _____
DATED _____ (See block 9)
☒ MODIFICATION OF CONTRACT/ORDER NO. F33657-67-C-1224
DATED 1 Mar 1967 (See block 11)

9. THIS BLOCK APPLIES ONLY TO AMENDMENTS OF SOLICITATIONS
☐ The above numbered solicitation is amended as set forth in block 12. The hour and date specified for receipt of Offers ☐ is extended, ☐ is not extended.
Offerors must acknowledge receipt of this amendment prior to the hour and date specified in the solicitation, or as amended, by one of the following methods: (a) By signing and returning _____ copies of this amendment; (b) By acknowledging receipt of this amendment on each copy of the offer submitted; or (c) By separate letter or telegram which includes a reference to the solicitation and amendment numbers. FAILURE OF YOUR ACKNOWLEDGMENT TO BE RECEIVED AT THE ISSUING OFFICE PRIOR TO THE HOUR AND DATE SPECIFIED MAY RESULT IN REJECTION OF YOUR OFFER. If, by virtue of this amendment you desire to change an offer already submitted, such change may be made by telegram or letter, provided such telegram or letter makes reference to the solicitation and this amendment, and is received prior to the opening hour and date specified.

10. ACCOUNTING AND APPROPRIATION DATA (If required)
Not Applicable

MAILING DATE AUG 30 1967

11. THIS BLOCK APPLIES ONLY TO MODIFICATIONS OF CONTRACTS/ORDERS
(a) ☐ This Change Order is issued pursuant to _____
The Changes set forth in block 12 are made to the above numbered contract/order.
(b) ☐ The above numbered contract/order is modified to reflect the administrative changes (such as changes in paying office, appropriation date, etc.) set forth in block 12.
(c) ☒ This Supplemental Agreement is entered into pursuant to authority of the "Government Property" clause of the General Provisions.
It modifies the above numbered contract as set forth in block 12. at no change in estimated cost and fixed fee.

12. DESCRIPTION OF AMENDMENT/MODIFICATION

Part I (b) of the Schedule is amended by deleting the last two lines and substituting the following in lieu thereof:

"facilities and the equipment listed below, subject to the 'Government Property' clause of the General Provisions"

Three (3) W/112 Galvoes, Contractor's Model 4300
Three (3) Power Supplies, Contractor's Model 4304
One (1) Galvo, Contractor's Model 4100-112
One (1) Develocorder, Contractor's Model 4000."

Copy: Budget Branch (5)
Ron Canada

ADMINISTRATIVE INFORMATION

Subject: Transfer of Government Property
Change in Estimated Cost: None
Change in Fixed Fee: None
Finance Office: DCASR, Dallas
Attn: Office of Data and Financial Management
500 South Ervay Street
Dallas, Texas 75201

Except as provided herein, all terms and conditions of the document referenced in block 8, as heretofore changed, remain unchanged and in full force and effect.

13. ☐ CONTRACTOR/OFFEROR IS NOT REQUIRED TO SIGN THIS DOCUMENT ☒ CONTRACTOR/OFFEROR IS REQUIRED TO SIGN THIS DOCUMENT AND RETURN 3 COPIES TO ISSUING OFFICE

14. NAME OF CONTRACTOR/OFFEROR See Block 7 above
BY J. L. Wood (Signature of person authorized to sign)

15. NAME AND TITLE OF SIGNER (Type or print)
J. L. Wood, Vice President

16. DATE SIGNED
17 Aug 67

17. UNITED STATES OF AMERICA
BY Thomas B. Kain (Signature of Contracting Officer)

18. NAME OF CONTRACTING OFFICER (Type or print)
THOMAS B. KAIN

19. DATE SIGNED
22 AUG 1967

30-101

REPRODUCTION

23 AUG 1967

Contract DCASR Dallas

F-16541-13

STANDARD FORM 30, JULY 1966
GENERAL SERVICES ADMINISTRATION
FED. PROC. REG. (41 CFR) 1-16.101

AMENDMENT OF SOLICITATION/MODIFICATION OF CONTRACT

PAGE 1 OF

1. AMENDMENT/MODIFICATION NO.	2. EFFECTIVE DATE	3. REQUISITION/PURCHASE REQUEST NO.	4. PROJECT NO. (If applicable)
P002	31 Oct 67	None	VTL 8/7703

5. ISSUED BY	CODE	6. ADMINISTERED BY (If other than block 5)	CODE
Hq ASD (ASRKS) Wright-Patterson AFB, Ohio 45433 BUYER: [illegible]/53202		DCASR, Dallas 500 South Ervay Street Dallas, Texas 75201	JAN 2[illegible] 1968 32952

7. CONTRACTOR NAME AND ADDRESS (Street, city, county, state, and ZIP Code)	CODE	FACILITY CODE
TELEDYNE INDUSTRIES, INC. (Geotech Division) 3401 Shiloh Road Garland, Texas 75041		

8. ☐ AMENDMENT OF SOLICITATION NO. _____,
DATED _____ (See block 9)
☐ MODIFICATION OF CONTRACT/ORDER NO. F33657-67-C-1[illegible]
DATED 1 Mar 1967 (See block 11)

9. THIS BLOCK APPLIES ONLY TO AMENDMENTS OF SOLICITATIONS

☐ The above numbered solicitation is amended as set forth in block 12. The hour and date specified for receipt of Offers ☐ is extended, ☐ is not extended.

Offerors must acknowledge receipt of this amendment prior to the hour and date specified in the solicitation, or as amended, by one of the following methods: (a) By signing and returning _____ copies of this amendment; (b) By acknowledging receipt of this amendment on each copy of the offer submitted; or (c) By separate letter or telegram which includes a reference to the solicitation and amendment numbers. FAILURE OF YOUR ACKOWLEDGMENT TO BE RECEIVED AT THE ISSUING OFFICE PRIOR TO THE HOUR AND DATE SPECIFIED MAY RESULT IN REJECTION OF YOUR OFFER. If, by virtue of this amendment you desire to change an offer already submitted, such change may be made by telegram or letter, provided such telegram or letter makes reference to the solicitation and this amendment, and is received prior to the opening hour and date specified.

10. ACCOUNTING AND APPROPRIATION DATA (If required)

11. THIS BLOCK APPLIES ONLY TO MODIFICATIONS OF CONTRACTS/ORDERS

(a) ☐ This Change Order is issued pursuant to: _____
The Changes set forth in block 12 are made to the above numbered contract/order.

(b) ☒ The above numbered contract/order is modified to reflect the administrative changes (such as changes in paying office, appropriation data, etc.) set forth in block 12.

(c) ☐ This Supplemental Agreement is entered into pursuant to authority of _____
It modifies the above numbered contract as set forth in block 12.

12. DESCRIPTION OF AMENDMENT/MODIFICATION

a. The Security Requirements, dated 29 November 1966, for subject contract was reviewed on 31 October 1967 in accordance with the policy set forth inn Para 7-103 of DOD Industrial Security Regulations 5220.22-R.

b. The review has indicated that the Security Classification as noted on the current form remains unchanged except as follows:

"SPECIAL INSTRUCTIONS: Foreign national employees of the contractor or subcontractors including those possessing Canadian or United Kingdom reciprocal clearance are not authorized access to classified information resulting from, or used in the performance of, this contract unless authorized in writing by the procuring contracting activity."

"All classified material generated under this Project Authorization will be placed in Group I in accordance with Appendix II, Industrial Security Manual (DOD 5220.22-M) and marked in accordance with DOD 5220.22-R Industrial Security Regulations, both dated 1 July 1966."

DUPLICATE ORIGINAL

MAILING DATE JAN 24 1968

Except as provided herein, all terms and conditions of the document referenced in block 8, as heretofore changed, remain unchanged and in full force and effect.

13. ☒ CONTRACTOR/OFFEROR IS NOT REQUIRED TO SIGN THIS DOCUMENT ☐ CONTRACTOR/OFFEROR IS REQUIRED TO SIGN THIS DOCUMENT AND RETURN _____ COPIES TO ISSUING OFFICE

14. NAME OF CONTRACTOR/OFFEROR		17. UNITED STATES OF AMERICA	
BY _____ (Signature of person authorized to sign)		BY Thomas F. Kain (Signature of Contracting Officer)	
15. NAME AND TITLE OF SIGNER (Type or print)	16. DATE SIGNED	18. NAME OF CONTRACTING OFFICER (Type or print) THOMAS F. KAIN	19. DATE SIGNED 31 Oct 67

30-101

REPRODUCTION

5 Jan 1968

* U.S. GOVERNMENT PRINTING OFFICE: 1966 O—255-145—16-61

UNCLASSIFIED

Security Classification

DOCUMENT CONTROL DATA - R&D

(Security classification of title, body of abstract and indexing annotation must be entered when the overall report is classified)

1. ORIGINATING ACTIVITY (Corporate author)	2a. REPORT SECURITY CLASSIFICATION
Geotech, A Teledyne Company 3401 Shiloh Road Garland, Texas 75040	Unclassified
	2b GROUP

3. REPORT TITLE

Deep Well Array Operations

4. DESCRIPTIVE NOTES (Type of report and inclusive dates)

Final Report, 1 March 1967-31 May 1968

5. AUTHOR(S) (Last name, first name, initial)

Der, Zoltan A.
Douze, Eduard J.
Simmons, A.W.

6. REPORT DATE	7a. TOTAL NO. OF PAGES	7b. NO. OF REFS
25 June 1968	78	11

8a. CONTRACT OR GRANT NO.	9a. ORIGINATOR'S REPORT NUMBER(S)
. F33657-67-C-1224 b. PROJECT NO. VELA T/7703 c. d.	Technical Report No. 68-24 9b. OTHER REPORT NO(S) (Any other numbers that may be assigned this report)

10. AVAILABILITY/LIMITATION NOTICES

Qualified requesters may obtain copies of this report from DDC.

11. SUPPLEMENTARY NOTES	12. SPONSORING MILITARY ACTIVITY
	HQ USAF (AFTAC/VELA Seismological Center) Washington, D.C. 20333

13. ABSTRACT

A deephole array consisting of 12 short-period triaxial seismometers was operated at a test site near Grapevine, Texas (GVTX) until 23 February 1968. The system was then put in a standby status until additional software could be developed to provide additional filtering capabilities. The complete system was shut down and all of the instrumentation and equipment was moved into storage areas at the Geotech plant in Garland, Texas, during the last week of May.

The information gathered from the short-period triaxial array at the GVTX site was used to study short-period noise and signals, to develop signal enhancement, and filtering techniques. Most of the time was used in trying techniques based on least-mean-square filtering. In general, it can be concluded that because the noise is not stationary, these filters degrade too rapidly to be of practical interest for online processing. Several non-optimum filtering techniques were also tried and were found to be as effective as the optimum filters.

DD FORM 1 JAN 64 1473

Security Classification

14. KEY WORDS	LINK A		LINK B		LINK C	
	ROLE	WT	ROLE	WT	ROLE	WT
Triaxial seismometers						
Vertical array						
Optimum filtering						
Non-optimum filtering						
VT/7703						

INSTRUCTIONS

1. ORIGINATING ACTIVITY: Enter the name and address of the contractor, subcontractor, grantee, Department of Defense activity or other organization *(corporate author)* issuing the report.

2a. REPORT SECURITY CLASSIFICATION: Enter the overall security classification of the report. Indicate whether "Restricted Data" is included. Marking is to be in accordance with appropriate security regulations.

2b. GROUP: Automatic downgrading is specified in DoD Directive 5200.10 and Armed Forces Industrial Manual. Enter the group number. Also, when applicable, show that optional markings have been used for Group 3 and Group 4 as authorized.

3. REPORT TITLE: Enter the complete report title in all capital letters. Titles in all cases should be unclassified. If a meaningful title cannot be selected without classification, show title classification in all capitals in parenthesis immediately following the title.

4. DESCRIPTIVE NOTES: If appropriate, enter the type of report, e.g., interim, progress, summary, annual, or final. Give the inclusive dates when a specific reporting period is covered.

5. AUTHOR(S): Enter the name(s) of author(s) as shown on or in the report. Enter last name, first name, middle initial. If military, show rank and branch of service. The name of the principal author is an absolute minimum requirement.

6. REPORT DATE: Enter the date of the report as day, month, year; or month, year. If more than one date appears on the report, use date of publication.

7a. TOTAL NUMBER OF PAGES: The total page count should follow normal pagination procedures, i.e., enter the number of pages containing information.

7b. NUMBER OF REFERENCES: Enter the total number of references cited in the report.

8a. CONTRACT OR GRANT NUMBER: If appropriate, enter the applicable number of the contract or grant under which the report was written.

8b, 8c, & 8d. PROJECT NUMBER: Enter the appropriate military department identification, such as project number, subproject number, system numbers, task number, etc.

9a. ORIGINATOR'S REPORT NUMBER(S): Enter the official report number by which the document will be identified and controlled by the originating activity. This number must be unique to this report.

9b. OTHER REPORT NUMBER(S): If the report has been assigned any other report numbers *(either by the originator or by the sponsor)*, also enter this number(s).

10. AVAILABILITY/LIMITATION NOTICES: Enter any limitations on further dissemination of the report, other than those imposed by security classification, using standard statements such as:

(1) "Qualified requesters may obtain copies of this report from DDC."

(2) "Foreign announcement and dissemination of this report by DDC is not authorized."

(3) "U. S. Government agencies may obtain copies of this report directly from DDC. Other qualified DDC users shall request through _____."

(4) "U. S. military agencies may obtain copies of this report directly from DDC. Other qualified users shall request through _____."

(5) "All distribution of this report is controlled. Qualified DDC users shall request through _____."

If the report has been furnished to the Office of Technical Services, Department of Commerce, for sale to the public, indicate this fact and enter the price, if known.

11. SUPPLEMENTARY NOTES: Use for additional explanatory notes.

12. SPONSORING MILITARY ACTIVITY: Enter the name of the departmental project office or laboratory sponsoring *(paying for)* the research and development. Include address.

13. ABSTRACT: Enter an abstract giving a brief and factual summary of the document indicative of the report, even though it may also appear elsewhere in the body of the technical report. If additional space is required, a continuation sheet shall be attached.

It is highly desirable that the abstract of classified reports be unclassified. Each paragraph of the abstract shall end with an indication of the military security classification of the information in the paragraph, represented as *(TS)*, *(S)*, *(C)*, or *(U)*.

There is no limitation on the length of the abstract. However, the suggested length is from 150 to 225 words.

14. KEY WORDS: Key words are technically meaningful terms or short phrases that characterize a report and may be used as index entries for cataloging the report. Key words must be selected so that no security classification is required. Identifiers, such as equipment model designation, trade name, military project code name, geographic location, may be used as key words but will be followed by an indication of technical context. The assignment of links, rules, and weights is optional.